GRI-92/0471

SECONDARY NATURAL GAS RECOVERY: TARGETED TECHNOLOGY APPLICATIONS FOR INFIELD RESERVE GROWTH IN DELTAIC SAND-RICH, LOW- TO CONVENTIONAL-PERMEABILITY RESERVOIRS IN THE WILCOX GROUP, LAKE CREEK FIELD, TEXAS

TOPICAL REPORT

(September 1, 1989–December 31, 1992)

Prepared by

Jeffry D. Grigsby, Edgar Guevara, and Raymond A. Levey
Bureau of Economic Geology
W. L. Fisher, Director
The University of Texas at Austin
Austin, Texas 78713-7508

Mark A. Sippel
Research and Engineering Consultants, Inc.

W. E. Howard and José M. Vidal
ResTech, Inc.

James Ballard
Envirocorp Services and Technology, Inc.

for

GAS RESEARCH INSTITUTE
Contract No. 5088-212-1718
GRI Project Manager, Raymond W. Owens

U.S. DEPARTMENT OF ENERGY
DOE Contract No. DE-FG21-88MC25031
DOE Chief, Unconventional Gas Recovery Branch
Charles W. Byrer

December 1992

DISCLAIMER

LEGAL NOTICE This report was prepared by the Bureau of Economic Geology as an account of work sponsored by the Gas Research Institute (GRI). Neither GRI, members of GRI, nor any person acting on behalf of either:

a. Makes any warranty or representation, expressed or implied, with respect to the accuracy, completeness, or usefulness of the information contained in this report, or that the use of any apparatus, method, or process disclosed in this report may not infringe privately owned rights; or

b. Assumes any liability with respect to the use of, or for damages from the use of, any information, apparatus, method, or process disclosed in this report.

50272-101

REPORT DOCUMENTATION PAGE	1. REPORT NO. GRI-92/0471	2.	3. Recipient's Accession No.

4. Title and Subtitle
Secondary Natural Gas Recovery: Targeted Technology Applications for Infield Reserve Growth in Deltaic Sand-Rich, Low- to Conventional-Permeability Reservoirs in the Wilcox Group, Lake Creek Field, Texas

5. Report Date December 1992

6.

7. Author(s) Jeffry D. Grigsby, Edgar Guevara, Raymond A. Levey, Mark A. Sippel, W. E. Howard, José M. Vidal, and James Ballard

8. Performing Organization Rept. No.

9. Performing Organization Name and Address

Bureau of Economic Geology
The University of Texas at Austin
University Station, Box X
Austin, Texas 78713–7508

10. Project/Task/Work Unit No.

11. Contract(C) or Grant(G) No.
(C) 5088-212/1718(GRI)
(G) DE-FG21-88MC25031 (DOE)

12. Sponsoring Organization Name and Address

Gas Research Institute
8600 West Bryn Mawr Avenue
Chicago, IL 60631
Project Manager: Raymond W. Owens

13. Type of Report & Period Covered
Topical Report
9/1/89 – 12/31/92

14.

15. Supplementary Notes

16. Abstract (Limit: 200 words)

The potential for secondary incremental recovery of natural gas exists in complex fluvial-deltaic reservoirs of the Texas Gulf Coast. Four deltaic parasequences were identified using well logs calibrated to cores in the G sandstone. Engineering evaluations of production performance and pressures are compared with reservoir facies; these evaluations demonstrate the importance of identifying reservoir facies in maximizing recovery of natural gas. A well-log-based model to predict the free-water level and effective gas permeabilities was tested and calibrated using Wilcox gas reservoirs. Key reservoir parameters of porosity, water saturation, permeability, and capillary pressure are related in a single equation. Analysis of natural gas reservoirs from the Wilcox Deltaic sandstones in the Houston Embayment (WX-1) in East Texas indicates that reserve growth potential of approximately 60 percent over the current estimate of ultimate recovery is possible in deltaic sandstone reservoirs in the Lake Creek Unit. Detailed geologic, engineering, and petrophysical evaluation of the G sandstone reservoir in the Lake Creek Unit indicates that the maximum additional incremental gas opportunities exist in the flank region adjacent to the area currently developed in the Lake Creek field. The location, number, and economic feasibility of additional wells required to convert this resource to producible reserves were not evaluated.

17. Document Analysis a. Descriptors

capillary presssure, cooperative wells, depositional facies, East Texas, free-water level, parasequences, secondary natural gas recovery, well-log model, Wilcox Group

b. Identifiers/Open-Ended Terms

Integrated geologic, engineering, and petrophysical evaluation of deltaic gas reservoirs, identification of secondary natural gas resources

c. COSATI Field/Group

18. Availability Statement	19. Security Class (This Report)	21. No. of Pages
Release unlimited	Unclassified	105
	20. Security Class (This Page) Unclassified	22. Price

RESEARCH SUMMARY

Title	Secondary Natural Gas Recovery: Targeted Technology Applications for Infield Reserve Growth in Deltaic Sand-Rich, Low- to Conventional-Permeability Reservoirs in the Wilcox Group, Lake Creek Field, Texas
Contractor	Bureau of Economic Geology, The University of Texas at Austin, GRI Contract No. 5082-211-1718, titled "Secondary Natural Gas Recovery: Targeted Technology Applications for Infield Reserve Growth"
Principal Investigators	Robert J. Finley and Raymond A. Levey
Report Period	September 1989–December 1992
Objectives	The objective of this report is to better enable natural gas producers to develop additional natural gas resources in fields with low to conventional permeability and porosity. Heterogeneities in late Paleocene-age reservoirs are described and evaluated in Lake Creek field, a mature gas field located in the Wilcox Deltaic Sandstone in the Houston Embayment (WX-1) play in Texas. This field study serves as a model in its approach to incremental resource development for similar gas fields.
Technical Perspective	A major goal of the Infield Natural Gas Reserve Growth Joint Venture project is to assess the potential for maximizing economic recovery of natural gas, mainly in reservoirs with low to conventional porosity and permeability. These reservoirs may contain incompletely drained compartments that are defined primarily by a combination of depositional-facies and diagenetic heterogeneity and secondarily by structural heterogeneity. In many low- to conventional-permeability gas fields, complex deltaic reservoirs contain opportunities for identifying potentially undrained reservoir compartments. Remaining natural gas in these compartments can be contacted by the recompletion of existing wells that have bypassed these compartments or by the drilling of infield wells that contact compartments not effectively drained at current well spacing. Exploration for compartments or bypassed gas zones in old fields can be improved using detailed geologic studies that integrate engineering, petrophysical, and geophysical methods.
Results	This report summarizes the results of research designed to evaluate the potential for secondary gas recovery in deltaic reservoirs in the lower Wilcox Group in Lake Creek field. These reservoirs consist of delta-front, channel-mouth-bar, and distributary-channel reservoir sandstones that are bounded by prodelta and delta-plain nonreservoir siltstones and mudstones. Analyses of secondary gas recovery potential in these reservoirs at Lake Creek indicate that a technically recoverable resource potentially exceeds the expected

ultimate recovery from currently developed wells in the G reservoir. Some part of this resource will be recoverable through additional infield development of existing well bores and through new well bores.

No attempt has been made to estimate the number of wells that might be required to fully develop the incremental resources identified by this study. Reservoir heterogeneity has probably resulted in multiple independent or poorly connected reservoir compartments. The reserve growth potential estimated in this analysis assumes that enough wells will be drilled to penetrate and effectively drain all such compartments. Actual development strategy, however, will depend largely on economic factors, which are beyond the scope of this study.

Detailed stratigraphic analysis of the lower Wilcox indicates that the G sandstone in Lake Creek field is composed of at least four parasequences. An analog comparison of lower Wilcox deltaic reservoirs in the subsurface with laterally continuous outcrop exposures was analyzed as part of a concurrent GRI research effort in the Ferron Sandstone in Utah. Similar trends in permeability from nearly identical depositional facies, both in whole cores from the subsurface Wilcox deltas and in Ferron outcrops, were documented by extensive minipermeameter measurements.

A well-log-based model to predict free-water level and effective permeabilities was also successfully tested in these lower Wilcox gas reservoirs. This model relates the four important reservoir properties of porosity, water saturation, permeability, and capillary pressure with a single equation. Detailed petrographic analysis from whole cores obtained in a GRI cooperative well indicates that fibrous illites will cause artificially high permeability measurements when industry standard procedures using conventionally dried core plugs are used to assess permeability.

Technical Approach

The research integrated geologic subsurface mapping, petrophysical techniques, and engineering analysis to evaluate the impacts of both depositional and diagenetic reservoir heterogeneities on the recovery of incremental gas. The technical approach included the following:

(1) Subsurface mapping of the G sandstone using well logs calibrated to core data to determine genetic depositional units, reservoir variability, and stacking patterns.

(2) Acquisition of high-resolution well-log data in GRI cooperative wells to determine applicability of state-of-the-art logging techniques in identifying infield gas resources.

(3) Application of a well-log-based permeability model that relates porosity, water saturation, permeability, and capillary pressure with a single equation.

(4) Analysis of production history and pressure data to compare volumes of original gas in place with estimates of recoverable resources.

(5) Comparison of the permeability structure in identical depositional facies identified in subsurface whole cores and in depositionally analogous outcrops.

Implications

This report summarizes the results of the integrated geological, petrophysical, and engineering research as part of a broader project to investigate technology applications for infield reserve growth in Lake Creek field. Analysis of gas reservoirs in stratigraphically complex Tertiary deltaic deposits in the Lake Creek gas field indicates that reserve growth potential exists in sandstone-rich deltaic reservoirs.

Variability in the stratigraphic reservoir architecture and the diagenetic effects on reservoir quality in the Wilcox Deltaic Sandstone in the Houston Embayment (WX-1) gas play will require operators to assess these conditions to evaluate the secondary resource potential of other fields in this play or in similar gas plays. The Secondary Natural Gas Recovery project is currently transferring technology and reporting results from this research to the gas industry through publications, short courses, and workshops.

CONTENTS

Appendices

Figures

Tables

Appendix Figures

Appendix Tables

EXECUTIVE SUMMARY

The lower 48 states contain approximately 800 Tcf of technically recoverable natural gas resources in reservoirs with conventional porosity and permeability (Finley and others, 1988). A subset of this 800 Tcf is a resource target of more than 200 Tcf in existing gas fields in the lower 48 states. Many of these reservoirs contain incompletely drained compartments that are defined primarily by depositional-facies heterogeneity and secondarily by structural heterogeneity and local variations in porosity and permeability. Additional natural gas can be contacted and produced by recompleting in existing wells that have bypassed these reservoir compartments or by drilling infield wells that contact compartments undrained by current well and completion spacing. Infield exploration in mature gas fields can be improved through the use of detailed geologic studies integrated with reservoir engineering, petrophysics, and reservoir geophysics.

This report summarizes part of a multiyear, multifield research program, including results from project cooperative studies in deltaic gas reservoirs in Lake Creek field, which is producing gas resources from the Wilcox Deltaic Sandstone in the Houston Embayment (WX-1) gas play in Texas. The potential for secondary recovery of gas resources exists in the Texas Gulf Coast, where stratigraphically complex Tertiary deltaic reservoirs contain both lenticular distributary-channel sandstone and delta-front reservoirs interbedded with nonreservoir prodeltaic and delta-plain mudstone. The resource potential for secondary gas recovery is affected by both the depositional controls on reservoir stacking, reservoir facies, and permeability architecture and by the diagenetic effects on reservoir quality. Project pressure testing of reservoir intervals in the Lake Creek field was not feasible because of operational contraints, but access to the gas operator's records for pressure tests and production data allowed detailed analysis of individual completions.

Several controls affect the number, size, and distribution of reservoir compartments, including geologic controls such as sandstone architecture and reservoir diagenesis and operational controls such as completion spacing and vertical extent of perforations through a gas-charged reservoir. In deltaic depositional systems, sandstone architecture is controlled by variations in the relative base level that reflect changes in eustasy, sediment supply, subsidence, and climate. In addition to undergoing potential reservoir compartmentalization resulting from reservoir architecture and depositional-facies heterogeneity, deltaic reservoirs in the Texas Gulf Coast are commonly overprinted by structural complexity (faults and folds) and by diagenetic variations in reservoir quality. Natural gas in the Lake Creek field is trapped in reservoirs on the rollover anticline along the Wilcox growth-fault zone. Detailed well-log correlations and seismic reflection lines indicate no major structural heterogeneity or discontinuity exists across the gas-productive part of the field.

The acquisition of preserved core from the LCU No. 48 well in Lake Creek field, a GRI cooperative well, provided the opportunity to apply petrophysical model based on logs, rock data, and well-test results. This model effectively provides log-derived reservoir parameters by modeling shaly sands, capillary pressures, and permeabilities of the lower Wilcox sandstones. With this model it was possible to predict the free-water level (FWL) for the G-2 sandstone and closely match the well-test permeability-feet (kh) results with log-derived kh values. Results of an investigation of the effects of fibrous illites on core measurement revealed that convection oven-dried permeability measurements on cores can be from two to seven times greater than preserved core permeability measurements in the lower Wilcox sandstones.

Production characteristics of 12 wells completed in the lower Wilcox G reservoir at Lake Creek field were evaluated. Pressure-buildup data and/or Texas Railroad Commission open-flow tests (G-1 reports) were used to calculate estimates of effective permeability-thickness (kh) from specific intervals. Core-analysis results were used to

calibrate log-derived estimates of kh that compare favorably with kh from production tests. Producing-rate data were used to determine ultimate recovery and were compared with an estimate of recoverable gas. The volumetrically determined recoverable original gas in place for the Wilcox G reservoir is greater than the projected ultimate recovery of the existing Wilcox G reservoir completions. Integrated geologic, engineering, and petrophysical analyses indicate that a reserve growth potential of 60 percent over the current well development in the G sandstone reservoir. Most of this reserve growth potential exists on the flank of the Lake Creek field.

OBJECTIVES

The chief objective of the research was to evaluate the potential for stratigraphic and diagenetic compartmentalization in natural gas reservoirs in fields with low to conventional permeability and porosity. The study area for this report was Lake Creek field, a mature onshore gas field in the Wilcox Deltaic Sandstone in the Houston Embayment (WX-1) play in Texas. In addition to subsurface evaluation of well logs and cores, a comparative analysis of permeability trends established in a parallel GRI-sponsored study to evaluate reservoir architecture in the Ferron Sandstone Research was also undertaken. Tasks to achieve the major project objective included

(1) calibrating well logs to cores to delineate productive reservoir facies in stacked deltaic depositional systems,

(2) determining permeability trends within depositional facies,

(3) applying a log-based permeability model to predict the free-water level in low- to conventional-permeability and porosity reservoirs,

(4) evaluating the effects of depositional facies on gas reservoir performance, and

(5) determining the reserve growth potential of stratigraphically complex deltaic reservoirs.

INTRODUCTION

Wilcox Deltaic Sandstone in the Houston Embayment (WX-1) Play

Lake Creek field, which contains 49 wells over 4.3 mi^2 (fig. 1), is part of the Wilcox Deltaic Sandstone in the Houston Embayment (WX-1) natural gas play defined by Kosters and others (1989). Fifty-four major reservoirs in the Wilcox WX-1 gas play have produced more than 3.8 Tcf of gas through January of 1987 (Kosters and others, 1989). In this gas play, hydrocarbons are trapped in rollover anticlines along the Wilcox growth-fault zone. Reservoirs in this play, confined to the Paleocene to lower Eocene Wilcox Group, consist of distributary-channel, channel-mouth-bar, and delta-front sandstones. These sandstones represent the first major progradational episode into the northern part of the Gulf Coast Basin (fig. 2).

Structural and Stratigraphic Framework

The major control on hydrocarbon production within Lake Creek field is a fault-bounded rollover anticline (fig. 3). Studies within Lake Creek field have focused on gas reservoirs of the G sandstone, one of 18 gas-condensate reservoirs ranging in depth from 9,200 to 14,500 ft (fig. 4). The G sandstone, composed of individual multistoried, stratigraphically heterogeneous reservoirs, is one of several 150- to 500-ft-thick, upward-coarsening intervals that form part of the fluvial-dominated Brazos delta of the lower Wilcox Rockdale delta system delineated by Fisher and McGowen (1967). At the LCU No. 48 well (fig. 1), the G sandstone is 290 ft thick and consists of a repetitive series of upward-coarsening, upward-thickening sandstones separated by mudstone-rich intervals. Thick, laterally persistent mud-rich intervals subdivide the G sandstone into four operational units (parasequences) that, from youngest to oldest, are named G-1 through G-4 (fig. 5). Each of these parasequences corresponds to a period of deltaic progradation. The G-2 and G-4 units

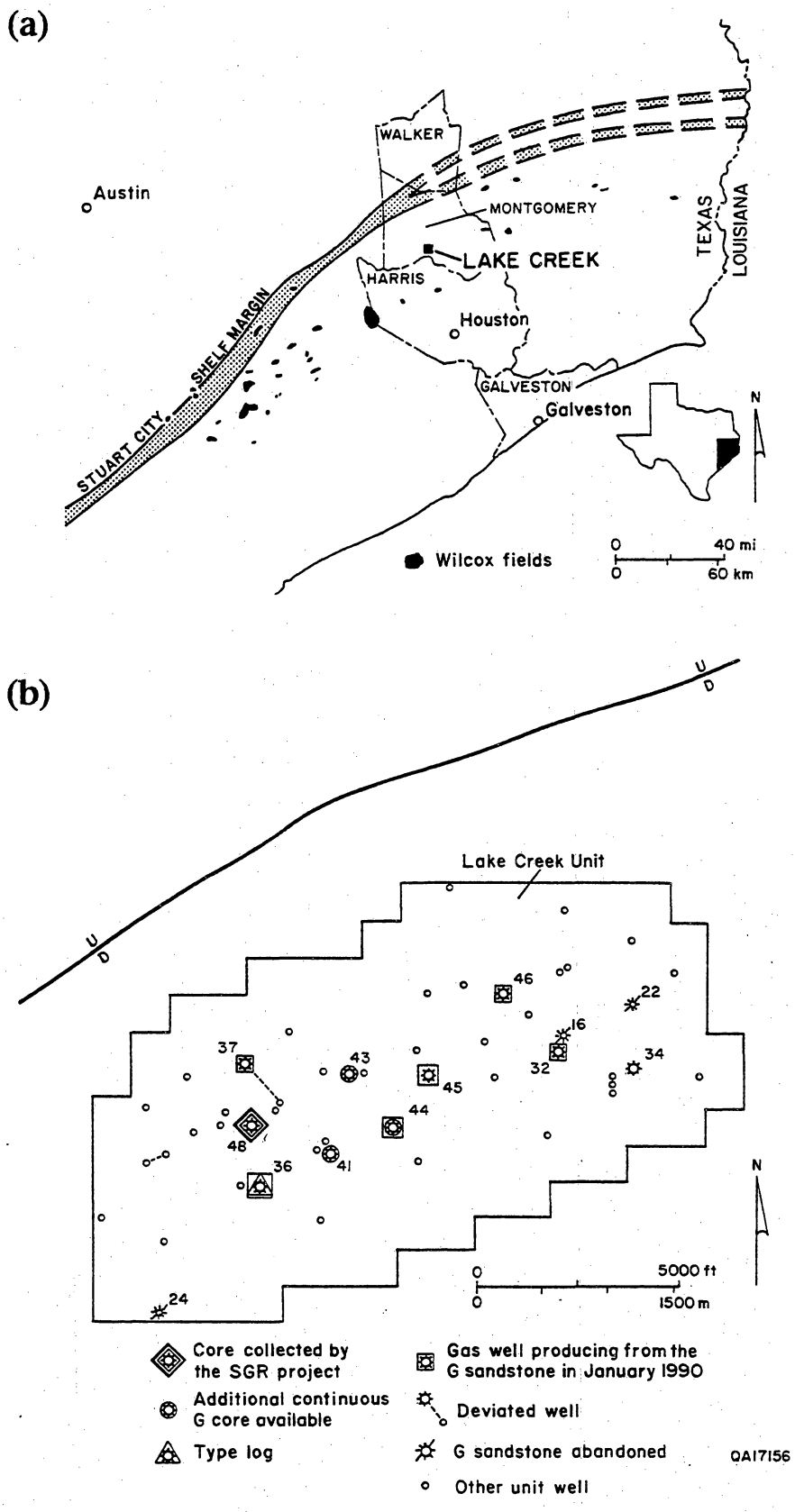

Figure 1. (a) Location map of Lake Creek field (modified from Kosters and others, 1989); (b) index map of wells in Lake Creek field (after Guevara and Grigsby, 1992).

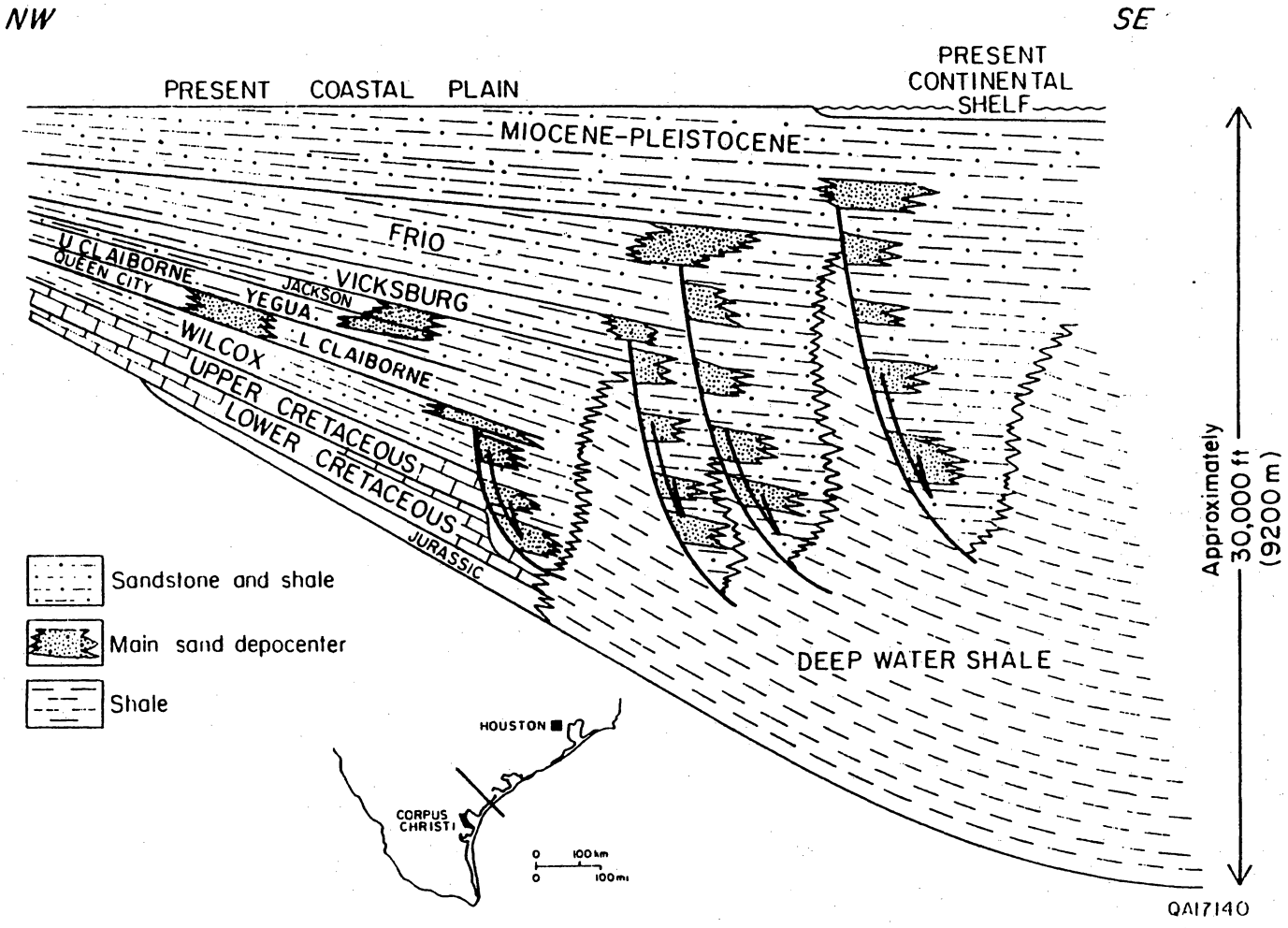

Figure 2. Schematic dip-oriented depositional cross section through the Central Texas Gulf Coast Basin illustrating the position of the Wilcox Group relative to other major sandstone deposits (after Bebout and others, 1982).

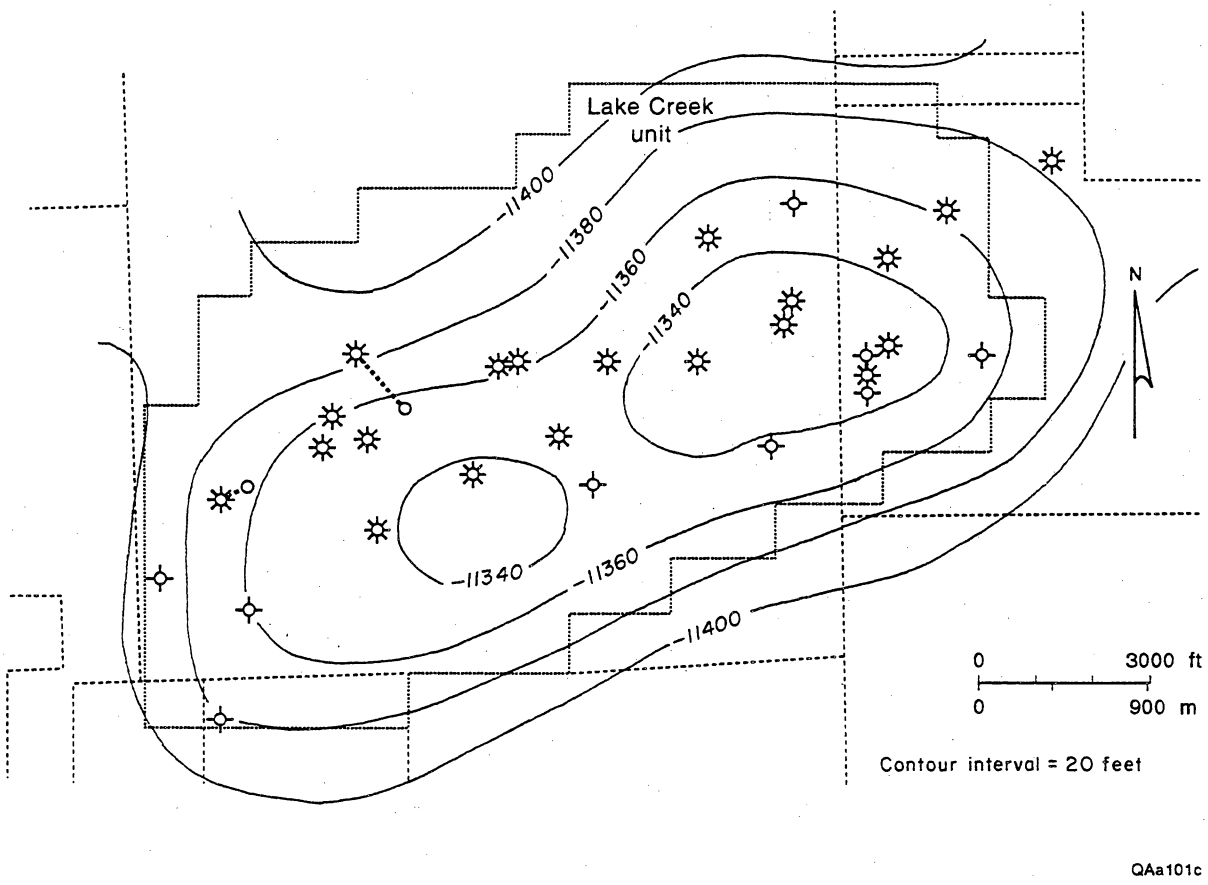

Figure 3. Map showing the structure of the Wilcox on the top of the G-2 sandstone. Structural closure is interpreted at –11,327 ft.

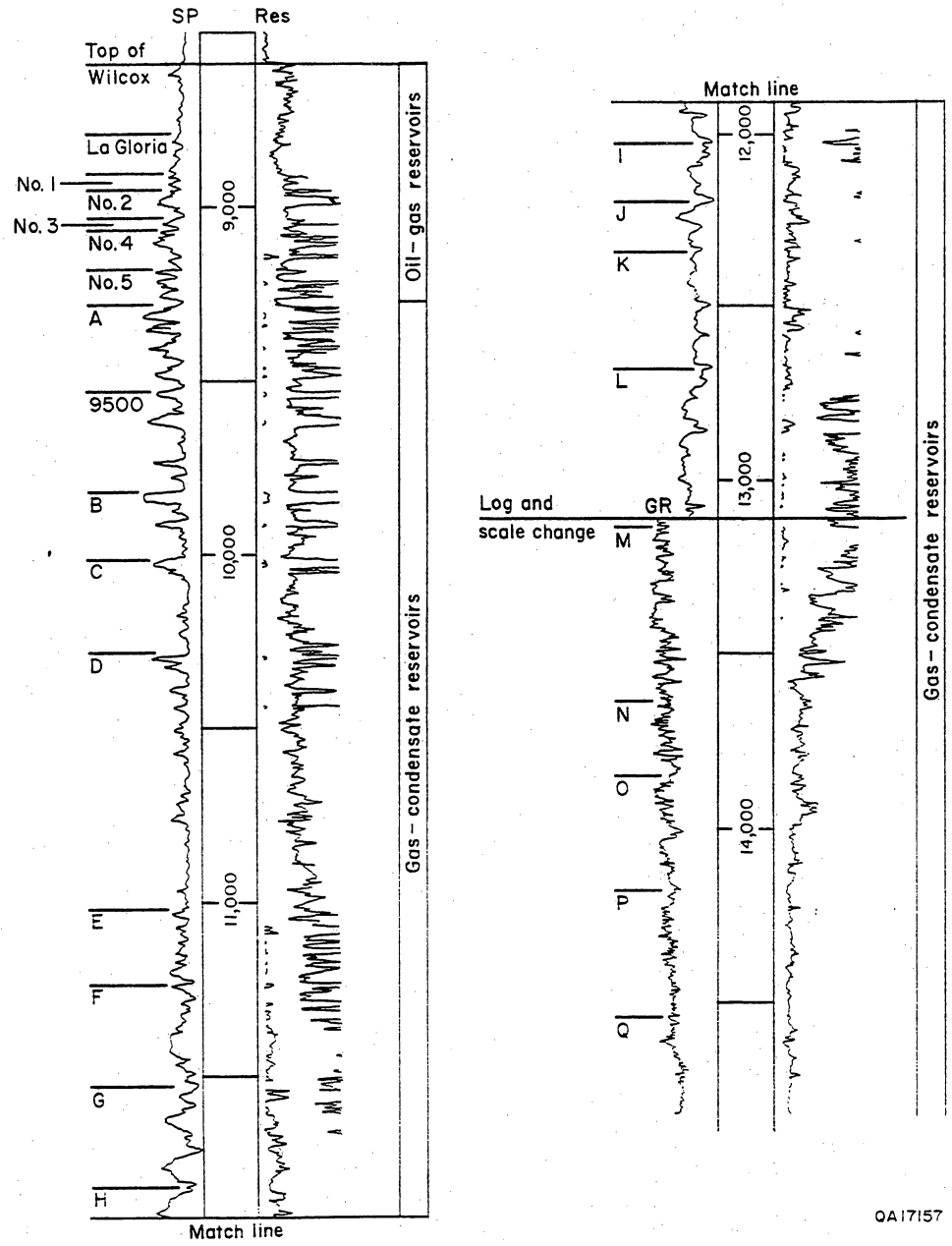

Figure 4. Type log (LCU No. 36) for Lake Creek field showing oil/gas reservoirs (La Gloria and G-1 through G-5 sandstones) and the underlying gas-condensate reservoirs (A to Q sandstones) of the Wilcox Group (after Guevara and Grigsby, 1992). Reservoir nomenclature after Clarke (1962).

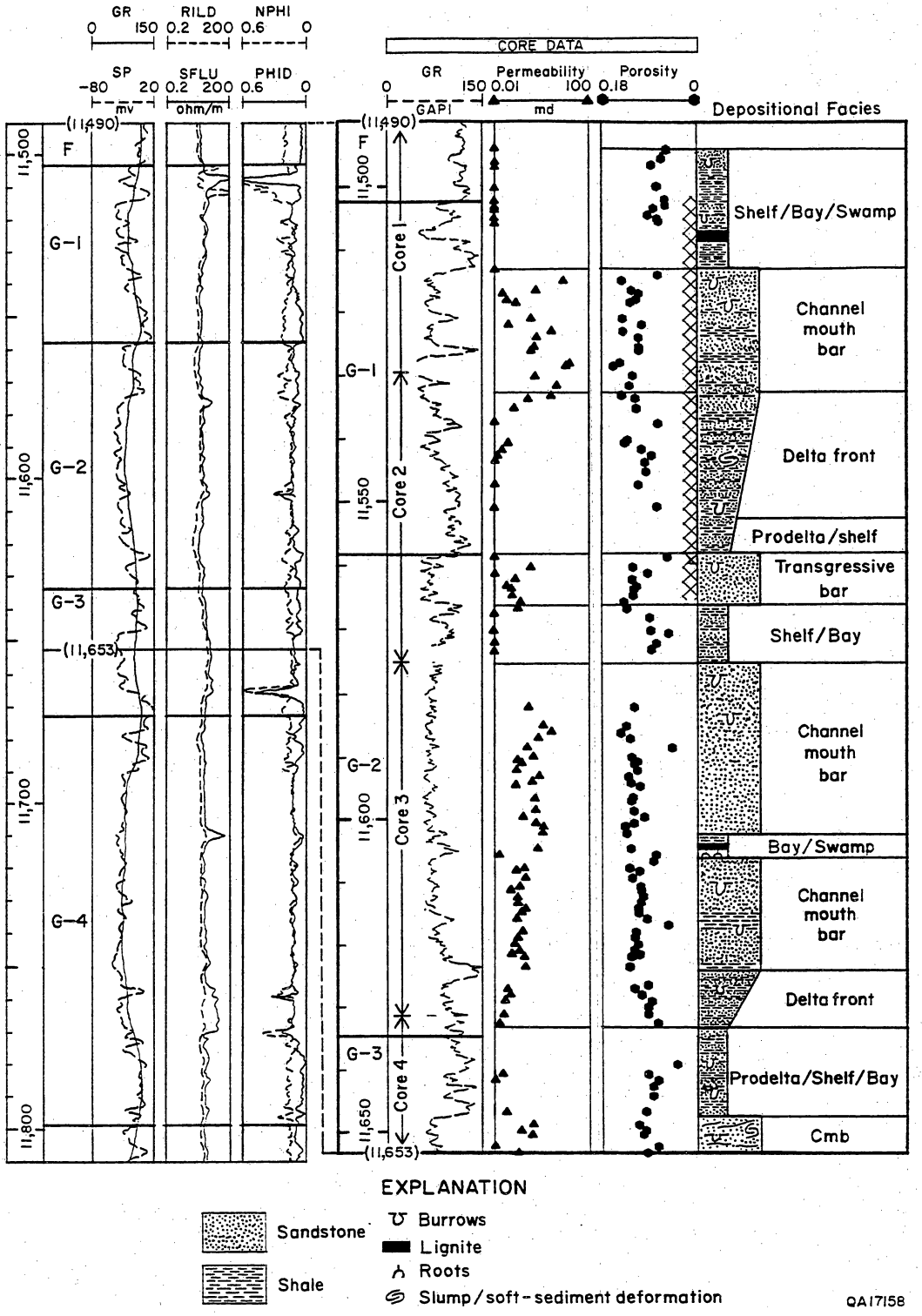

Figure 5. Well log (to left) from the LCU No. 48 well showing the major subdivisions (parasequences) of the lower Wilcox G sandstone. Core was collected from the G-1, G-2, and the top of the G-3 parasequences. Petrophysical data and a core graph depicting depositional environments are illustrated at right (after Guevara and Grigsby, 1992). Cmb = channel-mouth bar.

represent major progradations, each overlain by a smaller progradation (G-1 and G-3). Because progradation of these parasequences occurred during an overall relative sea-level rise, the G sandstone represents a retrogradational system (Guevara and others, in press).

Field History

Both oil and gas were discovered in Lake Creek field in 1941. Lake Creek field was initially produced in 1944 as a pressure-maintenance, gas-cycling operation to maximize recovery of liquid hydrocarbons. Gas-cycling extended through the mid-1950's. Cumulative gas production through January 1990 was 120 Bcf of gas and 15.7 MMbbl of condensate.

The Wilcox G reservoir at the Lake Creek field was first produced with one well in 1944. Two subsequent completions were made in 1948 and 1961. The cumulative production from these three early wells was 2,514 MMcf. Further development of the reservoir began again in 1984; since that time, nine additional wells have been completed in the G reservoir. The distance between completions in the G reservoir varies from 1,500 to 2,200 ft. The total reported production as of April 30, 1992, was 8,849 MMcf of gas and 279 Mbbl of condensate. The projected ultimate recovery of the past and current completions is 14,808 MMcf.

DEPOSITIONAL ENVIRONMENTS OF THE G SANDSTONE

Shelf/Prodelta Mud Facies

The shelf and prodelta mud-rich facies compose the lower part of each parasequence. The shelf facies consists of mostly bioturbated shales interbedded with laminae and thin beds of siltstone and sandstone, commonly bioturbated, massive, or rippled. The prodelta facies overlies the shelf facies, and the siltstones and sandstones of the prodelta facies generally thicken upward, are more abundant, and show less intense bioturbation.

Delta-Front Facies

Overlying the shelf/prodelta mud-rich facies is the delta-front facies. This facies can be divided into two subfacies: the distal delta-front facies and the channel-mouth-bar facies.

Distal Delta-Front Facies

The distal delta-front facies (or delta-front facies) occurs in the lower part of the delta-front complex. It consists of interbedded shales and sandstones increasing in abundance and thickness upward. These sandstones commonly exhibit hummocky cross-stratification and current and wave ripples. The more sand-rich intervals at the top of these shoaling-upward sequences commonly show slumping and soft-sediment deformation. The distal delta-front facies is often laterally extensive. Spontaneous-potential and gamma-ray log suites are typically funnel shaped.

Channel-Mouth-Bar Facies

The channel-mouth-bar facies (or proximal delta-front facies) occurs locally in the upper part of the delta-front complex. These sandstones are not as laterally extensive as the distal delta-front facies and consist of massive, crossbedded and parallel bedded, locally rippled, and burrowed sandstones interbedded with shales. Sandstones commonly coarsen upward. Spontaneous-potential and gamma-ray log suites, typically blocky and serrate, often indicate the coarsening-upward trend.

Distributary-Channel Facies

Distributary-channel facies examined from core from Lake Creek field are characterized by sand-rich intervals containing massive to crossbedded sandstones that fine upward. Spontaneous-potential and gamma-ray log suites are typically blocky in character. Abundant

rip-up clasts (clay and siderite) are common at the base of individual channels. These rip-up clasts often occur as pebble conglomerates that strongly affect the gamma-ray log by creating above-normal GR-API response within the basal part of the channel system. Individual distributary-channel-fill facies range from 10 to 90 ft in thickness and can range from several hundred to more than 2,000 ft in width. The smaller channels are interpreted to be interdistributary-bay-filling channels, and the larger channels represent the major distributary-channel trends. The two channel types are well developed in the G-4 parasequence (fig. 6). These channels are oriented parallel to depositional dip and are generally aligned in a northwest-southeast direction.

Delta-Plain Facies

Mud-rich facies, commonly rich in organic matter and locally displaying root molds and lignite deposits, represent the delta-plain facies. These sediments flank the distributary channels and are deposited in floodplain, swamp, and marsh depositional environments. Sandstones within these intervals, associated with crevasse-splay deposits, commonly have current and wave-ripple laminations.

Transgressive, Delta-Destructional Facies

Thin, bioturbated sandstones locally occurring in the upper parts of the operational units represent delta-margin, barrier-island, and sheet sandstones comprising transgressive, delta-destructional facies. These deposits, resulting from the reworking of the delta-front and delta-plain facies of the underlying, abandoned delta, grade up into and are interbedded with the shelf mud facies.

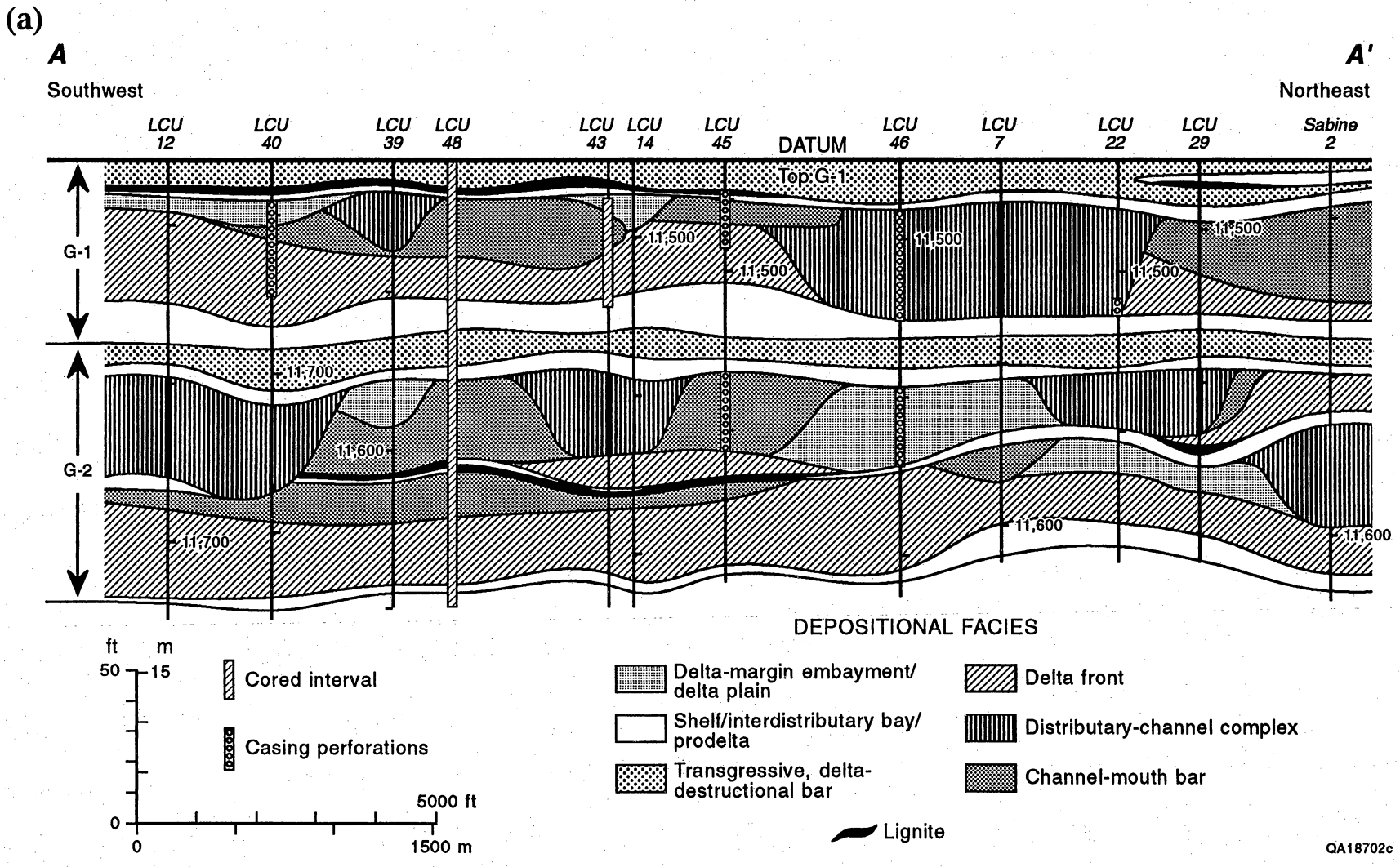

Figure 6. (a) Depositional strike-oriented cross sections showing (a) parasequences G-1 and G-2 and (b) G-3 and G-4 in the G sandstone interval across Lake Creek field.

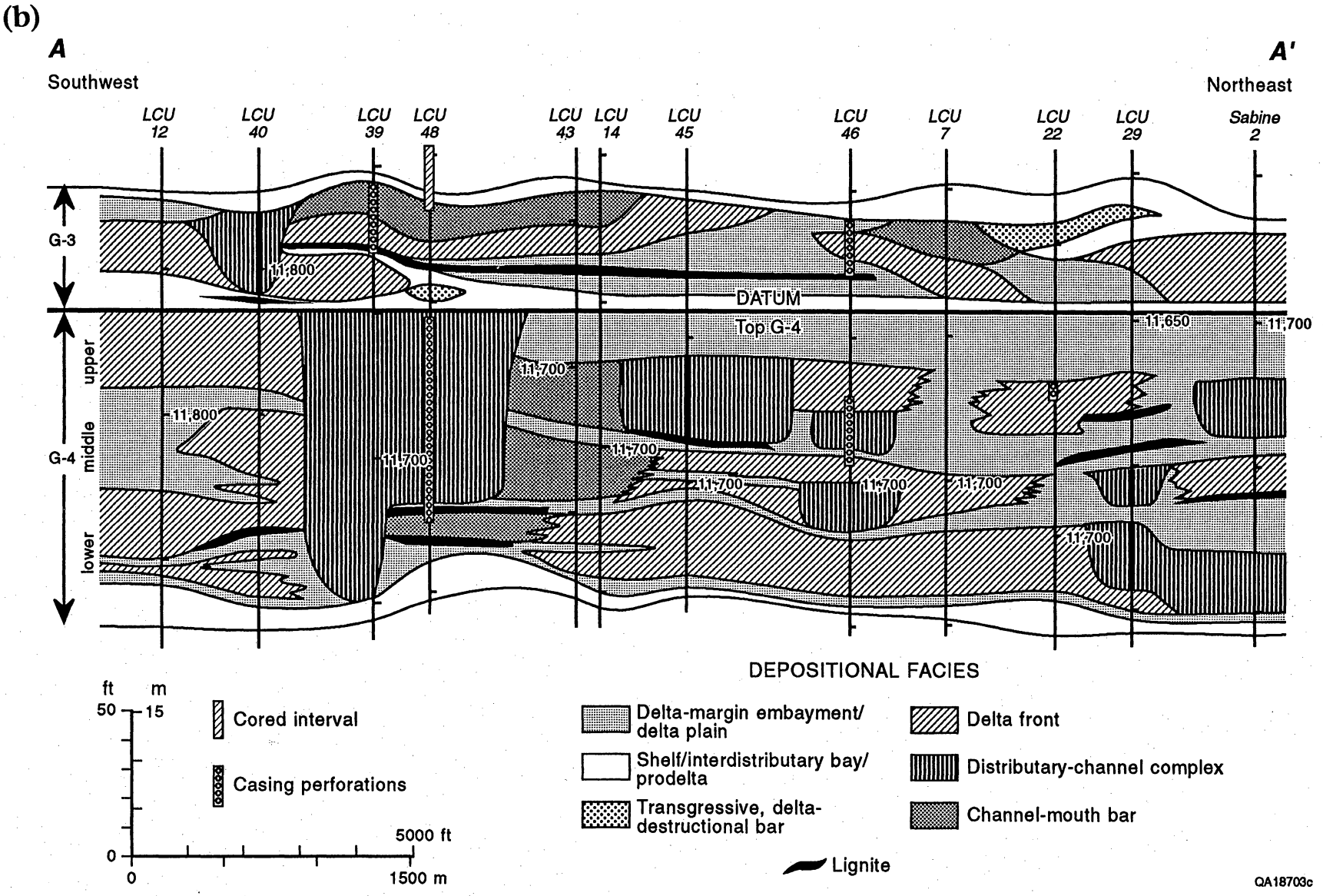

Figure 6. (continued)

FACTORS AFFECTING GAS RESERVOIR HETEROGENEITY

Stratigraphic Architecture of the G Sandstone

Characterization of stratigraphic architecture in the subsurface is dependent on the use of well-log profiles calibrated to lithologic information from core holes. Well-log profiles (spontaneous potential and gamma ray) define depositional facies and their three-dimensional extent and geometries. This approach formed the basis for the characterization of the G sandstone parasequences. However, information recently developed through work on the Cretaceous Ferron deltaic system in central Utah (Tyler and others, 1991), a deltaic system similar to the lower Wilcox deltaic sandstones, allowed for a more rigorous constraining of facies limits and internal structure.

Spontaneous-potential and gamma-ray logs of the operational units of the G sandstone generally display funnel-shaped log traces in the lower and upper parts and blocky-serrate log shapes in the middle part. Slabbed cores indicate that these log shapes reflect the subdivision of the operational units into three components. The funnel-shaped log traces, present in the lower and upper parts of the units, represent bioturbated shales with thin, locally parallel-laminated, rippled, and hummocky crossbedded sandstones. Sandstones may also be bioturbated and bounded by locally carbonaceous and lignitic shales. The blocky-serrate log shapes in the middle of these units represent massive crossbedded and rippled sandstones interbedded with thin shales. Because the operational units are stacked, the upper unit is also the base of the overlying unit.

The tripartite division of operational units (parasequences) can be interpreted as follows. Each operational unit is overlain, and underlain, by a thick shale unit that can be traced across the entire field. This mud-rich unit comprises the shelf and prodelta facies. Beginning at the base of the unit, the mud-rich shelf and prodelta facies are overlain by distal delta-front facies sandstones and mudstones. This facies grades upward into the thick, massive sandstones of the proximal delta-front or distributary-channel facies, which is

locally interbedded with delta-plain and interdistributary-bay-fill muds. The unit above the sandstone-rich interval of the proximal delta-front or distributary-channel facies is a return to the more distal delta-front facies and associated muds. This, in turn, is overlain by the mud-rich shelf and prodelta facies.

Cores and wireline logs of the G sandstone in the LCU No. 48 well and vicinity illustrate deltaic progradation and subsequent local, transgressive flooding of abandoned deltas. Each operational unit (G-1 through G-4, fig. 5) corresponds to a period of deltaic progradation (units G-2 and G-4 representing relatively major progradations), each overlain by smaller progradations (G-1 and G-3). Distal delta-front facies are locally overlain or replaced by channel-mouth-bar facies, which, in turn, are locally overlain and truncated by distributary-channel facies. This variation in stratigraphic architecture is illustrated in the net-sandstone maps of the G-4 and G-2 progradational units (figs. 7 through 9) and the cross section in figure 6.

Effects of progradation on reservoir architecture are well represented in the lower and upper/middle intervals of operational unit G-4 (figs. 6 through 8). The net-sandstone map in figure 7 illustrates that the lower G-4 represents the filling of an interdistributary bay by a delta lobe. The cross section in figure 6 indicates that the lower G-4 is dominated by laterally continuous distal delta-front and delta-plain deposits. Conversely, the upper/middle intervals of the G-4 unit are more sand rich and heterogeneous. This interval is dominated by a large distributary channel that downcuts through the delta-front and delta-plain facies of the lower G-4 unit. In addition, several smaller distributary-channel sandstones are seen. This pattern is repeated in the G-2 unit where the lower G-2 is dominated by laterally continuous distal delta-front and delta-plain deposits and is overlain by the more heterogeneous channel-mouth-bar and distributary-channel facies of the upper G-2 (figs. 6 and 9). Retrogradation (progradation during overall sea-level rise) analogous to that displayed in the upper Ferron Sandstone (Tyler and others, 1991) is well represented by

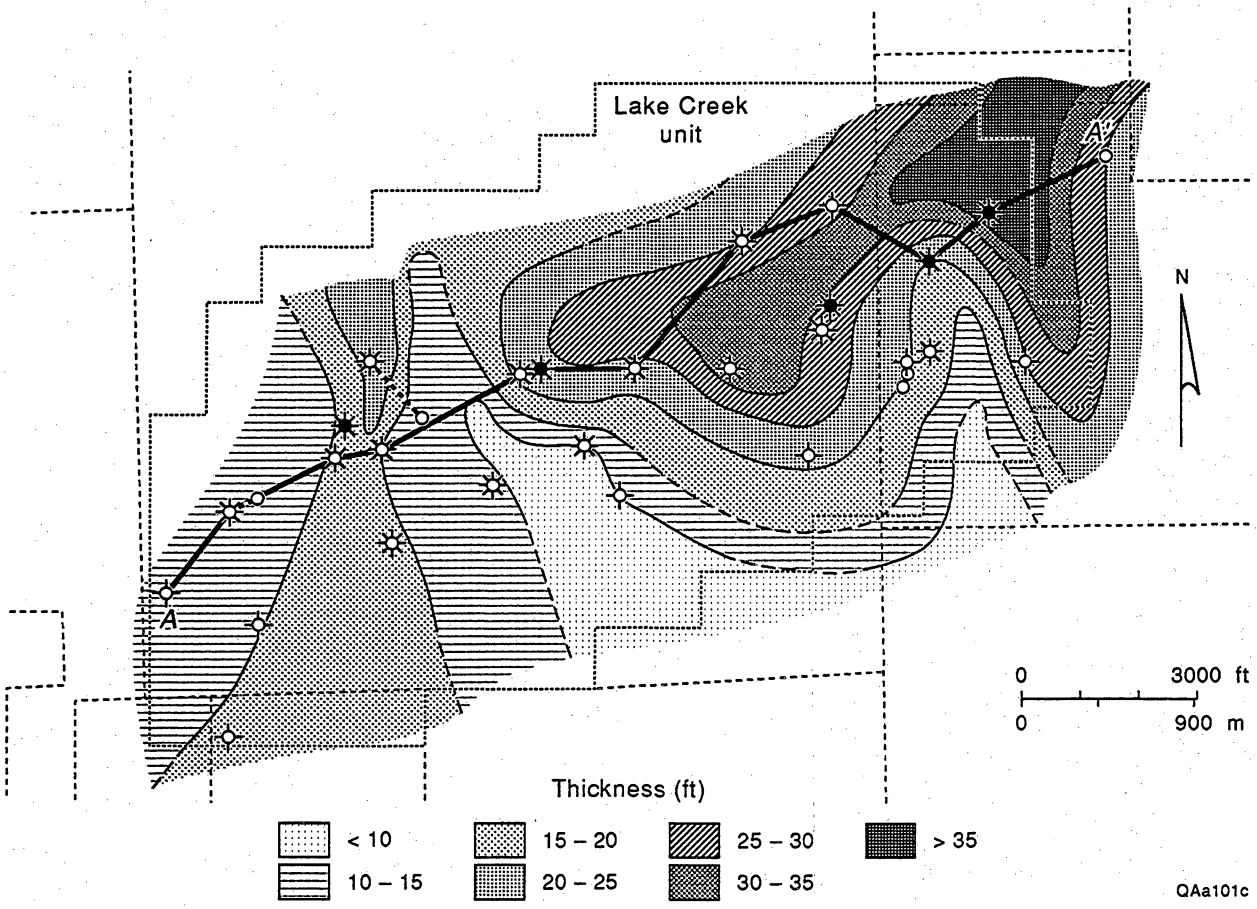

Figure 7. Net-sandstone map of the G-4 lower interval. Note well-developed delta lobe.

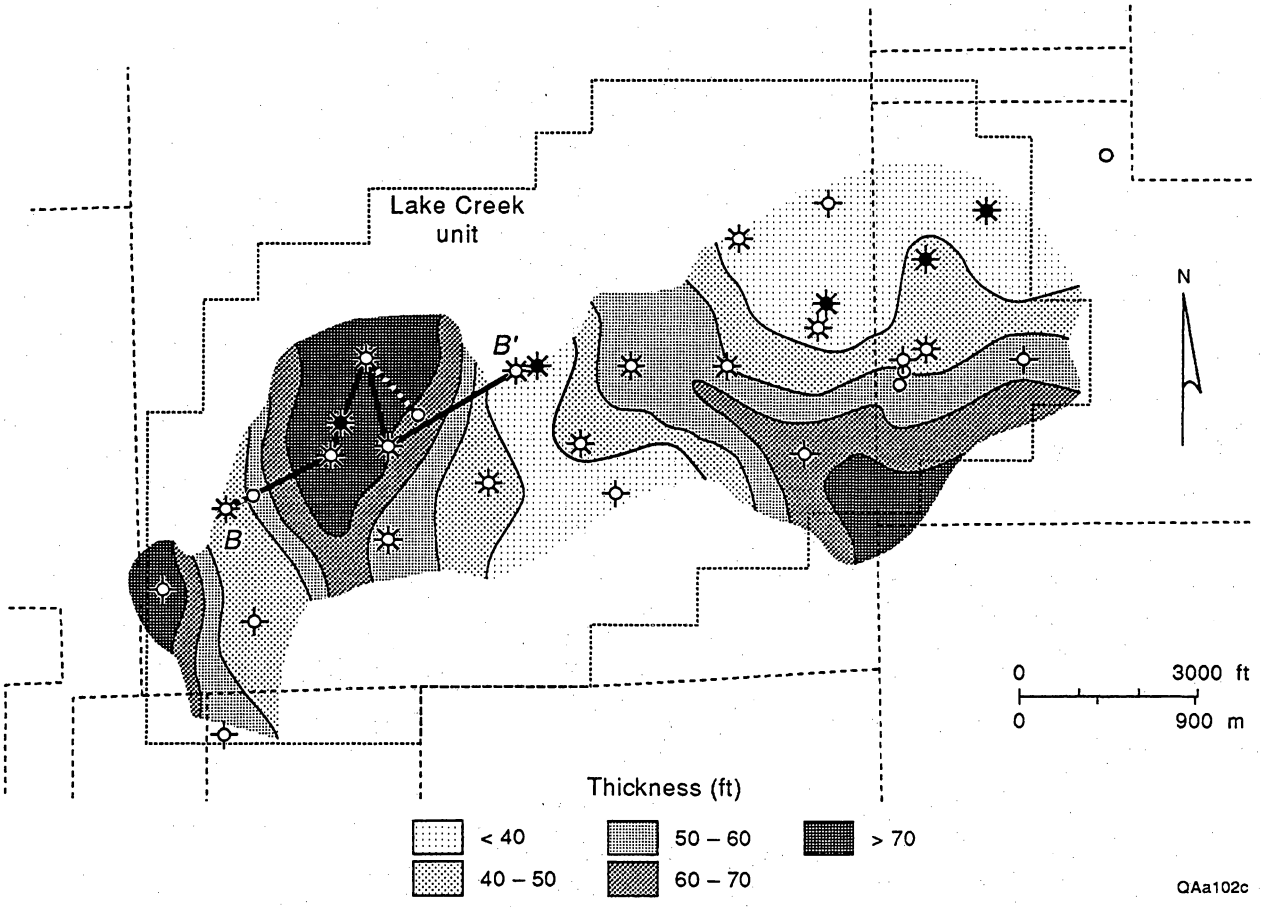

Figure 8. Net-sandstone map of G-4 upper/middle interval.

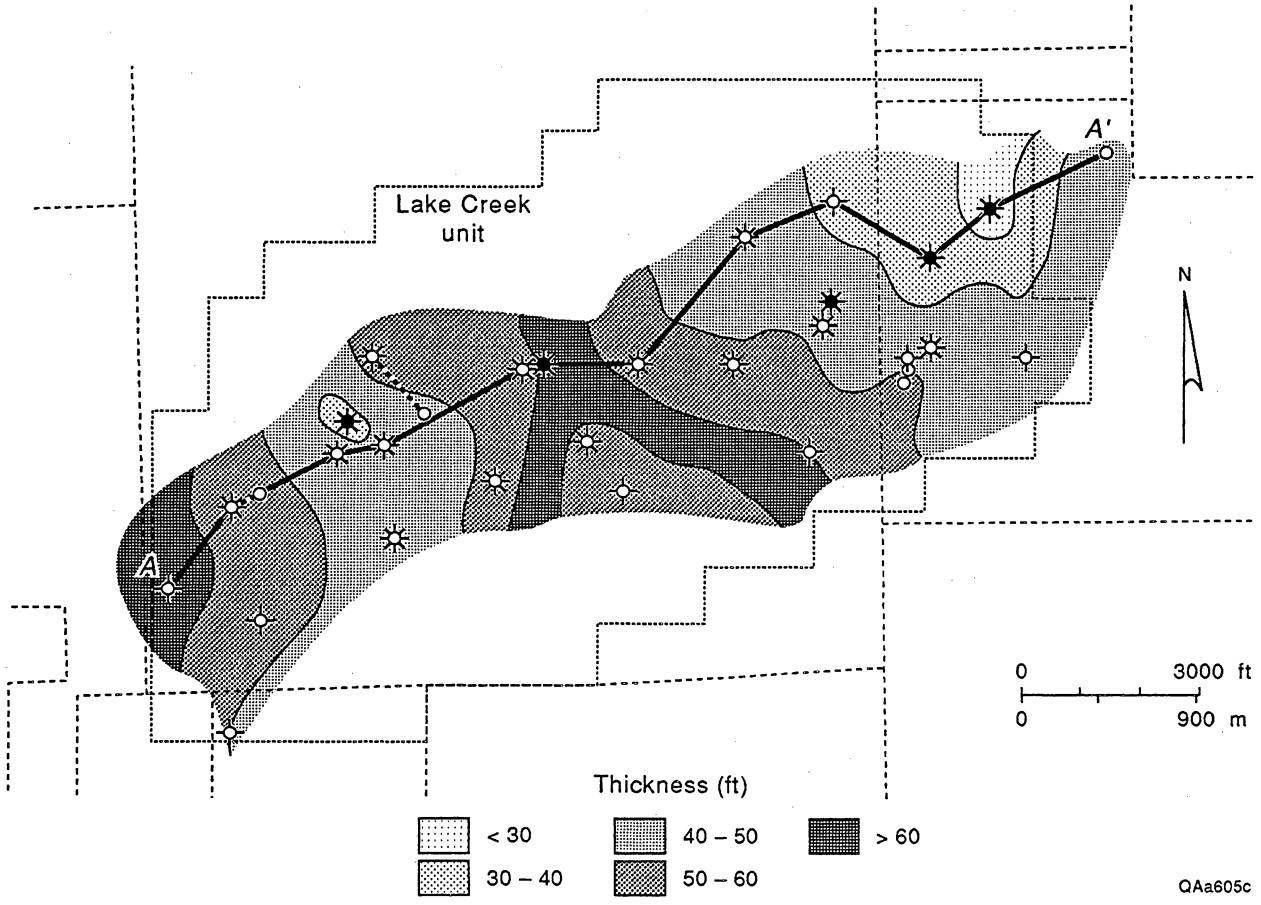

Figure 9. Net-sandstone map of G-2 undivided interval.

the G sandstone, which has operational units G-4, G-2, and G-1 becoming thinner vertically in the section.

Between-well heterogeneity in the G sandstone becomes readily predictable in the context of outcrop-constrained reservoir characterization and is well displayed in the strike cross section A–A′ across the crest of the field (fig. 6). The G sandstone parasequences compose a multistoried reservoir suite separated by shelf-deposited flooding surfaces. The mud-rich flooding surfaces provide the primary barriers to vertical gas flow and provide vertical compartments within the G sandstone. Secondary barriers to vertical flow occur within the parasequence units and are represented by laterally continuous interdistributary-bay-filling, delta-plain, and distal delta-front muds.

Lateral heterogeneity within a parasequence is a response to deep incision of channel-mouth-bar and distal delta-front sandstones by distributary channels. The distal delta-front facies are the most laterally persistent, the mouth-bar facies (proximal delta front) have intermediate continuities, and the distributary-channel deposits are the most areally restricted (fig. 6). Outcrop characterization of analogous deposits in the Ferron Sandstone has demonstrated that mud-clast-rich zones, which compose the fringes of the distributary-channel sandstones, form low-permeability barriers that effectively segment the reservoir (Fisher and others, 1992). Therefore, the mosaic of amalgamated distributary-channel, channel-mouth-bar, and delta-front sandstones provides a highly heterogeneous reservoir interval in the lower Wilcox G sandstones at Lake Creek field.

Permeability Characteristics of the G Sandstone: A Comparison with the Ferron Sandstone

Within the G sandstone, porosity averages 11.0 percent and ranges from 3.5 to 17.5 percent; air permeability averages 0.44 md and ranges from 0.009 to 22.5 md. The best

permeabilities are generally found in the channel-mouth-bar and distributary-channel sandstones of the G-1, G-2, G-3, and G-4 parasequences.

Recent investigations of the permeability characteristics of distributary-channel, channel-mouth-bar, and distal delta-front facies in the Ferron Sandstone (Fisher and others, 1992), located in east-central Utah, have provided an analog for the deltaic deposits of the lower Wilcox G sandstone. Comparison of permeability distribution by facies in the G sandstone shows the mean permeability of the distributary-channel facies (1.32 md) to be almost an order of magnitude higher than that of the delta front (0.17 md) and more than 50 percent greater than the mouth-bar facies (0.64 md) (fig. 10). Although the Ferron sandstones have mean permeabilities in the tens to hundreds of millidarcys (Tyler and others, 1991), permeability distribution trends similar to those measured at Lake Creek field have been found.

To document spatial variability in distributary-channel and channel-mouth-bar facies of the G sandstone, permeability profiles were constructed from log-derived permeability data at 0.5-ft intervals for 14 wells across the field. These permeability profiles, when used in conjunction with the spontaneous-potential and gamma-ray logs, have led to a better characterization of the depositional environments of the lower Wilcox G sandstones.

Distributary-Channel Facies

As discussed previously, the distributary-channel facies are characterized by sand-rich intervals containing massive to crossbedded sandstones that fine upward. Log-derived permeability profiles through these intervals indicate a cyclic pattern of permeabilities having high permeability peaks at the base of fining-upward sequences and a gradual decrease in permeability up the well (fig. 11). Comparison of the G-4 profile of the LCU No. 39 well with a typical profile from the Ferron Sandstone illustrates the similarities. Production in the G-4 reservoir at Lake Creek field is dominated by the large distributary

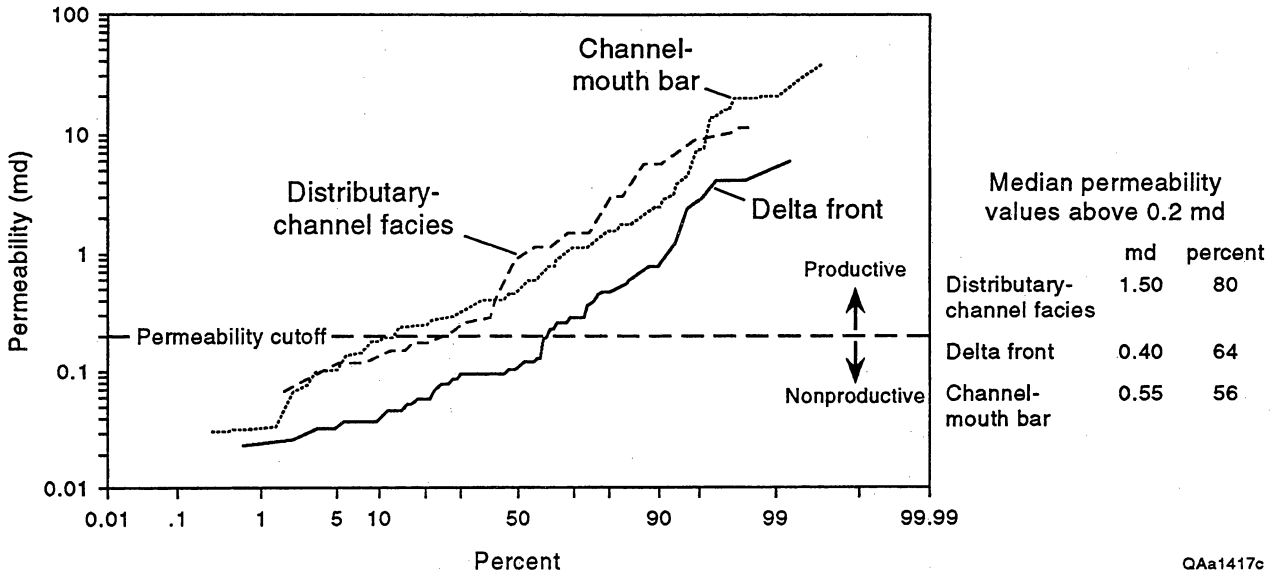

Figure 10. Facies cumulative frequency plot of the G sandstone in Lake Creek field.

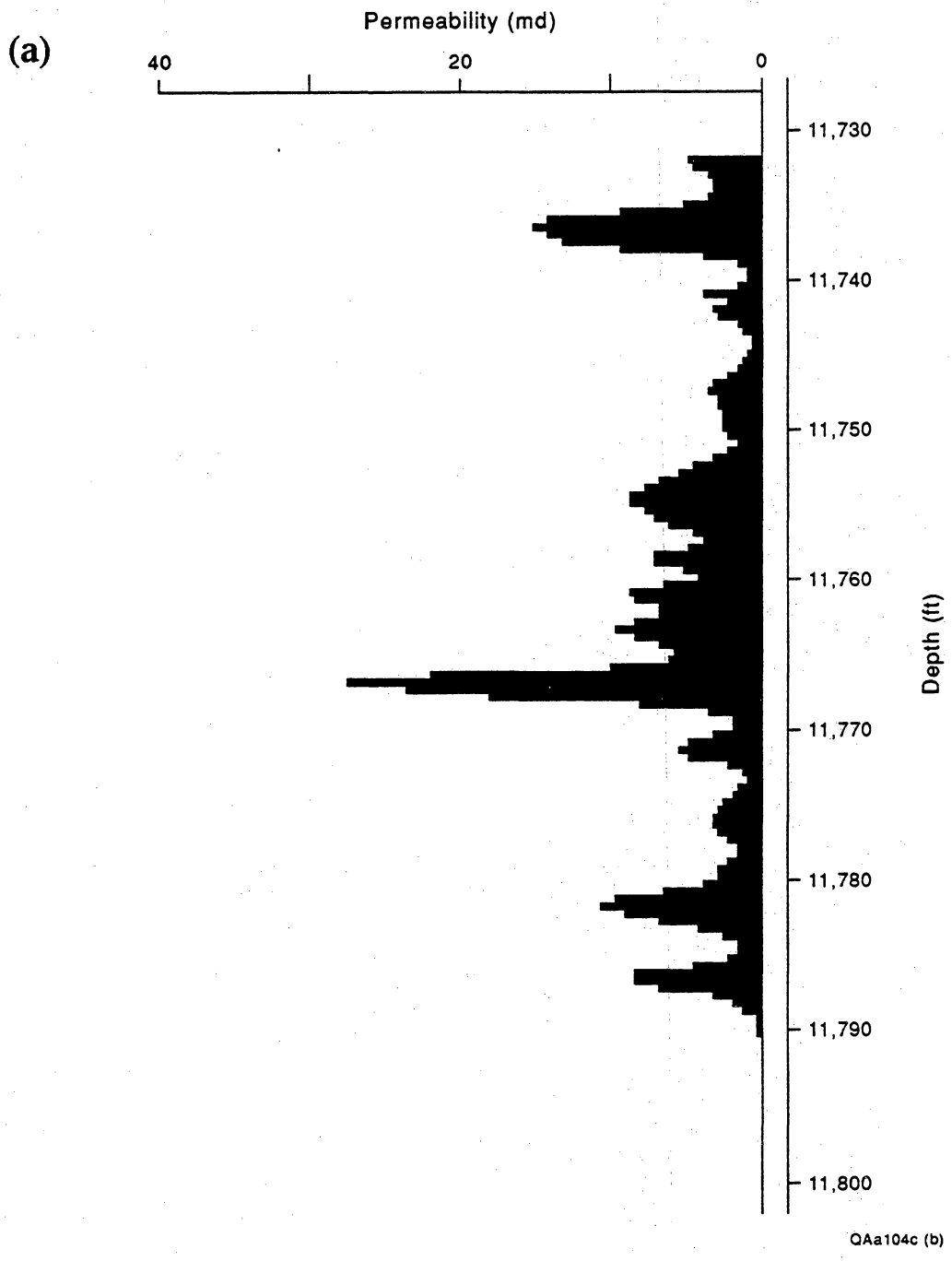

Figure 11. (a) Vertical permeability profile from log data through the distributary-channel facies of the G-4 reservoir in LCU No. 39 well. (b) Vertical permeability profile from minipermeameter data collected from a distributary channel of the Ferron Sandstone (after Fisher and others, 1992).

(b)

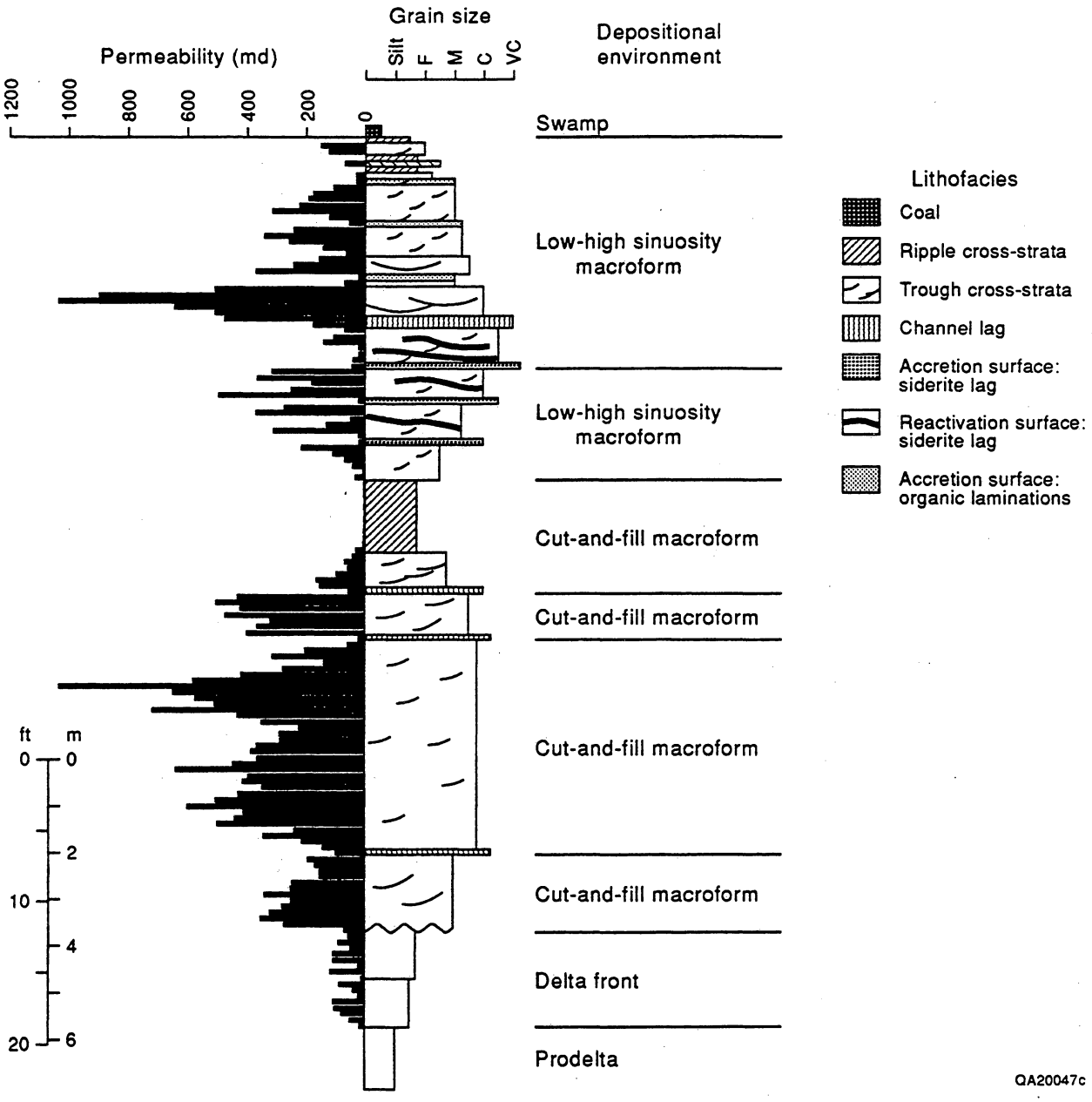

Figure 11. (continued)

channel that cuts through the southwest section of the field (fig. 6). A permeability profile (cross section) constructed through this distributary channel demonstrates the permeability characteristics of channel sandstones in Lake Creek field (fig. 12). These characteristics are similar to those found during the Ferron outcrop study (fig. 13). Similar permeability profiles have also been recognized in smaller channels in both the G-4 and G-2 reservoirs. These smaller channels are often difficult to distinguish from channel-mouth-bar sands using spontaneous-potential and gamma-ray logs and can be easily missed as potentially productive sands. This is demonstrated in the G-2 reservoir in the LCU No. 43 well, which is much more productive than surrounding wells penetrating the channel-mouth-bar facies (see later discussion of LCU No. 43 through No. 45 wells).

Channel-Mouth-Bar Facies

Permeability profiles constructed through wells containing sandstones of the channel-mouth-bar facies reflect the coarsening-upward trend that is representative of these sandstones (fig. 14). In general, there is an overall increase in permeability upward throughout the channel-mouth-bar facies. However, this increase is cyclic, with each cycle occurring between interbedded mudstones. Comparison with outcrop data from the Ferron sandstones shows similar cyclicity (fig. 14). The channel-mouth-bar facies is most prevalent in the G-2 reservoir and has been an important producer in both the LCU No. 44 and No. 45 wells.

Composition of Wilcox G Sandstones

The major authigenic minerals in the lower Wilcox G sandstones are quartz overgrowths and fibrous illite. Although quartz overgrowths have resulted in a permanent reduction in intergranular porosity in G sandstone reservoirs, this study found that fibrous illite, extending into and bridging pore throats, plays a major role in reducing permeability.

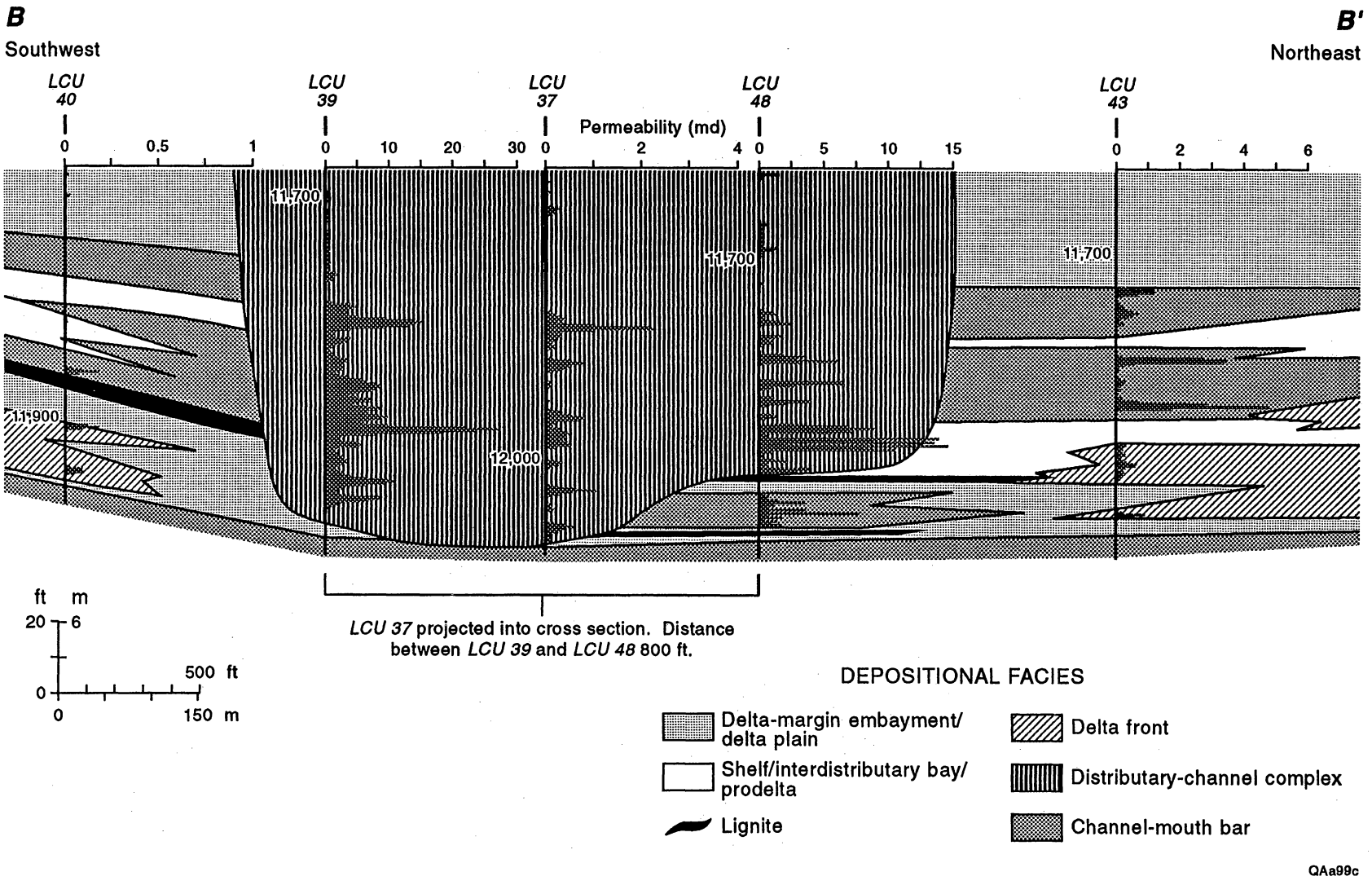

Figure 12. Permeability profiles of a channel of the G-4 reservoir, Lake Creek field.

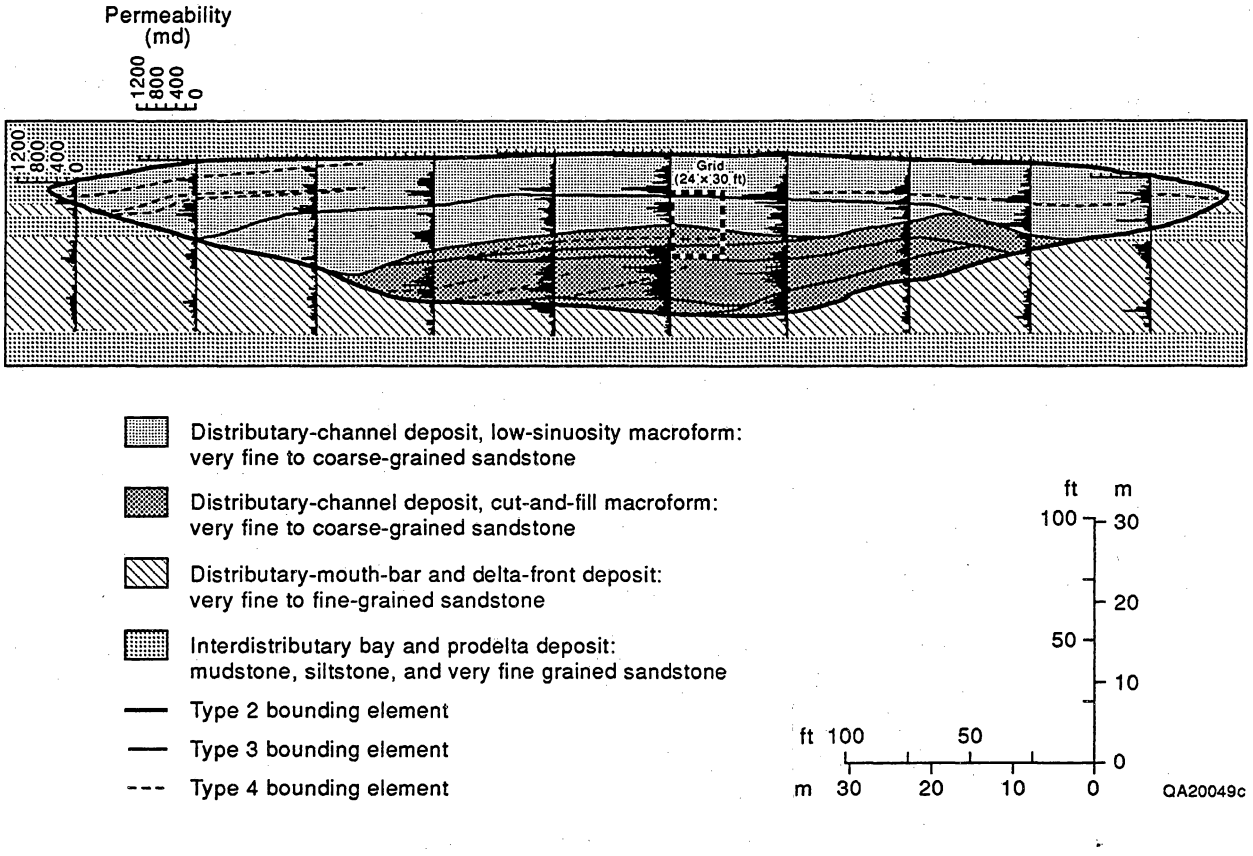

Figure 13. Distributary-channel architecture and permeability profiles, Ferron GS-2 at IH-70 location (after Fisher and others, 1992).

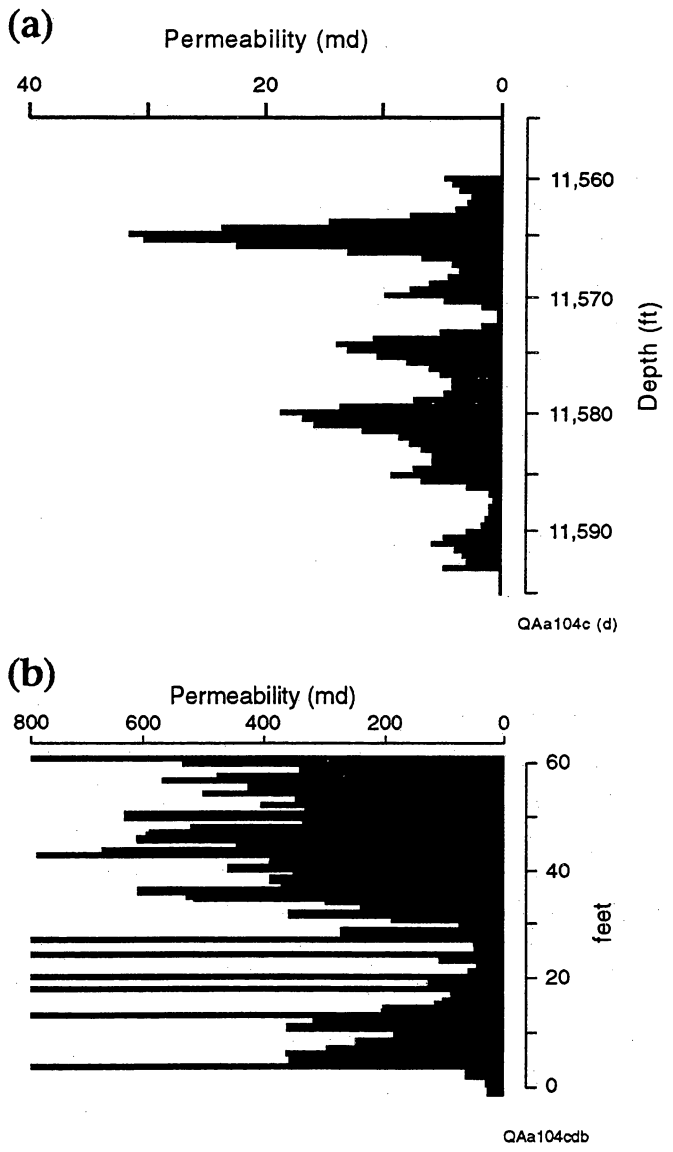

Figure 14. (a) Vertical permeability profile of a channel-mouth-bar deposit of the G-2 reservoir at Lake Creek field (LCU No. 41 well). (b) Vertical permeability profile in the channel-mouth-bar facies of the Ferron Sandstone.

Fibrous illite is rare in upper Wilcox gas and oil sandstones in South Texas (May and Stonecipher, 1990), but its presence in lower Wilcox gas sandstones and its possible effects on reservoir quality and production have been suggested in a previous work (Guven and others, 1980). The acquisition of preserved core from the LCU No. 48 well in Lake Creek field, located approximately 30 mi northwest of Houston in Montgomery County, Texas (fig. 1), has provided the opportunity to determine the effects of drying on fibrous illite morphology and on permeability measurements. The effects of drying are discussed in the following sections, and the effects on permeability measurements will be discussed later in this report.

Methods

Petrographic studies included thin-section point counts (200 points per sample) of 135 thin sections sampled at representative intervals throughout the G sandstone from the LCU No. 48, No. 41, No. 43, and No. 44 wells. In addition, wafers from nine preserved core plugs from the LCU No. 48 well were examined by X-ray diffraction (XRD) and scanning electron microscopy (SEM). To assess the effects of drying on illite morphology, each SEM sample was divided into three parts. One part was air dried at 60°F. A second part was flash frozen in liquid nitrogen and vacuum dried for 48 hr. To limit the possible damage caused by the formation of ice crystals during this process, the entire container was submerged in a methanol and dry-ice bath. A third part of the SEM sample underwent Dean-Stark extraction, methanol leaching, and vacuum oven drying at 240°F, which allowed a comparison of the effects of drying on illite morphology.

Detrital Mineralogy

G sandstones of the lower Wilcox Group are poorly to moderately well sorted, fine-grained, quartz-rich arkoses to lithic arkoses having an average composition of

$Q_{62}F_{26}L_{12}$ (table 1; fig. 15). Lithic fragments consist of subequal amounts of volcanic, plutonic, and metamorphic rock fragments. Sedimentary rock fragments, which are rare, are dominated by chert and siderite rip-up clasts. Pseudomatrix is common. Plagioclase is the dominant feldspar (table 1), although K-feldspar can make up as much as 6.5 percent of the rock volume. Seritization is the most common form of alteration in plagioclase, and both plagioclase and K-feldspar show variable degrees of dissolution. Detrital quartz averages 42.5 percent of the rock volume and ranges from 31.5 to 52.5 percent. Plutonic and metamorphic quartz are the dominant varieties, but volcanic quartz is also present. Depositional matrix, which averages 1.5 percent, is a minor constituent in G reservoir sandstones.

Diagenesis

Quartz, as overgrowths, is the most abundant authigenic mineral in the G sandstone of the lower Wilcox Group, averaging 12 percent of the whole rock volume (table 1; fig. 15). Quartz overgrowths can totally occlude intergranular pore spaces (fig. 16) and effectively reduce primary intergranular porosity, which averages 4 percent of the whole rock volume. Quartz overgrowths are predated by the precipitation of Fe-rich chlorite, which forms a thin coating on detrital grains (fig. 16a), and illite, which occurs as fibrous blades that extend into and bridge primary, and to a lesser extent, secondary, pores (fig. 16b and 16c). Illite is the most common clay and the second most abundant authigenic mineral in the G sandstone (tables 1 and 2). Kaolinite, which has been identified in thin section but not in XRD analyses (tables 1 and 2), is rare, and the time of its precipitation could not be determined.

Carbonate cements (ankerite, ferroan calcite, and siderite) are not common in lower Wilcox G sandstones (table 1). Siderite occurs as euhedral crystals that predate and overlap in time with quartz precipitation. Ferroan calcite postdates quartz overgrowths and occurs as

Table 1. Results of thin-section analyses (n=46).

	Average (%)	Range (%)
Framework grains:		
Quartz	42.5	31.5 - 52.5
Plagioclase	12.0	6.5 -17.5
K-feldspar	3.0	0.5 - 6.5
MRF*	2.0	0.0 - 5.5
PRF*	3.0	0.5 - 6.0
VRF*	4.5	2.0 - 8.5
SRF*	1.5	0.0 - 4.0
Matrix	1.5	0.0 - 8.0
Cements:		
Quartz	12.0	3.0 - 20.5
Illite	3.0	0.5 - 6.0
Chlorite	0.3	0.0 - 2.5
Kaolinite	0.2	0.0 - 3.0
Carbonates†	1.8	0.0 - 21.0
Feldspar	0.4	0.0 - 1.5
Pyrite	0.4	0.0 - 4.5
Porosity		
Primary	4.0	0.0 - 11.5
Secondary	5.0	1.0 - 9.0
Grain size (phi)	3.19	3.93 - 2.49

*MRF=metamorphic rock fragments, PRF=plutonic rock fragments, VRF=volcanic rock fragments, SRF=sedimentary rock fragments (chert, siderite, mud rip-up clasts)

†Carbonates=ankerite, ferroan calcite, and siderite

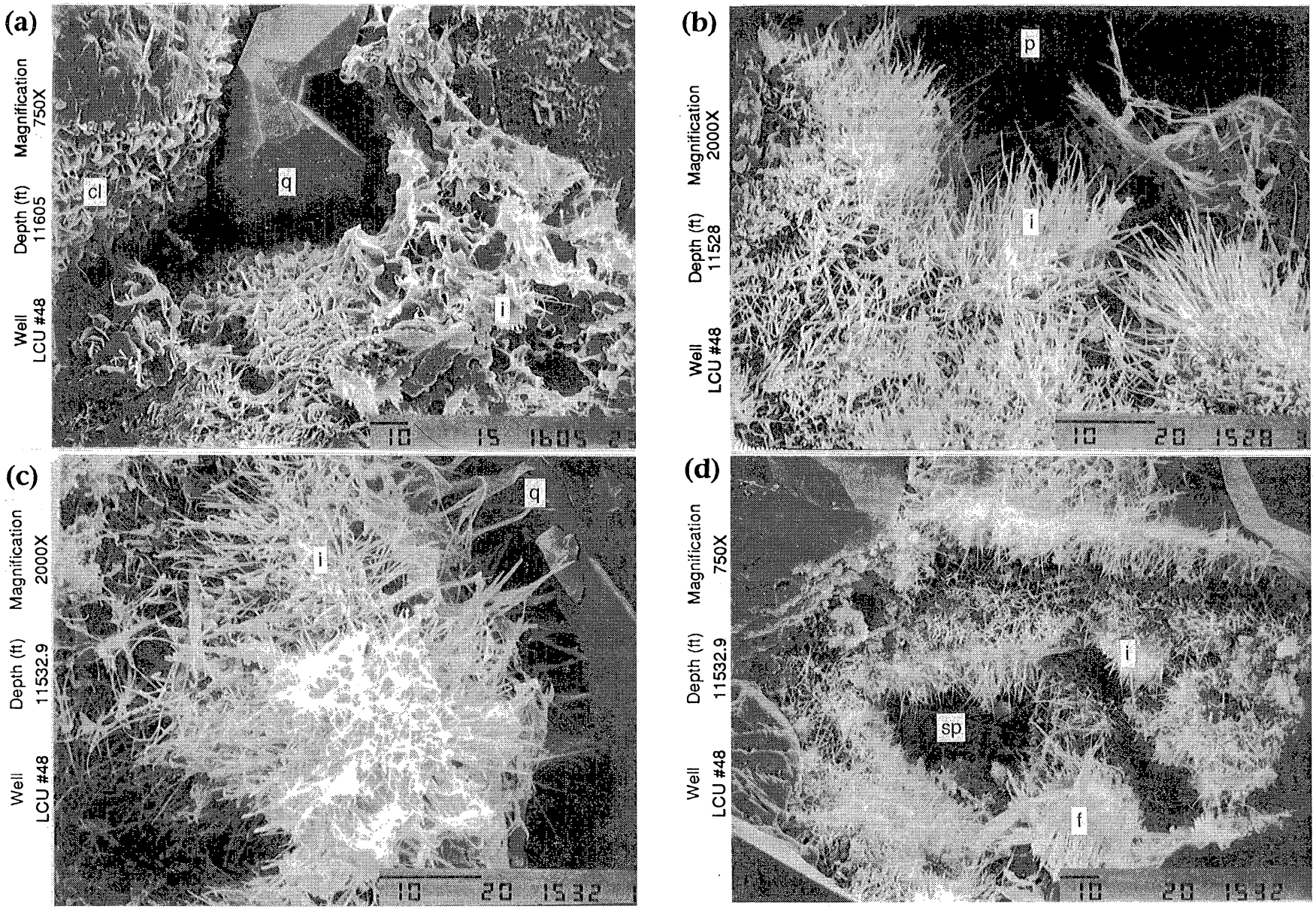

Figure 16. SEM photomicrographs of lower Wilcox G sandstones. (a) Diagenetically early chlorite (cl) forming a grain coat on detrital grains. Quartz overgrowth (q) postdates formation of this clay coat and fills primary pores. Note the presence of collapsed illite fibers (i) closely associated with the chlorite. This sample was air dried at 240°F after undergoing Dean-Stark extraction and methanol leaching. Magnification is 750×. (b–c) Examples of fibrous illite (i) extending into primary pores (p). Note the enclosure of illite fibers by quartz overgrowths (q) in the upper right corner of (c). Magnification is 2,000×. (d) Example of fibrous illite (i) occurring in a secondary pore (sp) formed by the dissolution of detrital feldspar (f). Magnification is 750×. Bar scales equal 10 μm.

Table 2. Clay analysis from X-ray diffraction.

Core depth (ft)	Illite (%)	Chlorite (%)	Total clay (%)
11,523.0	3	Tr	3
11,526.1	5	Tr	5
11,528.1	4	Tr	4
11,532.9	6	1	7
11,592.0	3	1	4
11,596.5	7	2	9
11,599.4	5	1	6
11,605.4	8	2	10
11,607.4	5	2	7

a sparry cement filling intergranular pores and as grain replacements. Following precipitation of ferroan calcite, secondary porosity developed by the leaching of feldspar, unstable rock fragments, and calcite cement. Ankerite postdates secondary porosity and commonly fills secondary pores. Prior to ankerite precipitation, secondary porosity may have been as much as 60 percent of total porosity. Because secondary porosity is predominantly intragranular, much of it is poorly connected. Therefore, primary pores form the main permeability pathways.

Other authigenic minerals that have been recognized in lower Wilcox G sandstones, but are rare, include feldspar (as overgrowths) and pyrite.

Illite Morphology

SEM analyses of freeze-dried and air-dried samples were used to examine the morphology, distribution, and effect of drying on authigenic illite in the G sandstone at the LCU No. 48 well. SEM analyses of freeze-dried samples indicate that most framework grains are coated by fibrous radial illite that is less than 1 μm thick at its base, thins at its tips, and projects 10 to 20 μm into pore throats (fig. 16b and 16c). Fibrous illite is most commonly found projecting into primary pores (fig. 16b and 16c), but it has also been recognized in secondary pores formed by the leaching of detrital feldspar (fig. 16d). Although fibrous illite does not form on quartz overgrowths, it is commonly found enclosed by these overgrowths (fig. 16c).

SEM analyses of air-dried samples indicate that fibrous illite coalesces and collapses against pore walls during the drying process. For example, figure 17a illustrates the partial collapse of illite fibers in a sample air dried at 60°F. Note how the individual illite fibers have coalesced to form a bladed morphology approximately 2 μm thick at the base. These blades thin upward, with remnants of the fibrous character remaining at their tip. In addition,

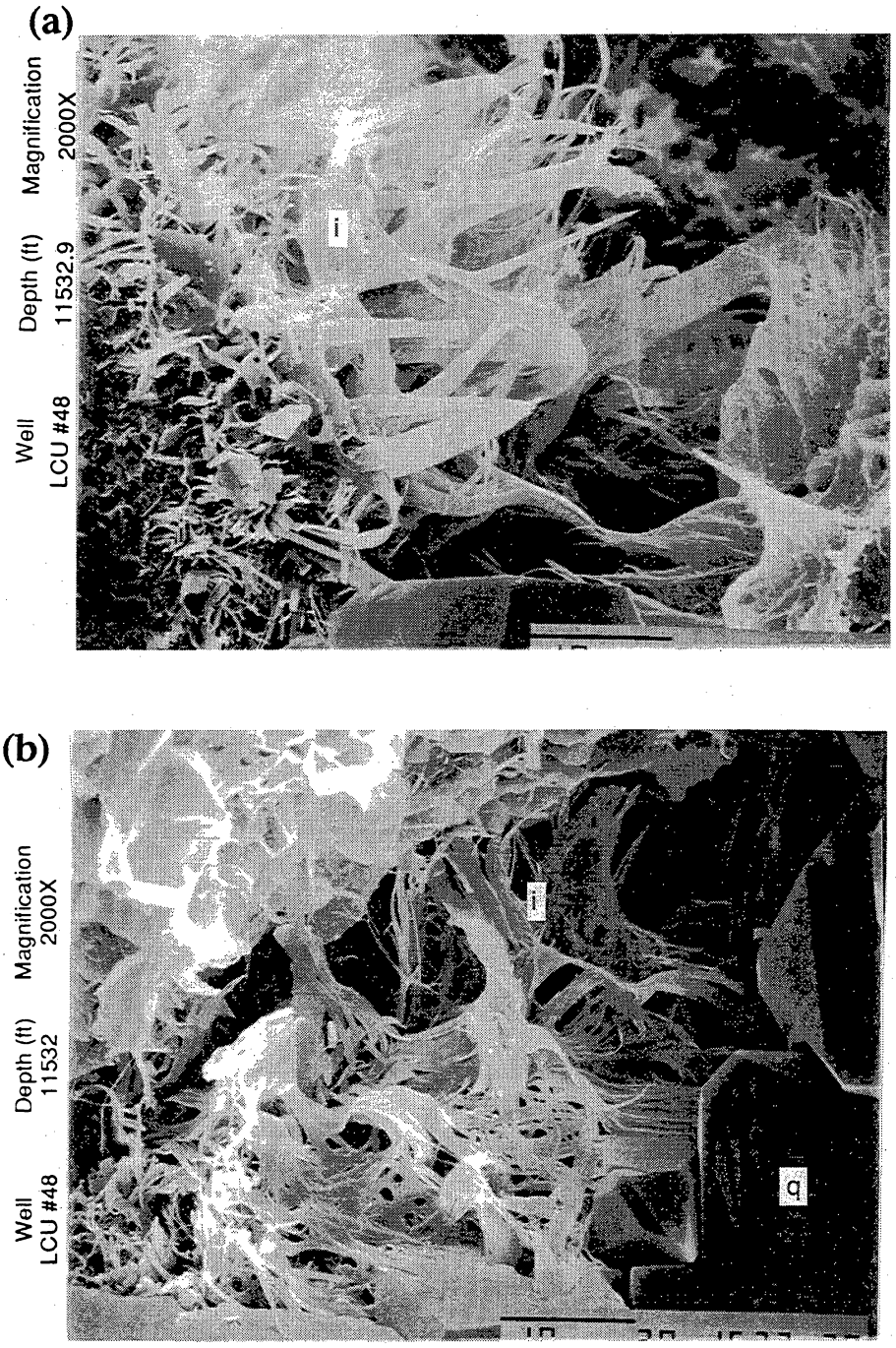

Figure 17. SEM photomicrographs of lower Wilcox G sandstones showing the effects of air drying on illite morphology. (a) Sample air dried at 60°F. Note the coalescence and partial collapse of illite fibers (i). (b) Sample that has undergone Dean-Stark extraction, methanol leaching, and air-drying at 240°F. Note the total collapse of illite (i) against the pore walls (q = quartz overgrowths). Magnification is 2,000×. Bar scales equal 10 μm.

these blades show early evidence of collapse when the tips bend down toward the grain surface.

Core plug samples analyzed in the laboratory for permeability commonly undergo Dean-Stark extraction, methanol leaching, and air drying at 240°F. Figure 17b illustrates the effects of these methods on fibrous illite in lower Wilcox G sandstones. As drying proceeds, the illite, which was originally a fibrous mesh (fig. 17b), coalesces into blades similar to those seen in figure 17a. These blades then collapse and become matted against the pore walls, thus increasing the size of permeability pathways.

PERMEABILITY AND PRODUCTIVITY BY FACIES

Transient well tests and production tests support the calculation of permeabilities that are approximately one order of magnitude lower than permeabilities in distributary-channel and proximal mouth-bar facies and in the more distal mouth-bar and delta-front facies. The same distinction has been found to exist in the Ferron Sandstone outcrop studies.

Production characteristics of 12 wells completed in the lower Wilcox G reservoir at Lake Creek field were evaluated. Pressure-buildup data and/or Texas Railroad Commission open-flow tests (G-1 reports) were used to calculate estimates of effective permeability-thickness (kh) from specific intervals.

Transient Well-Test Permeability of Distributary Channel

The Wilcox G-4 in the LCU No. 37 well consists predominantly of distributary-channel and proximal distributary-mouth-bar facies. Conventional core-plug permeability measurements give an average permeability for these facies of 1.7 md. Transient well-test analysis indicates an effective permeability of about 0.7 md.

A pressure-buildup test was performed on April 25, 1984, after the well was flowed for 70 hr at an average rate of 1,180 Mcf/d. The bottomhole pressure was measured for 147 hr

after shut in. The effective gas permeability was determined by conventional Horner and type-curve analyses to be 0.7 md for 68 ft (ResTech evaluation) of net pay, or a total permeability-thickness of 51 md-ft. The final shut-in pressure was 5,347 psi. The extrapolated pressure in the 900-ft radius of investigation was determined to be 5,360 psi.

Transient Well-Test Permeability of Distal Channel-Mouth Bar

The Wilcox G-4 in the LCU No. 34 well consists predominantly of distal mouth-bar and delta-front facies. Conventional core-plug permeability measurements give an average of about 0.17 md for sandstones of this facies, which is comparable to well-test results.

A pressure-buildup test, performed on January 16, 1985, evaluated the G-4 perforations from 11,660 to 11,682 ft. The well was producing 176 Mcf/d, 7 bcpd, and 5 bwpd with a flowing well-head pressure of 353 psi. The conventional Horner and type-curve analyses of the pressure-buildup data indicate a gas permeability of about 0.03 md for the 42 ft of net pay (ResTech evaluation), which is permeability-thickness of 1.2 md-ft. The extrapolated pressure in the 100-ft radius of investigation was determined to be 4,890 psi. The final pressure was 4,783 psi after 118 hr. A wireline pressure measurement was taken in the G-4 interval at a depth of 11,682 ft on December 24, 1984, and a pressure of 5,078 psi was reported. This is in close agreement with the buildup test results. There has been no production reported for the completion in the G-4 interval, and it is concluded that the interval has been abandoned as noncommercial.

Effective Permeability from Production Tests

Back-pressure tests reported on state completion forms were used to evaluate well productivity and kh (assuming a skin value of zero). There were eight tests from wells completed in the G reservoir that were used for these evaluations. The possible effect of stimulation or damage to the producing interval requires that the kh results presented in

table 3 be interpreted as order-of-magnitude estimates of natural formation kh. A finite-difference radial-flow model was used to history match the reported flow rates and pressures from the completion reports. The log-derived hydrocarbon porosity-thickness was assumed to be constant in the drainage volume. The input permeability was varied until the best match of rates and pressures was achieved. These simulations indicated that the successful Wilcox G reservoir completions have effective permeability-thicknesses (kh) to gas from 1.0 to 21 md-ft and effective permeabilities from 0.06 to 0.66 md. The channel-complex completions demonstrate nearly a threefold superiority of average effective kh over that of the nonchannel facies completions. This demonstrates that identification and completion in channel-complex facies should result in more efficient depletion of the reservoir.

PREDICTING EFFECTIVE GAS PERMEABILITY FROM A WELL-LOG MODEL

Core Analysis

Lake Creek field contains low-permeability shale-sandstone reservoirs. The G sandstones have average air permeabilities of .44 and range from .009 to 22 md. The Secondary Natural Gas Recovery project, in combination with Mobil Exploration and Producing U.S., Inc., obtained 189 ft of 4-inch-diameter conventional core from the lower Wilcox sandstone, which comprises the upper and middle part of the G reservoir in the LCU No. 48 well, a GRI cooperative well (table 4).

Precautions were taken at the well site during both the recovery operation and the laboratory plug cutting to minimize dehydration of the core and plugs by using air-tight plastic bags at the well site and aluminum bags in the laboratory. By taking these precautions, representative values of water saturation could be determined during routine core analysis, and more reliable permeability values could be determined during special core analysis.

Table 3. Effective kh from potential tests.

Reservoir facies	Well no.	Net pay* (ft)	Potential test (md-ft)	Effective permeability (md)
	LCU 32	65	3.8	0.06
	LCU 34	9	1.0	0.11
Channel complex	LCU 36	37	10.4	0.28
Channel complex	LCU 37	21	13.8	0.66
Channel complex	LCU 43	32	12.2	0.38
	LCU 44	37	8.4	0.23
	LCU 45	38	8.7	0.23
	LCU 46	31	4.0	0.13
Channel Complex	LCU 48	47	21.0	0.44
All	(average)	35.2	9.1	0.26
Channel complex	(average)	34.3	14.1	0.44
Nonchannel	(average)	36.0	5.2	0.15

*From log evaluation of perforated interval

Table 4. Petrophysical parameters, LCU No. 48 well.

Shale determination parameters

	Clean	Shale
Gamma ray	46	138
Apparent grain density	2.64	2.92

Water saturation parameters

R_w @ 199°F = .031 ohm-m
R_{wb} @ 199°F = .014 ohm-m
a=1 m=2.10 m–1.94

Shale parameters for porosity determination

	Shale
Density (litho-density tool [LDT])	2.69
Neutron (condensated-neutron log [CNL])	26

Matrix values for porosity

Density (LDT)	2.65
Neutron (CNL)	sandstone

For routine core analysis, 1.5-inch-diameter core plugs were taken every foot. Initial water saturations were determined by weight loss after drying the plugs in a 240°F convection oven. For all core plugs, measurements were made for porosity, permeability to air (k_{air}), and Klinkenberg-corrected permeability (k_∞) using helium at sleeve pressures to simulate a net effective stress of 800 psi and an in situ stress for net overburden (NOB) of .35 psi/ft.

Special core-analysis measurements were also performed to obtain parameters to determine lithology, water saturation, free-water level, and effective permeability. The effects of fibrous illites in permeability measurements were also investigated. Petrographic measurements were made on several samples, including thin-section analysis (200 points per sample) on 46 thin sections and X-ray diffraction and scanning electron microscopy (SEM) on wafers from 9 core plugs. The measurement of electrical properties at NOB stress and 77°F provided values for the cementation and saturation exponents (m and n) that were used in the saturation equation. A saturant of 100,000 ppm of sodium chloride was used to simulate formation water salinity. The composite cementation factor (m) is equal to 2.10 when "a" is constrained to 1, and the composite saturation exponent (n) is equal to 1.94. Core resistivity measurements were performed using a two-terminal method.

Capillary-pressure measurements were made to test the applicability of the advanced capillary-pressure curve model (ADCAP) under development at ResTech and to establish the irreducible water saturation. This model estimated the free-water level and the permeability of the G reservoir. The tests were conducted using centrifuge air/brine measurements on representative selected preserved plugs.

To determine the effects of core-measurement conditions on permeability-derived values, a comparison was made between the permeabilities obtained from preserved core samples and those obtained from the same samples after they were oven dried at 240°F. The comparison showed that conventional core-analysis procedures yield permeabilities from two to seven times greater than permeabilities from preserved core samples. Additionally,

using SEM analysis, the comparison further demonstrated that this anomaly was due to the presence of fibrous illites that line the pore network and reduce permeability in the lower Wilcox G sandstones in Lake Creek field. Detailed petrographic studies indicate that fibrous illite coalesces and collapses upon conventional core-plug extraction and oven drying, which results in high apparent dry-core-measured permeabilities.

Capillary-Pressure Modeling for Lake Creek

Model Derivation

The ADCAP model, under development at ResTech, Inc., was employed by the SGR project in the lower Wilcox sandstones in Lake Creek field to predict the free-water level and effective permeabilities. The generalized method is explained in appendix 1 of this report. Briefly, it consists of relating three empirical equations resulting from studies on capillary pressures by Thomeer (1960), Swanson (1981), and Pittman (1992). This model relates the four important reservoir properties of porosity, water saturation, permeability, and capillary pressure with a single equation. Therefore, any one of these properties can be found by knowing the other three.

In the LCU No. 48 well, regression analysis on core data from the G-2 sandstone was used to adjust these equations to obtain a local model. The equations for this model are

$$\log P_c = -F_g / \ln (1 - S_w) + \log P_d \qquad (1)$$

$$F_g = \left[\ln \left(2.54 \frac{k_{air} \cdot .009}{\emptyset} \right) \right]^2 / 2.303 \qquad (2)$$

and

$$P_d = 120 / k_{air}^{.72} \emptyset \qquad (3)$$

where

P_c = capillary pressure,

F_g = the pore geometrical factor, which reflects the pore-throat-size distribution,

P_d = extrapolated displacement pressure,

S_w = water saturation, and

$\emptyset$ = porosity.

The conversion of capillary pressure to height is given by

$$h = 0.217\ P_c \qquad (4)$$

The ADCAP model was applied to core and log data in the G-2 reservoir in the LCU No. 48 well. Both gas and water saturations in the G-2 reservoir were considered to be at gravity and capillary equilibrium prior to field discovery and gas production. Under the condition of gravity and capillary equilibrium, the gas and water saturations in the rock vary systematically in the reservoir. After capillary-pressure properties at each vertical position of the reservoir facies have been determined by the model, these saturations can be used to deduce the actual capillary pressure at each vertical position. Because capillary pressure (gas pressure minus water pressure) varies linearly with vertical position (for constant fluid densities), the depth at which the capillary pressure is zero (the free-water level) can be determined. However, the reservoir facies present in the LCU No. 48 well at the G-2 interval may not exist at the depth of the free-water level. That is, only a shale equivalent may be present. The principle of the calculation is still valid, however, and if a sand facies were present, it would be at 100 percent water saturation.

In previous reservoir studies it has been difficult to link capillary-pressure properties measured on a few discrete core samples in the laboratory with log-calculated porosity and water saturation to deduce actual capillary-pressure values in the reservoir. This is largely because of the wide fluctuation of both rock properties and saturations, such as those found in the Lake Creek field. The ADCAP model provides a practical method of linking these measurements.

Permeability within the G-2 parasequence is expected to vary from approximately 0.01 to 20 md, depending on the facies. Because of the extent of variation, thick or areally

extensive low-permeability units such as delta-front facies are expected to create barriers to gas flow. These barriers can effectively block gas flow during the 20- to 30-year period of reservoir gas production. However, during the long period of initial gas migration and accumulation in the reservoir, these low-permeability units will not act as barriers to gas flow. Therefore, during accumulation, gas and water should have been able to move through these low-permeability units in Lake Creek field, and a capillary-pressure equilibrium was almost certainly established.

There is a limit to how low the permeability can be in a poor grain-size facies and still act as a conduit for gas and water movement during gas accumulation. The shelf and prodelta mud-rich facies that compose the lower part of each parasequence probably constituted a vertical barrier to gas movement during accumulation. Therefore, the G-2 and G-4 intervals probably do not share a common free-water level. However, for the purpose of estimating gas in place, separate free-water levels were assumed to occur in the G-2 and G-4 reservoirs.

Example of Estimation of a Free-Water Level

A free-water level of 11,473 ft below sea level is estimated for the G-2 sandstone using regression analysis as described in appendix 1. Figure 18 shows how the capillary-pressure-curve model can be used to estimate the free-water level. An important result of the regression analysis is quantification of the uncertainty around the estimated free-water level. In this example the uncertainty is ±29 ft. Relating this estimated free-water level to the structure map indicates that productive limits are not controlled by structural closure. A structure map on top of the G-2 (fig. 3) sandstone shows a saddle to the northwest of the developed part of the field. This saddle is approximately 70 ft below the crest of the G-2 sandstone at approximately 11,387 ft below sea level, 86 ft above the estimated free-water level.

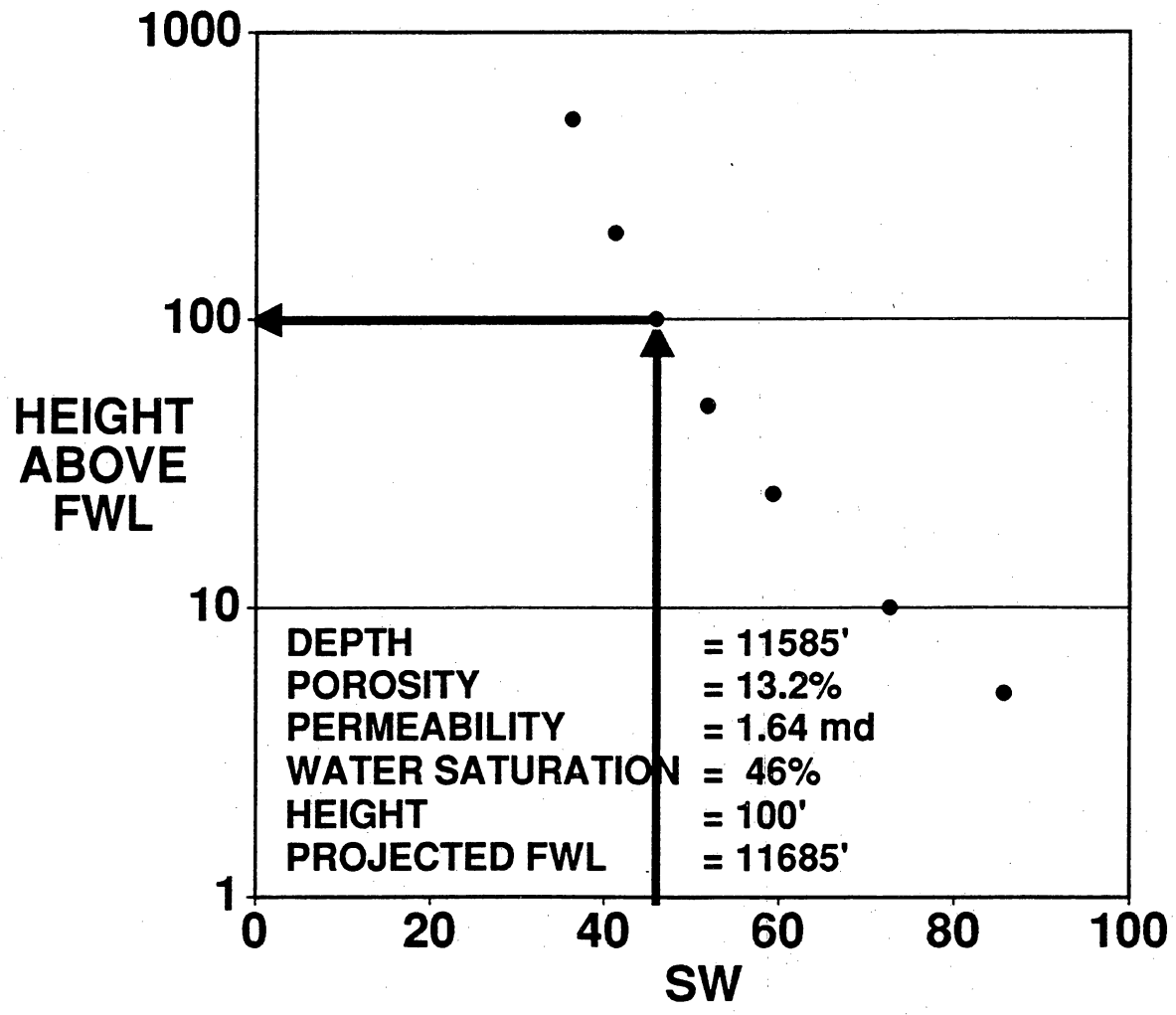

Figure 18. Example of free-water level (FWL) projection with the capillary-pressure model for G-2 sandstone in the LCU No. 48 well.

Although the estimated water level cannot be confirmed with available data in the field, the following results support the validity of the estimation. Among nearby wells, the LCU No. 44 and No. 24 tested dry gas at 11,395 and 11,401 ft below sea level, respectively. In another well, the LCU No. 40, the lowest known gas determined by log analysis of modern logs is found at 11,429 ft below sea level. In the LCU No. 12 well, an old electric log shows high apparent resistivity as low as 11,463 ft below sea level, but the interpretation here is uncertain because of the lack of porosity logs. Note that all of these measurements confirm the presence of producible gas below the saddle that is shown on the structure map mentioned previously. This indicates that stratigraphy plays a role in controlling productive limits.

About 2 mi from these wells, across the field to the east, the Superior MM1 well presents an anomaly. At the top of the G-2 sandstone, an apparent highest known water level of 11,383 ft below sea level is indicated from log-calculated water saturations of about 66 percent. Because this apparent water level is 12 to 18 ft above the lowest known gas produced in the LCU No. 24 and No. 40 wells, an explanation is necessary. If the apparent water level is valid, it seems reasonable to assume that a barrier exists between the MM1 and other wells to the west. Another possibility is that the high water saturations do not represent a true water level but are caused by the presence of very low permeability in the sand. In either case, the G-2 sandstone in the MM1 would not be considered productive.

Productive Limits

Productive limits for the G-2 sandstone are shown in table 5 for each of the principal rock types, which were calculated as follows. Assuming a productive limit of 100 barrels of water per million cubic feet of gas (bbl water/MMcf gas) leads to a k_g/k_w ratio of .6. Visual inspection of relative permeability curves shows that this ratio occurs at approximately 82 percent water saturation. Height above the free-water level was calculated for each rock

Table 5. Productive limits of G-2 sandstones at Lake Creek field.

Rock type	Average air permeability (md)	Productive limit (ft)
Channel	1.32	–11,463
Channel mouth bar	.64	–11,453
Delta front	.17	–11,429

Uncertainty ± 29 ft

type from the regressed capillary-pressure curves. These values were then added to the free-water level (11,473 ft below sea level) to obtain structural levels below which each rock type would produce more than 100 bbl water/MMcf gas.

Permeability Modeling

Estimation of Air Permeability

The capillary-pressure-curve equations described earlier were used to determine a log-derived permeability. Once the water contact is known, equations 1 through 4 can be rewritten into a single equation:

$$\ln k_{air} = 13 \left[\ln \frac{120}{\varnothing} - \ln P_c - \frac{\left(\ln \frac{2.54}{\varnothing}\right)^2}{\ln(1-S_w)} \right] \quad (5)$$

where

k_{air} = air permeability,

$\varnothing$ = porosity,

S_w = water saturation, and

P_c = capillary pressure.

This method shows a correlation between model and measured permeability that is superior to that obtained using porosity alone.

Illite Effects on Permeability

Permeability measurements from conventional core analysis were made at normal overburden pressures on oven-dried core samples (240°F). To relate these results to the effective permeability, the effects of fibrous illites on permeability must be taken into account. Petrographic studies reveal that the core cleaning and drying process during conventional core analysis alter illite morphology. The collapse of fibrous illites against the

pore walls causes an increase in the size of the permeability pathways, which results in measured air permeabilities that are higher than brine permeabilities from preserved core measurements. This increase in permeability is similar to that previously reported for the Frontier and Travis Peak Formations (Luffel and others, 1990, 1991a, b) in GRI Tight Gas Sands research. Table 6 shows the comparison of brine permeability from preserved core (k_w) and air permeability from dry core (k_{air}) at net overburden stresses (NOB) for six samples from the lower Wilcox G sandstones. The brine permeability measured from preserved core is two to seven times less than permeabilities obtained from conventional core analyses. If these laboratory data alone were used to estimate well productivity, a comparison with actual well-test productivity would lead to the conclusion that the well was damaged even when no damage was present. The relationship of k_w to k_{air} when both are measured at NOB pressure is shown in figure 19. A best-fit major axis (RMA) line for the six points is expressed as:

$$k_w = 0.21252\, k_{air}^{1.12053} \qquad (6)$$

where

k_w = preserved core brine permeability and

k_{air} = oven-dried (240°F) air permeability.

This relationship is used to estimate permeability to brine from the conventional dry core air permeabilities for Wilcox sandstones containing fibrous illites.

Relative Permeability

To proceed from brine permeability (k_w) of the preserved cores to effective permeability to gas (k_g) of the reservoir at connate water saturation, it is necessary to establish the relative-permeability properties. In the LCU No. 48 well, six relative permeabilities were obtained using preserved cores at NOB stresses. On the basis of these relative permeabilities

Table 6. Comparison of brine permeability (k_w) from preserved cores with dry core air permeability (k_{air}) at NOB from lower Wilcox G sandstones.

Sample depth (ft)	Porosity (%)	Air permeability (md)	Klinkenberg permeability (md)	Brine permeability (md)
11,526.1	10.7	0.255	0.146	0.072
11,528.1	16.0	19.8	18.1	7.8
11,532.9	13.2	1.94	1.51	0.56
11,592.0	13.9	2.55	1.99	0.29
11,596.5	10.8	0.050	0.023	0.008
11,605.4	11.8	0.485	0.311	0.072

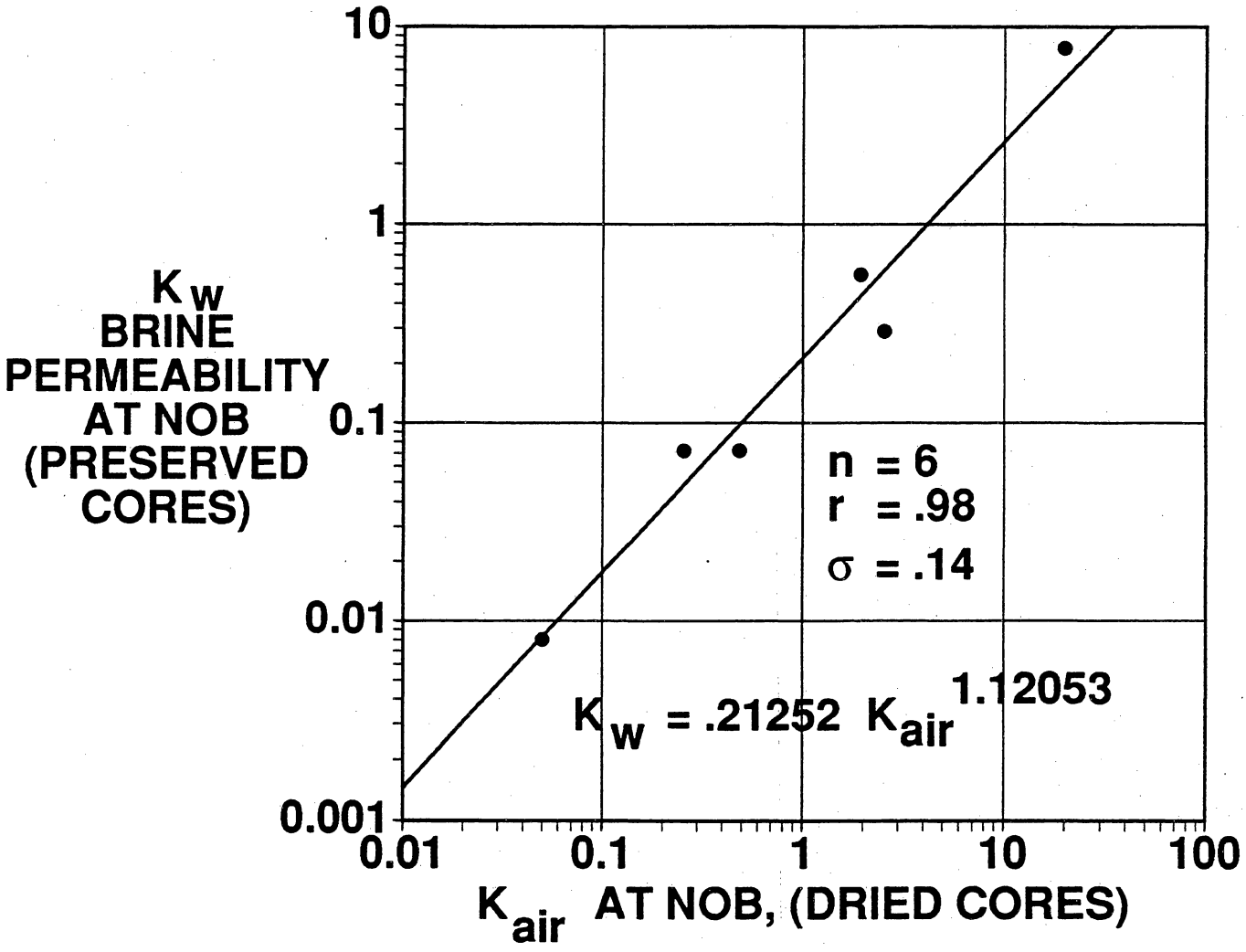

Figure 19. Plot of brine permeability (k_w) measured from preserved cores versus air permeability (k_{air}) measured from oven-dried cores, both at NOB.

for the lower Wilcox sandstones, a log-derived model was obtained using the Brooks-Corey approach (Brooks and Corey, 1984). These equations are the following:

$$k_{rg} = [(.97-S_w)/(1-S_{wi})]^{1.82} \quad (7)$$

$$S_{wi} = 4.5/\emptyset \quad (8)$$

where S_{wi} = irreducible water saturation. Knowing the relative permeability to gas and the brine permeability, the effective permeability to gas (k_g) for any gas saturation can be calculated using the following equation:

$$k_g = k_{rg} * k_w \quad (9)$$

where k_w is obtained from equation 6.

Comparison of Results

Log-Derived and Core-Derived Results

As an example of the match of log-derived results to core-derived results, the LCU No. 48 well is presented in the cored zone in figure 20. It should be noted that high-resolution (increased sample rate) neutron and density logs were run on the LCU No. 48 well. These types of logs have shown to be useful in identifying thinly bedded sandstones in previous Secondary Natural Gas Recovery research (Langford and others, 1992). This is important when defining the better permeability zones in the G reservoir known to be laminated by core or formation microscanner results. The petrophysical methods used to evaluate the Lake Creek wells were similar to those used in other clastic reservoirs.

To obtain a shale volume, the gamma-ray, neutron, and density logs were calibrated against the results of petrographic thin-section analysis. Porosity was derived from the density-neutron combination, with the appropriate matrix value based on core-analysis results and corrected for shale and gas effects. Water saturation was determined using the measured cementation factor (m) equal to 2.10 and the saturation exponent (n) being equal to 1.94. The formation water resistivity (R_w = 0.031 at 199°F) was determined from

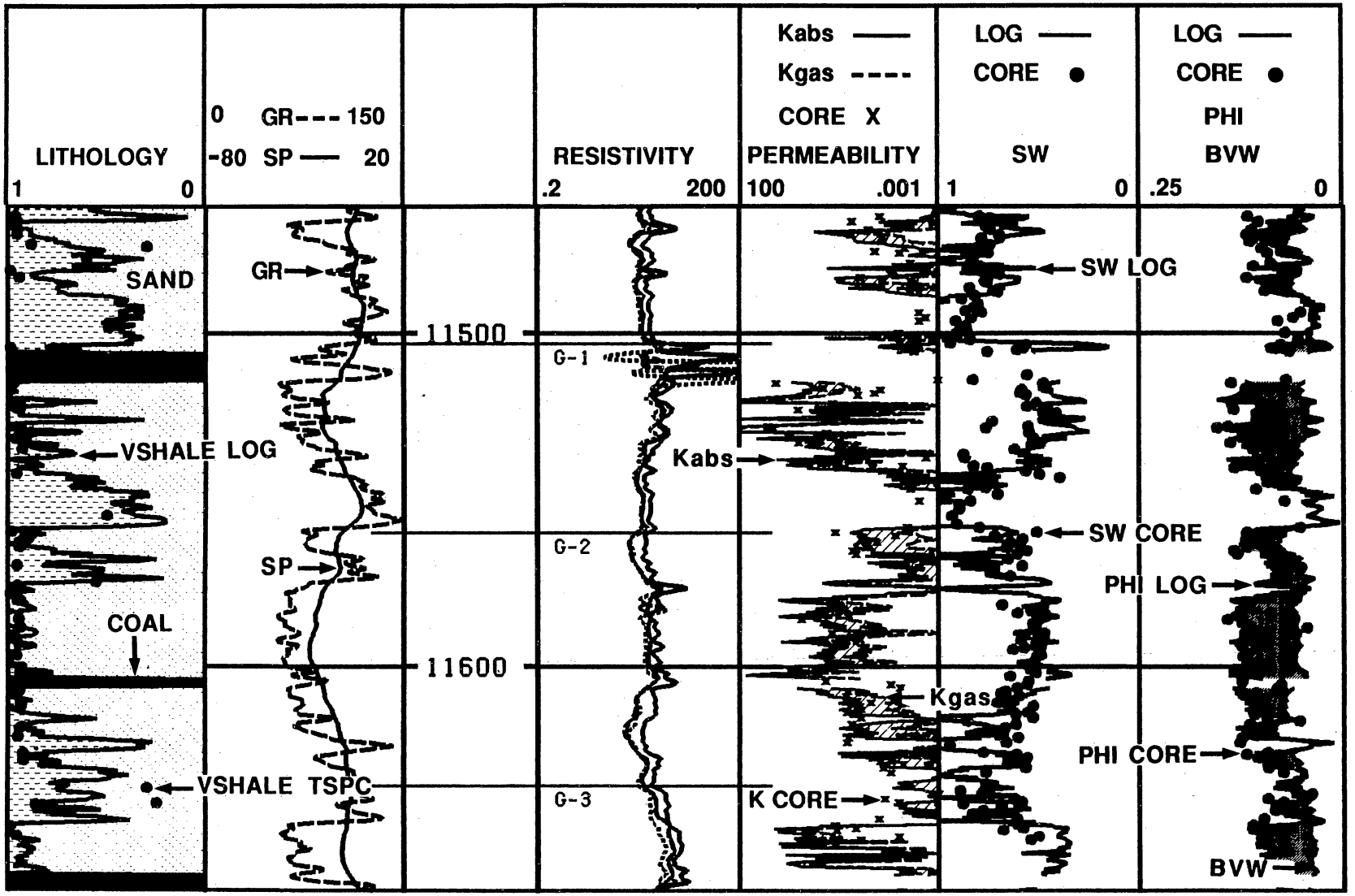

Figure 20. Results of log and core analysis for the cored interval of lower Wilcox G sandstone in the LCU No. 48 well.

representative formation water samples obtained from nearby wells producing from the lower Wilcox G sandstone in Lake Creek. The dual water saturation equation (Clavier and others, 1977) was used to account for the bound water in the shales. Overall, the results of the log-analysis model are in good agreement with the core-analysis results (at NOB) from the LCU No. 48 well. Establishment of the match is important to correctly estimate reservoir values in sandstones where core data are not available.

Log kh Compared with Well-Test kh

The petrophysical model that predicts reservoir parameters, permeabilities, and permeability-feet of potential producing zones in lower Wilcox G sandstones was in good agreement with well-test analysis in Lake Creek field. Because this model is calibrated with preserved core and relative permeabilities, the effects of fibrous illites on permeability measurements are taken into account. Table 7 shows the results of a five-well study performed in this field.

The LCU No. 48 well was tested in the G-4 reservoir and perforated from 11,690 to 11,766 ft (fig. 21). This procedure was followed by a frac treatment, sand propping, and cleaning of the well. The flow rate was shown to be 2.1 MMcf/d gas. From the flow data, an apparent postfracture permeability-feet of 21 md-ft was calculated using Darcy's radial flow model. No pressure-buildup test was available. Because the completion interval was stimulated, the true matrix permeability is expected to be less by a factor of 2 to 3.

Effective gas reservoir permeability determined using the well-log interpretation model for Lake Creek estimates the true matrix permeability/thickness (kh) as 18 md-ft. This is higher than the estimated matrix kh because the matrix kh could be 7 to 10 md-ft. However, because of the uncertainty factors involved in core- and log-derived permeabilities, this is considered to be an acceptable fit.

Table 7. Summary of results for five-well petrophysical study at Lake Creek field.

	LCU 48	LCU 44	LCU 43	LCU 37	LCU 34
Sand	G-4	G-2	G-2	G-4	G-4
Net pay (ft)	51.5	42.0	17.5	68.5	42.0
Porosity (percent), average	11.6	11.5	11.1	11.3	11.4
S_w (%), average	47.8	49.8	52.5	50.7	56.8
kh model (md-ft)	18.3	13.3	2.5	9.2	1.6
kh production test	21	8.4	12.2	51	1.3
Perforations (ft)	11,690 to 11,766	11,541 to 11,574	11,570 to 11,596	11,920 to 11,971	11,660 to 11,682
CAOF potential (Mcf/d)	2,355	1,700	2,089	2,110	180

(Cutoff parameters used: S_w <70 percent and porosity >10 percent)

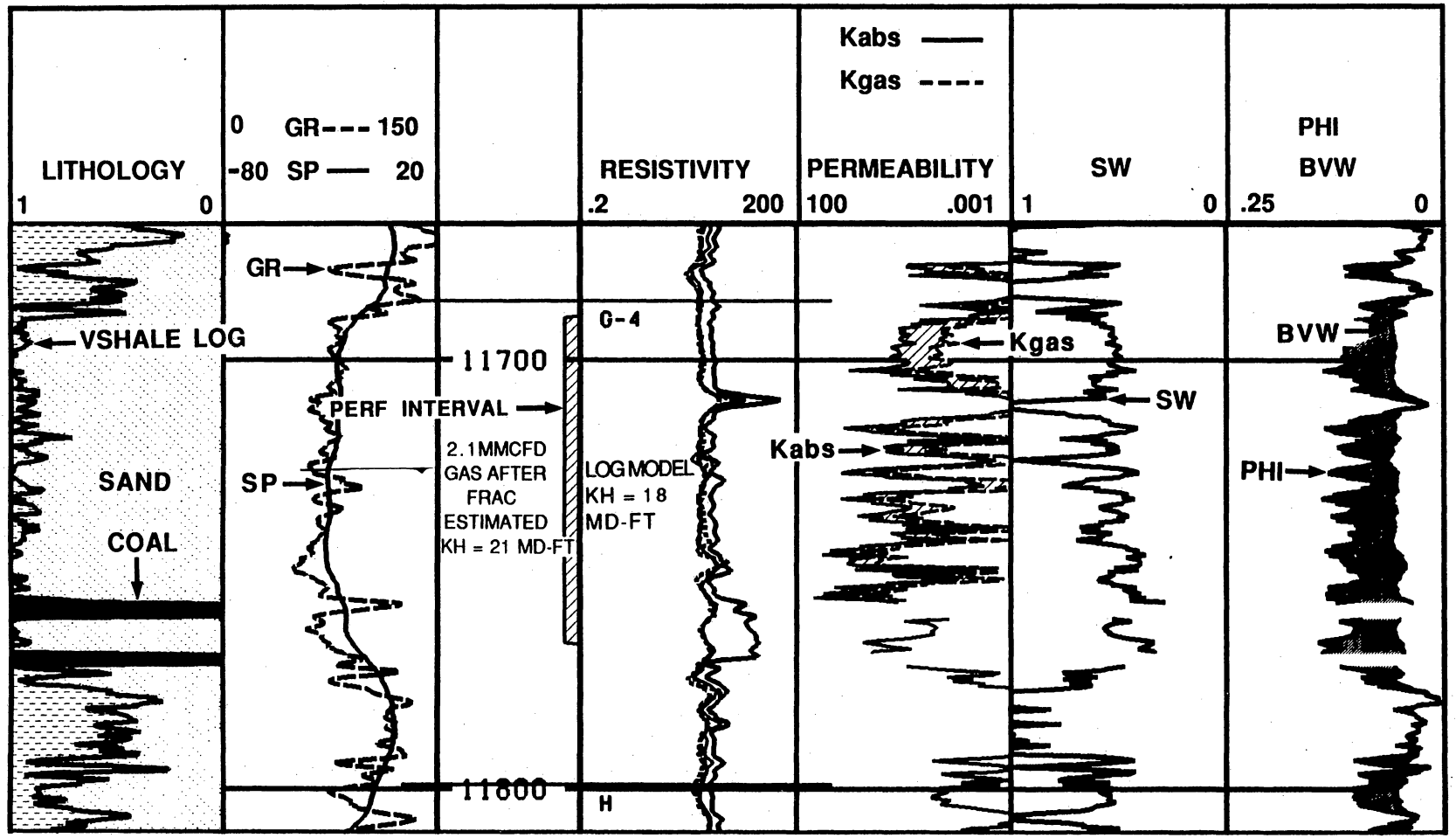

Figure 21. Comparison of permeability-thickness (kh), well-test versus log-derived values for perforated interval of lower Wilcox G sandstone in the LCU No. 48 well.

The LCU No. 44 well was tested in the G-2 reservoir and perforated from 11,541 to 11,574 ft. The initial potential test was 1,196 Mcf/d at a well-head flowing pressure of 1,327 psi. The completed interval was fracture stimulated. From a back-pressure test performed on March 29, 1989, the formation permeability thickness was estimated to be 8.4 md-ft. The log evaluation estimates a kh of 13.3 md-ft for the G-2 sandstone, with a net pay of 42 ft, average porosity of 11.5 percent, and average water saturation of 49.8 percent.

The LCU No. 43 well was also tested in the G-2 sandstone in the interval 11,570 to 11,596 ft. The initial potential test was 1,265 Mcf at 2,290 psi of well-head flowing pressure. No stimulation was reported. From a single back-pressure test, permeability-thickness was estimated to be 12.2 md-ft. The log-evaluation model estimates a kh of 2.5 md-ft for the G-2 sandstone, with a net pay of 17.5 ft, average porosity equal to 11 percent, and average water saturation of 52 percent.

The LCU No. 37 well was tested in the G-4 sandstone from 11,920 to 11,971 ft. The initial potential test was 1,180 Mcf/d with a flowing well-head pressure of 1,964 psi. From a pressure-buildup test, believed to have been performed prior to fracture treatment of the G-4 zone, a permeability-thickness of 51 md-ft is estimated. A history match of the initial completion back-pressure test indicates a kh of about 11 md-ft. The log-evaluation model estimates a kh of 9.2 md-ft, a net pay of 68 ft, an average porosity of 11 percent, and an average saturation of 50 percent.

The LCU No. 34 well was tested also in the G-4 sandstone from 11,660 to 11,682 ft. There was no flow information available with the pressure data. From a pressure-buildup test, a kh of 1.3 md-ft was estimated. The log evaluation confirms this low kh with a value of 1.6 md-ft. A net pay of 42 ft is determined with an average porosity of 11 percent and average water saturation of 57 percent. No production has been reported on this interval.

Applications to Other Fields

The technology developed above could be used in fields in the immediate vicinity of Lake Creek to calculate effective permeabilities to gas. The minimum required data for this would be well logs, although core data would be useful. If the free-water level is unknown, it could be estimated using the capillary-pressure model. The equations described above could then be used with well-log analysis to estimate the effective permeability to gas.

If cores are available, capillary-pressure measurements and relative-permeability measurements should be conducted at net overburden stress. The capillary-pressure measurements would be used to derive the constants for the capillary-pressure-curve model (eq. 2 and eq. 3). The relative-permeability measurements can be used to derive constants for calculating relative permeability with the Brooks-Corey approach (Brooks and Corey, 1964) (eq. 7 and eq. 8). In the absence of core data, equations 2, 3, 7, and 8 can be used in fields adjacent to Lake Creek.

If the free-water level is unknown, it can be determined through regression analysis. If conventional core data are available, values for porosity, permeability, and water saturation at each coring point can be entered into the model (eq. 1 through eq. 3). Regression analysis of this system can then be used to predict the free-water level. If core data are not available, log analysis results can be used in the regression. Along with log values for porosity and water saturation, permeability can be derived from a relationship such as the one presented in figure 22 for the Lake Creek No. 48 well from conventional core analysis.

With the knowledge of the free-water level, equation 4 can be used to calculate capillary pressure, which can be entered into equation 5 to calculate air permeability. Equation 6 gives the conversion to stressed brine permeability and equations 7 and 8 give the relative permeability to gas. Equation 9 is used to calculate the effective permeability to gas, which is then summed over the sandstone in question to arrive at a total kh value for the sandstone.

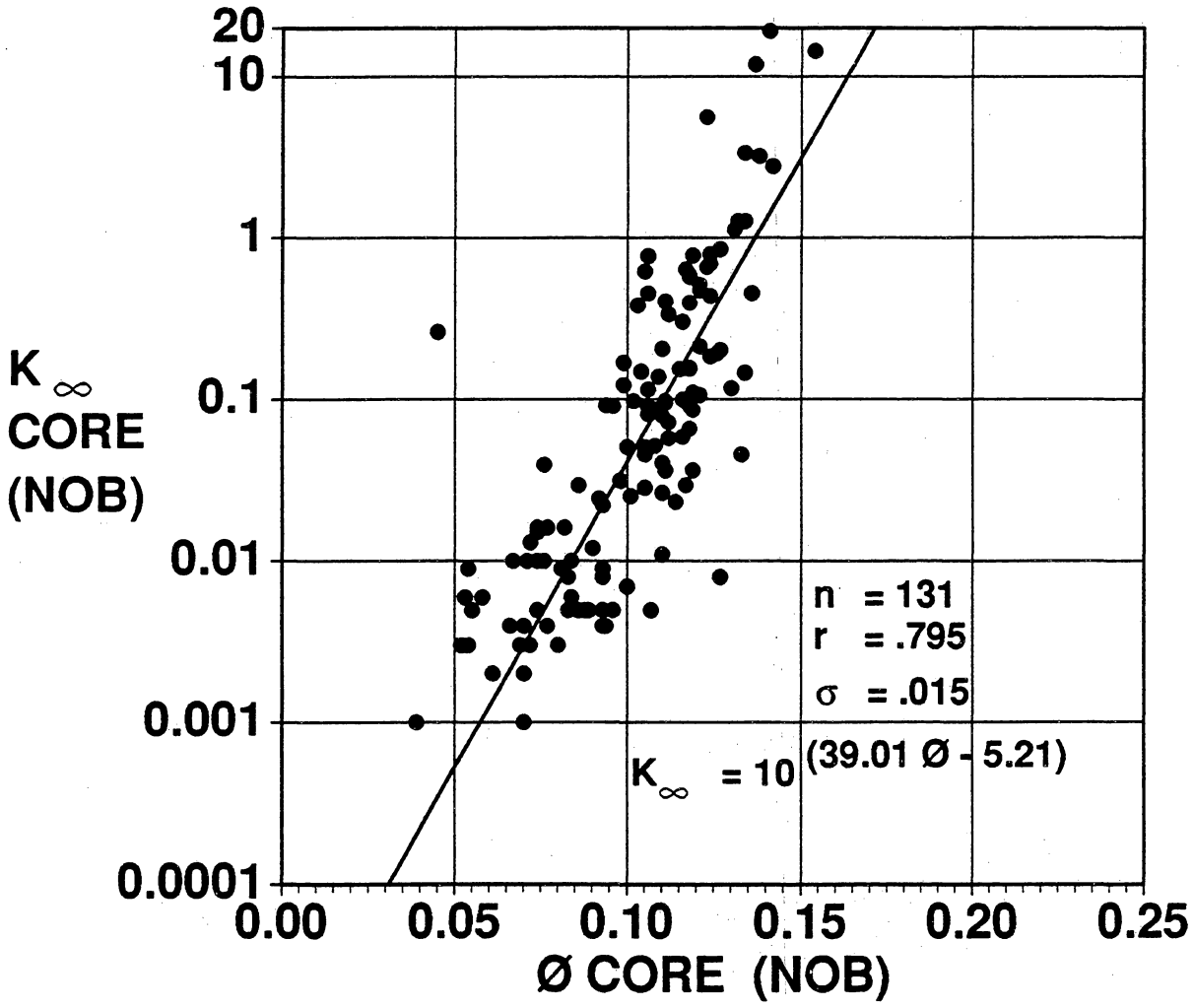

Figure 22. Plot of Klinkenberg-corrected permeability (k_∞) versus porosity (Ø), both at NOB, from core cut in the LCU No. 48 well, G reservoir.

Permeability-thickness profiles have been developed at Lake Creek field using a petrophysical model based on routine and special core analysis. Results for five wells are in good agreement with the well-test analysis. This model allows for the presence of illite, which if unaccounted for will tend to exaggerate permeabilities and predict significantly higher production rates.

CASE STUDIES OF DELTAIC RESERVOIR PRODUCTION CHARACTERISTICS

Production and pressure data indicate that channel-mouth-bar facies may not be effectively connected to distributary-channel-fill facies with a distance between wells of 1,800 ft. This hypothesis will be supported by the presentation of two case studies in this section. The productivity and projected recovery for wells completed in distributary-channel-fill facies appear to be superior to those of completions made in channel-mouth-bar and delta-front facies, indicating that understanding depositional systems is important in maximizing the recovery of natural gas.

Development of the G Sandstone Reservoir

The producing-rate history of the G sandstone is shown in figure 23, which illustrates the successful increase of producing rate as additional completions were made in the reservoir after 1984.

The reservoir temperature is about 280°F (determined from logs and bottomhole-pressure surveys). The original reservoir pressure was about 5,700 psi (determined from plotting wireline pressure data as a function of depth). The produced well-stream gas has an average gravity of 0.862 (air = 1.0) and an average gas/oil ratio of 19,608 cf/bbl (Texas Railroad Commission completion reports). The cumulative condensate and gas-production figures were used to estimate a reservoir gas mole fraction of 97.6 percent and a condensate mole fraction of 2.4 percent. The reported condensate production is considered negligible

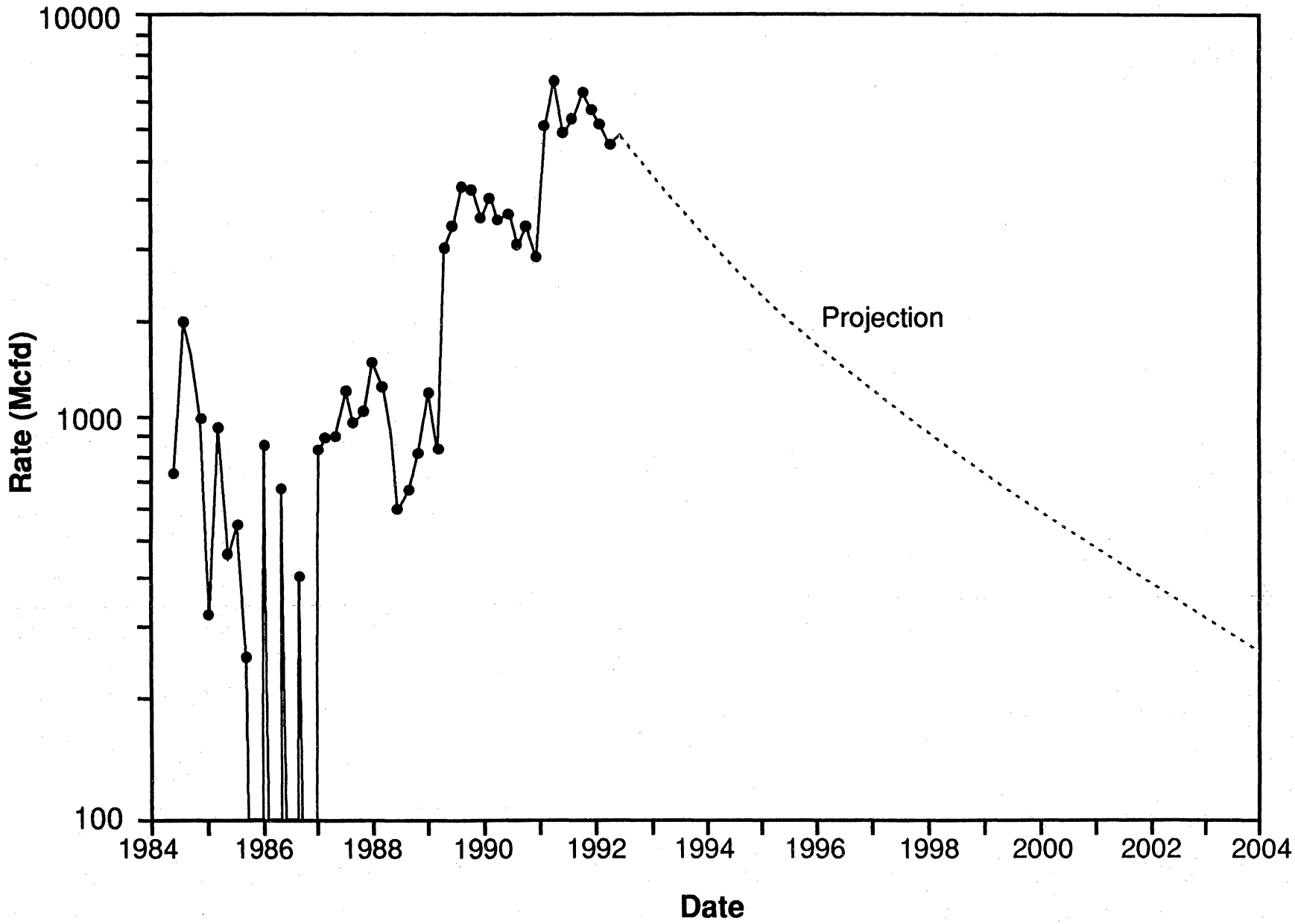

Figure 23. Production history and projection from Wilcox G completions in Lake Creek field since 1984. (a) Daily producing rate with time. (b) Daily producing rate with cumulative production since 1984.

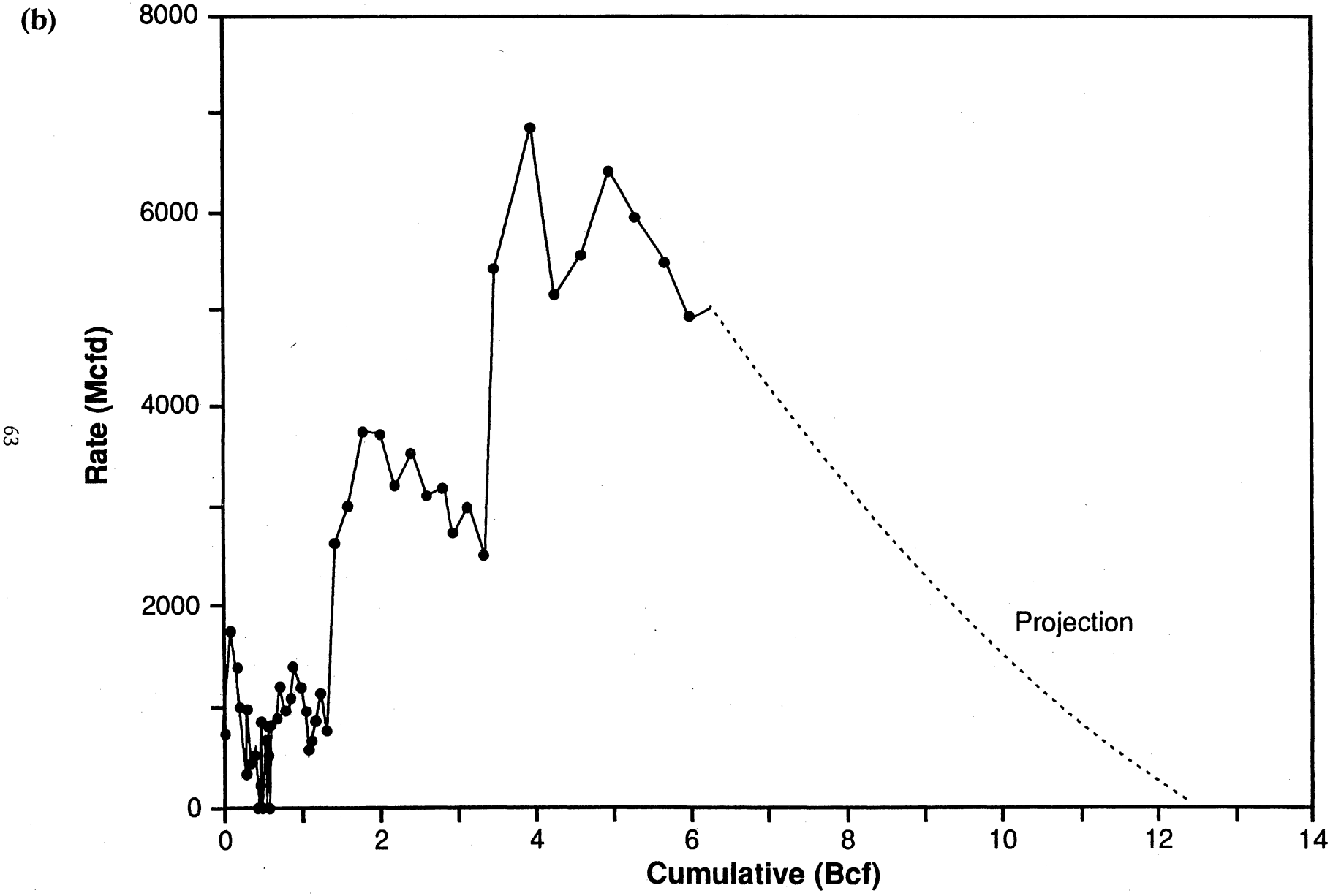

Figure 23. (continued)

for gas resource calculations, and it was assumed that there is no significant retrograde condensation dropout in the reservoir.

The average depth to the productive G interval is from 11,563 to 11,753 ft. The G reservoir has been divided into four units (G-1 through G-4) by this study. Two of these units, the G-2 and G-4, are the most frequently completed intervals in the G sandstone, across the field. These horizons have an average gross thickness of 49 ft in the G-2 and 71 ft in the G-4. The typical net productive thickness in each of these intervals is from 27 to 42 ft.

Description of Study Area

The Lake Creek Unit outline encompasses approximately 2,770 acres (fig. 24). The unit boundary encloses an area that approximates the structural closure of the Wilcox. Estimations of gas in place were made for the total unit area and for a more restricted, developed area. This study area is along the axis of the structure and subjectively encloses the Wilcox G reservoir completions based on average completion spacing of 1,800 ft. The study area shown in figure 24 is approximately 4,100 ft wide by 14,000 ft long, which is equivalent to about 1,310 acres.

The G-2 and G-4 sandstone intervals appear to be continuous across the field area. The productive G-2 sandstones within the outlined area lie at depths from 11,306 to 11,434 ft below sea level. The shallowest and deepest depths of net pay in the G-2 from log evaluations with cutoff values of 10 percent porosity and 70 percent water saturation were used in this evaluation. The difference in these depths suggests a minimum gas column height of 128 ft. The average gross sandstone thickness is 49 ft and the maximum thickness is 69 ft. Petrophysical evaluations of 10 wells in the outlined area indicate an average net-pay thickness of 27 ft.

The G-4 reservoir interval has a gas column height of 153 ft within the outlined area. The productive G-4 sandstones lie at depths from 11,441 to 11,594 ft below sea level. The

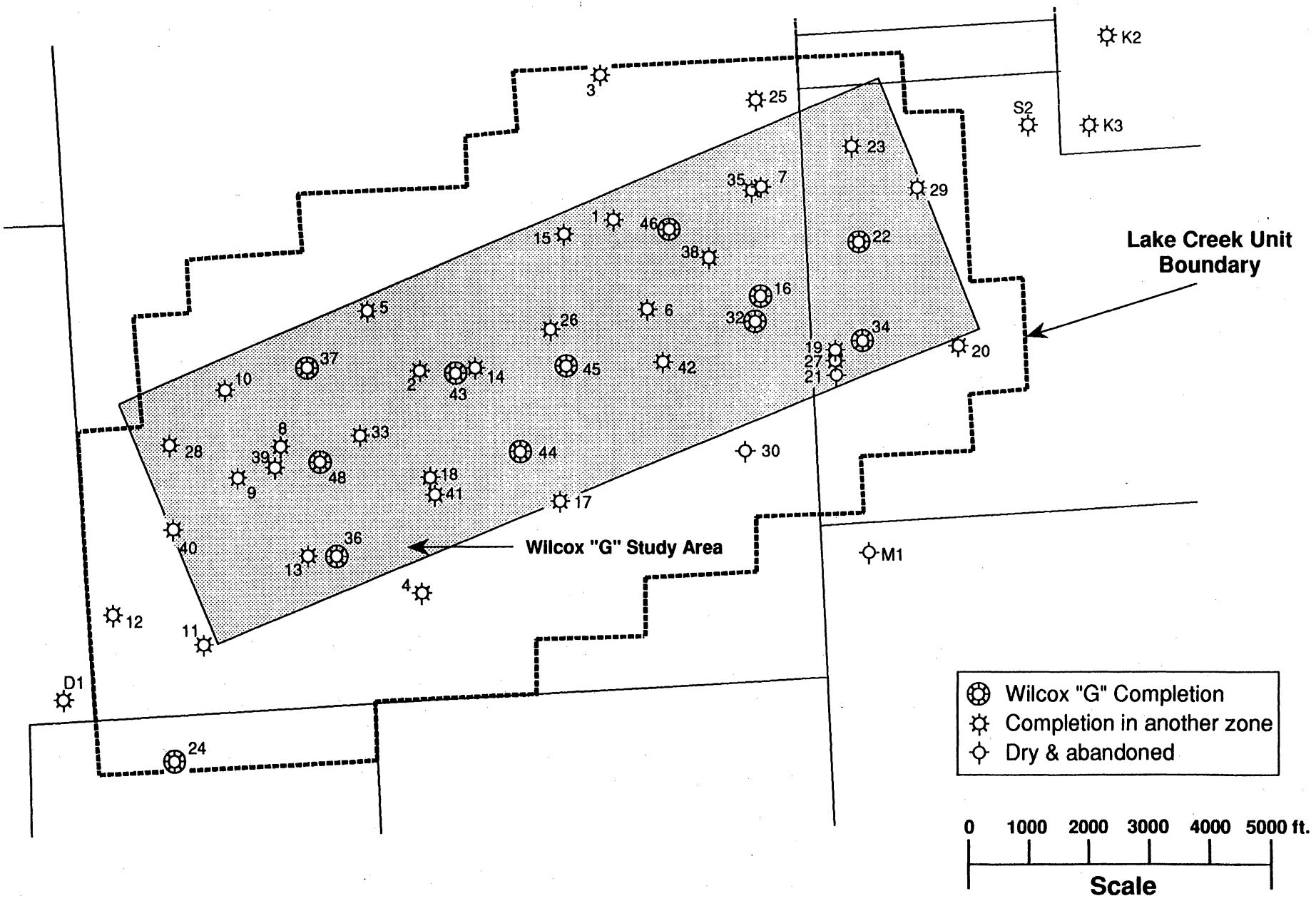

Figure 24. Map showing Lake Creek Unit outline boundary, location of wells, and completions made in the Wilcox G reservoir. The unit outline encompasses about 2,770 acres. The smaller rectangular enclosure is the minimum productive limit of the Wilcox G reservoir for volumetric estimates of original gas in place. The minimum area encompasses about 1,310 acres.

average gross sandstone thickness is 71 ft, with a maximum thickness of 111 ft. Petrophysical evaluations of 10 wells show an average net-pay thickness of 42 ft.

The apparent gas column height for these two intervals is almost twice that of the mapped structural closure across the field at the top of the Wilcox G level. The structure map of the G-2 shows about 70 ft of closure from the crest (11,330 ft below sea level) to the lowest contour (11,400 ft below sea level) on the northwest side of the field (fig. 3). Similarly, structural mapping of the G-4 intervals indicates from 70 to 80 ft of closure. This suggests that productive limits of these Wilcox sands may be more significantly influenced by reservoir architecture and stratigraphy than by structure.

Examples of Reservoir Heterogeneity

The productivity and projected recovery for wells completed in distributary-channel-fill facies appear to be significantly superior to those of completions in the channel-mouth-bar and delta-front facies, indicating that understanding depositional systems is important in maximizing the recovery of natural gas. Channel-mouth-bar facies may not be effectively connected to distributary-channel-fill facies at between-well distances of 1,800 ft, as indicated by pressure differentials and productivity. The combined drainage area for the two wells completed in the distributary-channel fill of the G-4 was determined to be 233 acres. A similar drainage area of 190 acres was estimated for the G-2 reservoir for a distributary-channel-fill facies completion, in contrast to a drainage area of only 40 acres per well for offsetting channel-mouth-bar facies completions.

Case 1: G-4 Reservoir Interval

Figure 25 shows the record of available bottomhole-pressure measurements in the Wilcox G-4 reservoir level. The pressures (adjusted for the gas deviation factor, z) are plotted against the cumulative production from the only well that was producing from this interval

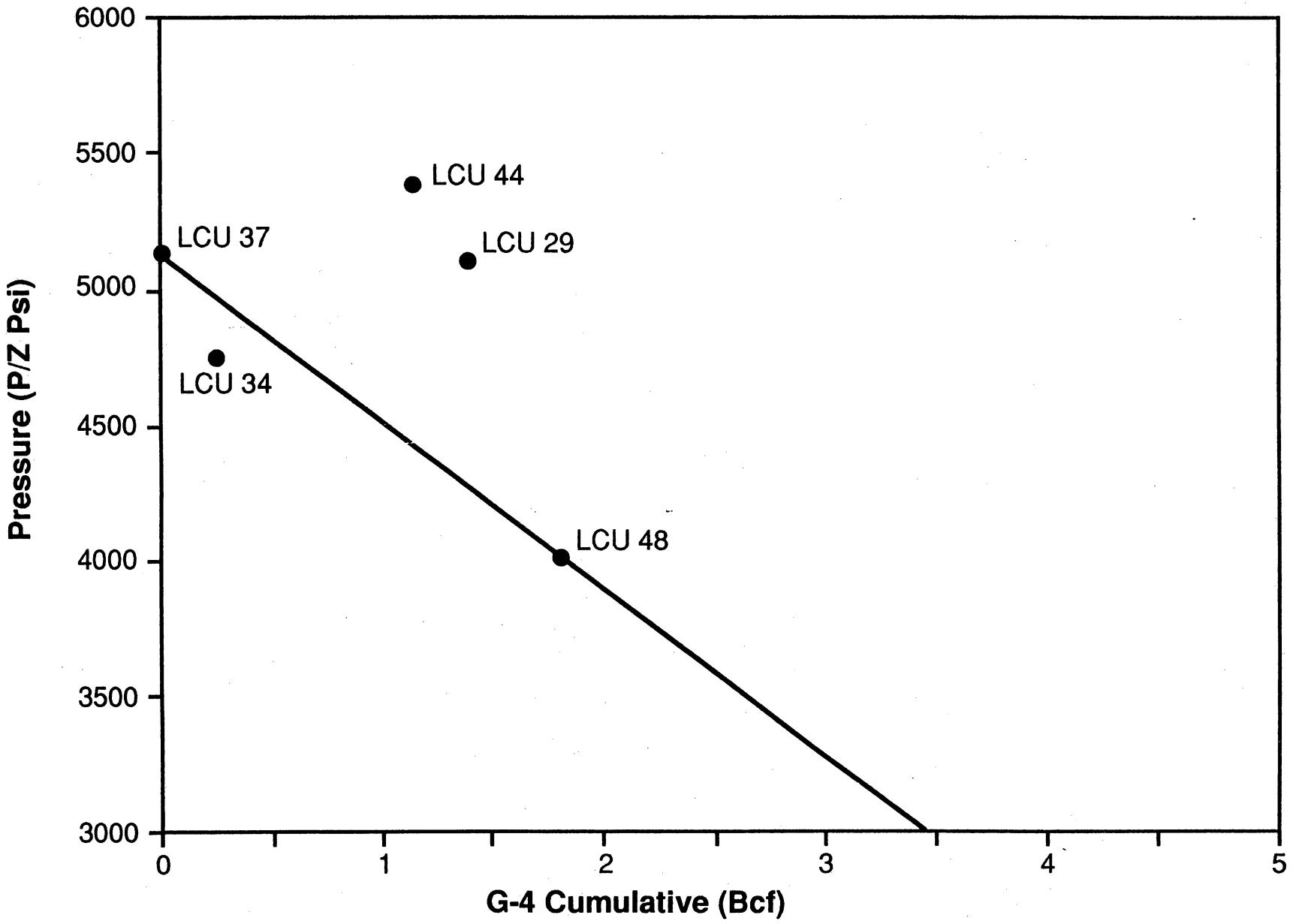

Figure 25. Plot of pressures (P/Z) with cumulative production from tests made in the Wilcox G-4 reservoir interval.

at the time of the pressure measurements. That well was the LCU No. 37. Figure 25 illustrates some of the heterogeneity in the G-4 interval. The LCU No. 37 and No. 48 wells are interpreted to be producing from a common drainage volume. The other wells are interpreted to be located in other poorly connected parts of the G-4 interval.

The LCU No. 37 well was measured by a pressure-buildup test at completion in 1984. The extrapolated pressure was 5,360 psi, which is close to the original pressure. The G-4 pressure in the LCU No. 48 well was measured by a wireline tool and reported to be 3,796 psi, a significant drawdown from the original pressure. Because of the proximity (1,700 ft) and log character similar to LCU No. 48, the drawdown is likely to have been the result of production from the No. 37 well. Both wells are completed in thick distributary-channel-fill facies in the G-4 upper parasequence. The LCU No. 37 well had produced 1,814 MMcf of gas and 57 Mbbl of condensate at the time of these wireline pressure measurements in the LCU No. 48 well. The LCU No. 37 well was the only completion producing from the G-4 interval at that time.

The pressure depletion and cumulative production indicate a drainage from a reservoir volume that initially contained 8,300 MMcf of gas (fig. 25). Using the average net-pay thickness of 61 ft (69 ft for the LCU No. 37 and 52 ft for the LCU No. 48), an effective drainage area of 233 acres can be calculated. The projected ultimate recovery from the G-4 reservoir interval by these two wells is 6,100 MMcf, based on a static reservoir pressure of 1,300 psia at abandonment. Plots of the combined producing rate with time versus cumulative production are shown in figures 26a and 26b. The extrapolated trend of rate to abandonment conditions shown in these figures has been made to match the ultimate recovery of 6,100 MMcf predicted from the pressure decline and cumulative production. The abandonment conditions were determined from equations for the pseudo-steady-state flow of gas that used the average well spacing, deliverability, and stimulation records from the completion reports. Details of these calculations are presented in appendix 5.

The LCU No. 37 and No. 48 wells account for 31 percent of the cumulative production and about 43 percent of the projected ultimate recovery from all Wilcox G reservoir completions that were producing in the Lake Creek Unit as of April 1992. The LCU No. 37 and No. 48 wells are also credited with more than 95 percent of the projected ultimate recovery from the G-4 completions.

The pressure in the LCU No. 34 was tested by both open-hole wireline and subsequent buildup tests after perforation. Both pressure tests were in good agreement. The wireline test measured a pressure of 5,078 psi and the pressure-buildup test extrapolated to a static pressure of 4,900 psi. This pressure is 700 to 800 psi less than it was originally, which indicates drawdown from production. The drawdown at the LCU No. 34 well is likely to have been caused by production from the LCU No. 22 well. The LCU No. 34 well is about 1,700 ft from the LCU No. 22 well, which is reported to have produced 684 MMcf from Wilcox G-4 perforations from 1961 through 1966. Both wells were perforated in the upper sequence of the G-4 interval. It is unlikely that any measureable drawdown could have been caused by the LCU No. 37 well. The LCU No. 37 well is almost 9,800 ft from the LCU No. 34 well and had produced only 267 MMcf for 8 months prior to the tests at the LCU No. 34 well.

The LCU No. 44 well was tested by wireline measurement in the middle sequence of the G-4 interval and was found to have an undepleted pressure of 5,788 psi. Petrophysical estimates of net pay in the G-4 interval indicate only 7 ft to be productive. The pressure in the G-4 may represent the effect of a barrier and additional undrained gas resources in nearby areas of the reservoir. The cumulative production of the LCU No. 37 well was 1,020 MMcf and the interpolated static pressure was 4,420 psi at the time of the pressure test at the LCU No. 44 well. The LCU No. 44 well is about 3,800 ft from the LCU No. 37 well and about 3,200 ft from the LCU No. 48 well. At these distances, the pressure at the LCU No. 44 would be about 4,600 psi if an average kh of 9.1 md-ft, determined from production tests in table 3, were continuous across the field.

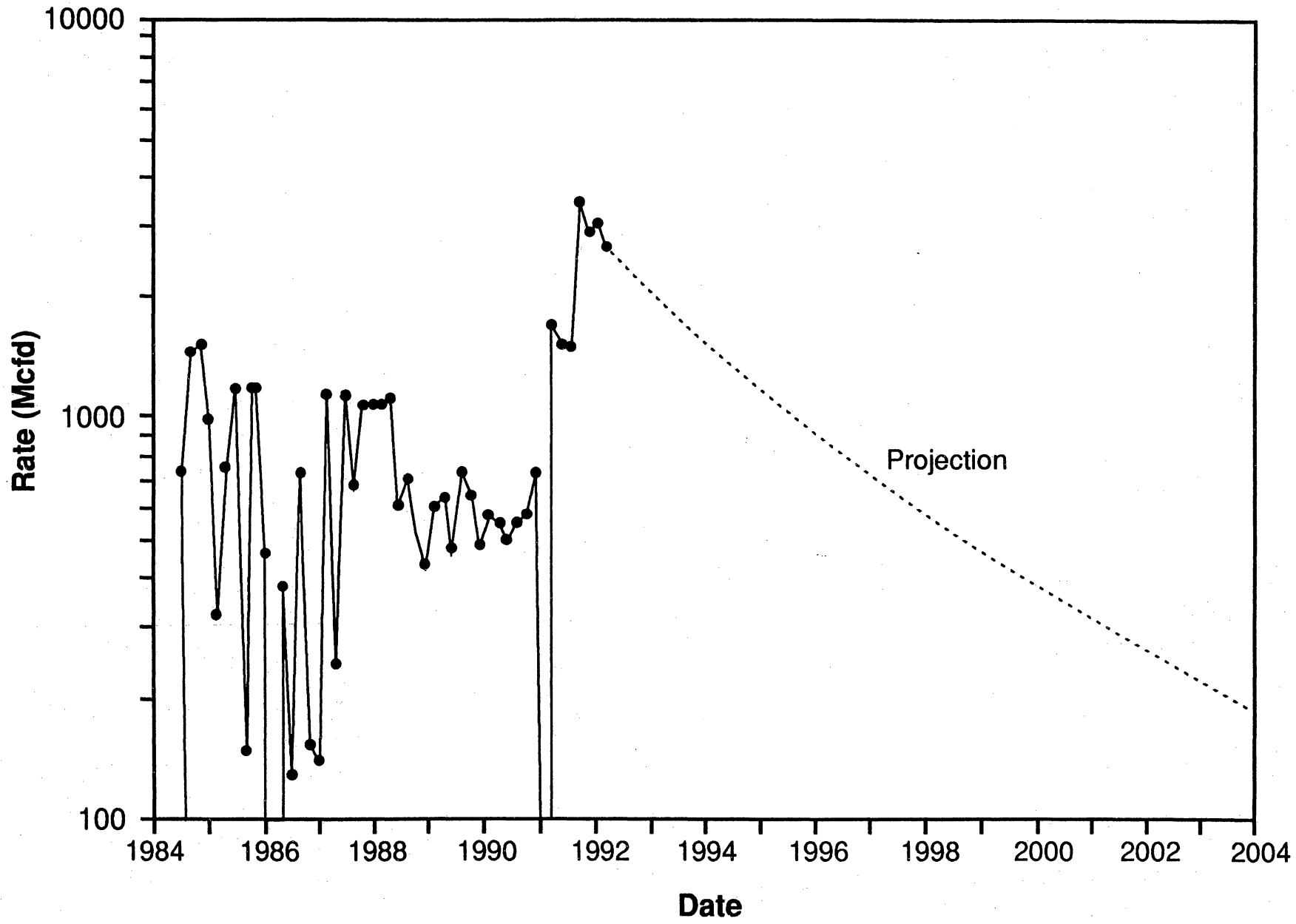

Figure 26. Production history and projection from LCU No. 37 well and No. 48 well. (a) Daily producing rate with time. (b) Daily producing rate with combined cumulative production.

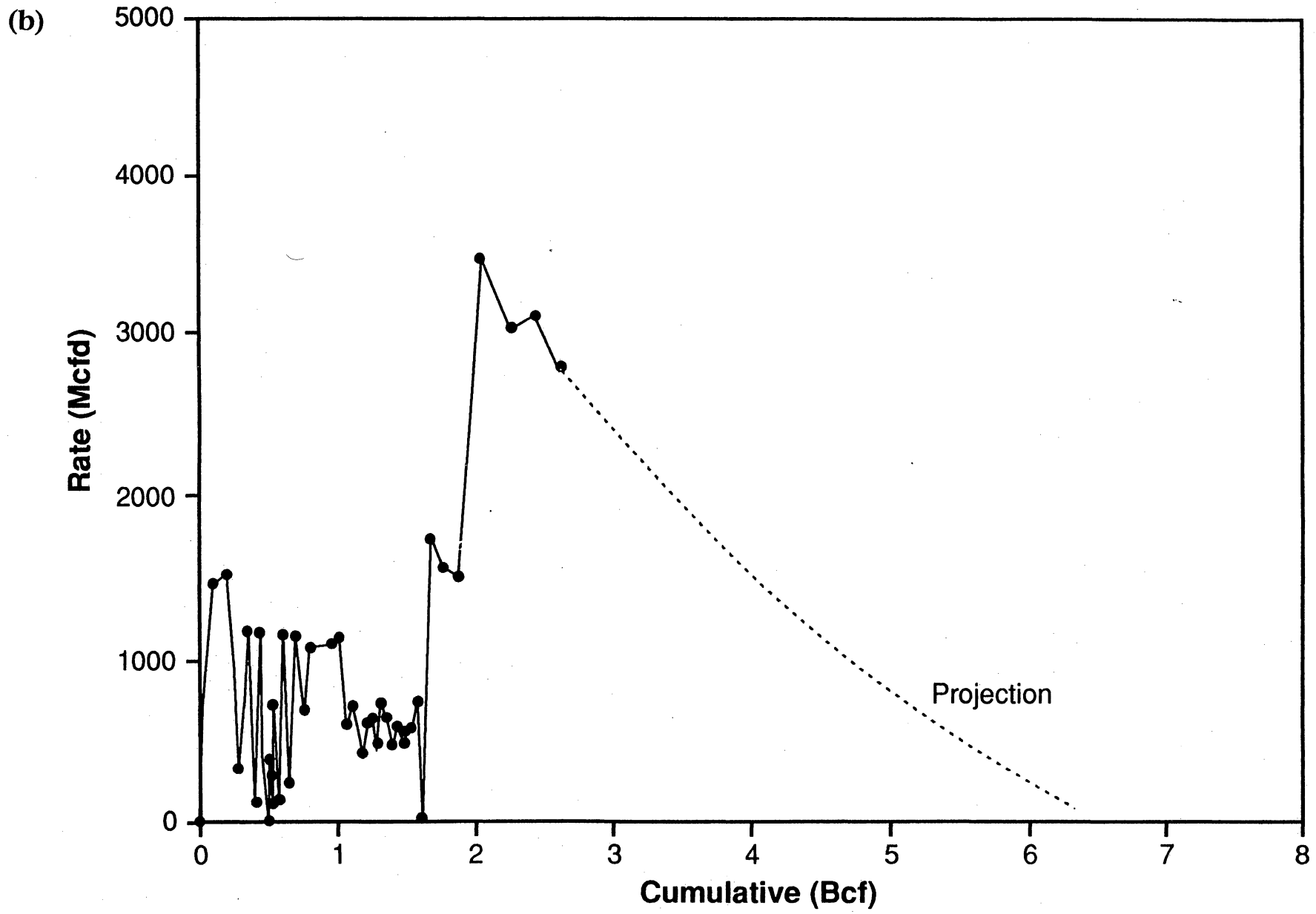

Figure 26. (continued)

The lower part of the G-4 interval was tested by wireline tools in the No. 29 well and found to have a pressure of 5,335 psi. The LCU No. 29 well is about 1,400 ft from the LCU No. 22 well, but did not exhibit pressure drawdown as did the LCU No. 34 well. It is believed that the distributary channel fill of the lower part in the G-4 interval at the LCU No. 29 well may be effectively isolated from the upper G-4 part produced by the LCU No. 22 well and tested by the LCU No. 34 well. A completion test of the channel complex in the lower G-4 may produce a previously untapped gas resource.

Case 2: G-2 Reservoir Interval

The LCU No. 43, No. 44, and No. 45 wells are nearby completions (1,600 to 2,200 ft) (fig. 24). The LCU No. 44 and No. 45 wells demonstrate similar reservoir properties of thickness and productivity and may be sharing reserves. The LCU No. 43 well appears to be separated from the LCU No. 44 and No. 45 wells and is projected to recover more reserves at a higher rate, despite a thinner net-pay thickness.

The LCU No. 44 and No. 45 wells were completed in the channel-mouth-bar facies of the G-2 reservoir interval in early 1989. Both had initial shut-in bottomhole pressures of nearly 4,800 psi and similar open-flow deliverabilities at completion, 1,700 and 1,530 Mcf/d, respectively. The projected ultimate recovery of the LCU No. 44 well is 664 MMcf, and the LCU No. 45 is projected to recover 523 MMcf. The similar production performance, proximity, log character, and initial pressure of these two wells indicate that they have similar reservoir properties and may be sharing reserves (fig. 27). Both wells have similar gross sandstone thicknesses of about 56 ft and net-pay thicknesses of about 36 ft. The combined drainage area of the two wells is indicated to be approximately 80 acres.

The LCU No. 43 well, at a distance of about 1,700 ft, is nearly equidistant to both the LCU No. 44 and No. 45 wells. The gross G-2 sandstone thickness in this well is 58 ft, and the net-pay thickness is 18 ft (ResTech evaluation). The primary facies of the G-2 at this well is

interpreted to be distributary channel fill. The initial pressure and rate history indicate that this well is not connected to the LCU No. 44 or No. 45 well in the G-2 interval. The LCU No. 43 well was completed in the G-2 interval in January 1991 with a reported initial static bottomhole pressure of 5,618 psi. The producing rate and production decline have been projected to an ultimate recovery of 1,608 MMcf. An effective drainage area of about 190 acres is determined from the projected ultimate recovery and 18 ft of net pay. Neither the LCU No. 44 nor the LCU No. 45 well exhibited a significant change in producing rate or trend after the completion of the LCU No. 43 well in the G-2 interval.

IMPLICATIONS FOR RESERVE GROWTH

Early completions in the Wilcox G sandstone producing from 1944 to 1966 did not decrease the reservoir pressure significantly across the field. New infield development commencing in 1984 found undepleted pressures.

Projections of downdip water saturations, based on the capillary-pressure model, predict productive reservoir limits below the mapped structural closure of the Wilcox G reservoir sandstone. Evaluations of modern logs and depths of perforation intervals support the projections based on the capillary-pressure model.

The analysis of the production performance of the distributary-channel completions indicates that they produce from larger drainage areas and that they recover more reserves than completions made in the channel-mouth-bar or delta-front facies. These observations imply that stratigraphy plays a role in controlling productive limits in this reservoir and that additional reserve growth potential exists.

A comparison of permeability-thickness (kh) and estimated ultimate recovery for distributary-channel and nonchannel reservoir facies indicates a strong correlation between primary depositional facies and productivity. Eleven wells (table 8a) with completions in the G-2 and G-4 intervals were analyzed using production and pressure data combined with log

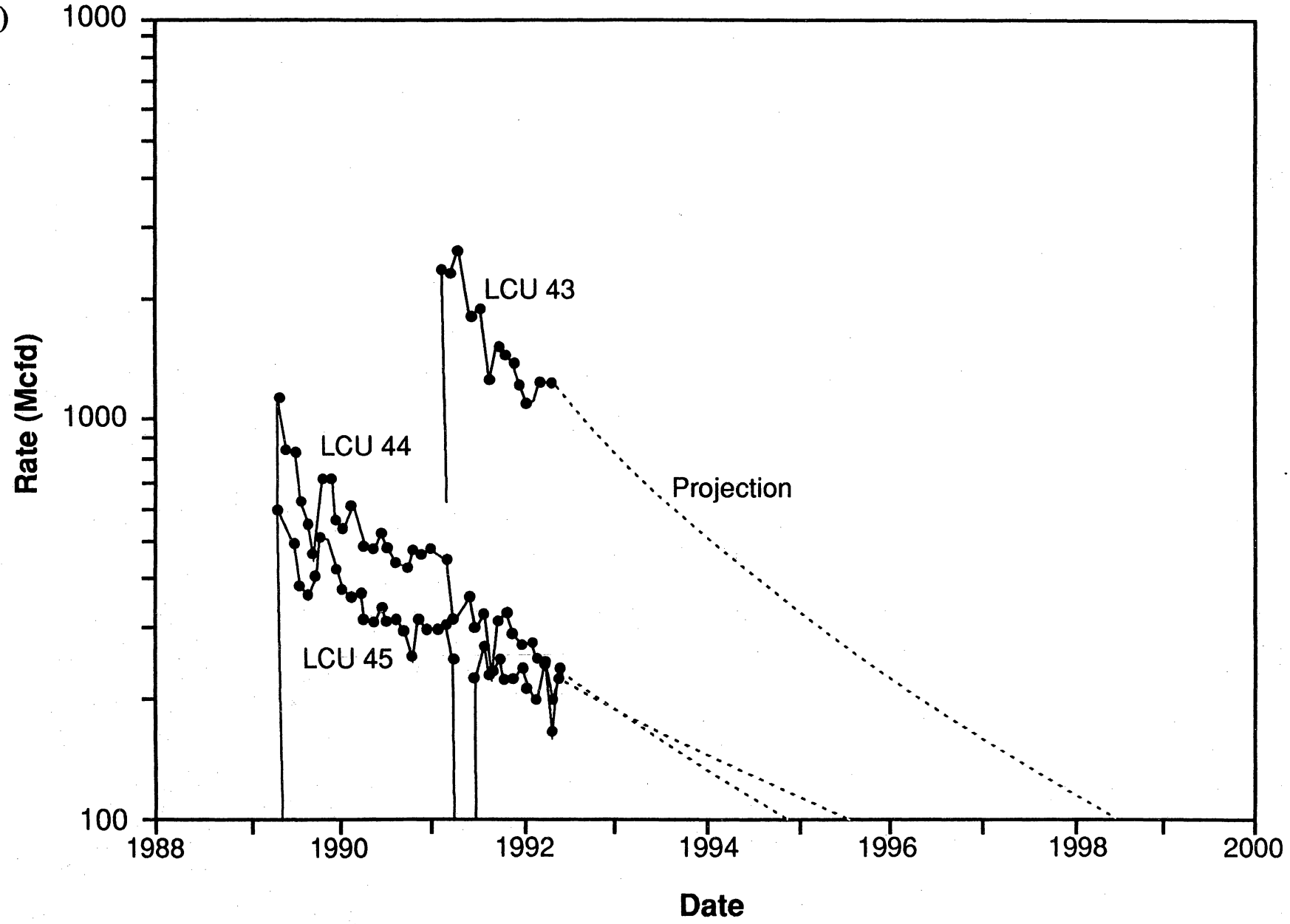

Figure 27. Production history and projection from Wilcox G-2 completions showing performance of channel-mouth-bar and distributary-channel completions. These wells are separated by a standard field spacing of about 1,800 ft. (a) Daily producing rate with time. (b) Daily producing rate with individual well cumulative production.

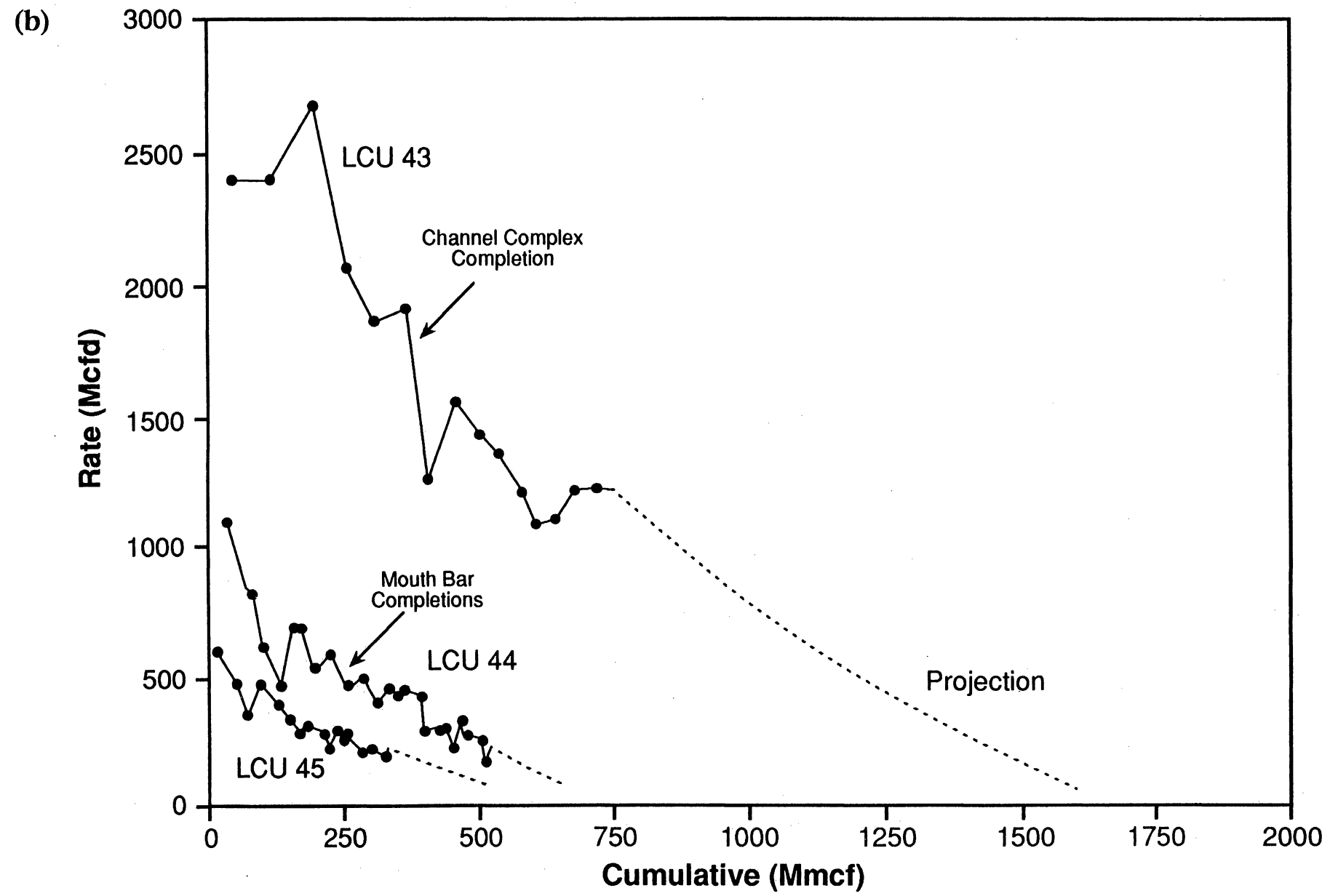

Figure 27. (continued)

Table 8a. Comparison of ultimate gas recovery and permeability thickness by well number.

LCU well number	Distributary channel ultimate recovery (MMcf)	Channel kh (md-ft)	Nonchannel ultimate recovery (MMcf)	Nonchannel kh (md-ft)
16	1,580			
36	1,791	10.4		
37	3,567	13.8		
43	1,608	12.2		
48	2,777	21.0		
22			684	
24			250	
32			509	3.8
44			664	8.4
45			523	8.7
46			855	4.0

Table 8b. Statistical comparison of productivity by reservoir facies.

	Distributiary Channel Complex		Nonchannel	
	Distributary channel ultimate recovery (MMcf)	Channel kh (md-ft)	Nonchannel ultimate recovery (MMcf)	Nonchannel kh (md-ft)
Minimum	1,580	10.4	250	3.8
Maximum	3,567	21.0	855	8.7
Sum	11,323	56.2	3,485	24.9
Samples	5	4	6	4
Mean	2,265	14.1	581	6.2
Median	1,791	13.0	594	6.2
Standard deviation	878	4.1	205	2.69

analysis. Productivity estimates in the G sandstone indicate that completions in the distributary-channel complex have approximately three times the effective kh as completions in the nonchannel part of the reservoir (table 8b). Projected ultimate recoveries for distributary-channel completions indicate that channel completions can obtain approximately four times the gas recovery of nonchannel completions (table 8b). This analysis indicates that it may be important strategically to identify the presence and location of specific reservoir facies to maximize the recovery of natural gas in the most timely and efficient manner.

Volumetric Estimates of Original Gas in Place

The capillary-pressure model described earlier suggests that productive Wilcox G sandstone should be found at depths greater than that of the mapped structural closure of the Lake Creek field. Because the unit outline of the Lake Creek field encompasses the approximate structural closure, it can be inferred that gas-productive Wilcox G sandstone should be found at the unit boundary and beyond. The capillary-pressure model predicts that productive Wilcox G-2 sandstone (with air permeabilities >0.17 md) should be found at depths as low as 11,429 (±29) ft below sea level. This prediction was based on the mean air permeability of the poorer delta-front facies. Higher permeability rock would be found productive at even deeper depths. The structural saddle on the northwest side of the field occurs at the top of the G-2 interval at approximately 11,390 ft below sea level and the base of porosity development at about 11,440 ft below sea level. The LCU No. 44 and No. 24 wells have produced gas from G-2 perforations at 11,401 and 11,395 ft below sea level, respectively. Given the relatively small change in structural depths for the G-2 and G-4 reservoir intervals, the porosity is not expected to change significantly across the Lake Creek unit. However, S_w will increase as we move closer to the free-water level. These observations

suggest that reserve growth should be possible from flank development, assuming a distribution of reservoir facies similar to that found on the crestal axis.

The original (mobile) gas in place (OGIP) and recoverable gas in place (RGIP) were estimated using volumetric calculation methods. The gas-in-place calculations were performed in the G-2 and G-4 intervals using the mapped facies distributions across the unit area. The fraction of reservoir rock containing mobile gas was estimated for each facies using an air-permeability cutoff of 0.2 md (fig. 10). Separate calculations were performed for each rock type and average structural position of the developed area and flank area. The OGIP estimates were determined from net area, net thickness, and water saturations that were calculated on the basis of average facies permeability and structural position. Recoverable gas estimates were based on a final or abandonment pressure in each facies unit. The lower permeability and structurally lower rock facies will have a higher final pressure at abandonment than will higher permeability rock on the crest of the field. This final abandonment pressure was calculated from Darcy's flow equation for gas, which would result in a flow rate of 100 Mcf/d at a flowing pressure of 1,000 psi if a well were completed at that facies unit. A detailed description of the method and results of these calculations are presented in appendix 5.

An approximation of the primary developed area of the Wilcox G reservoir is shown in figure 24. This area is along the axis of the structure and subjectively encloses the Wilcox G reservoir completions based on average completion spacing (1,800 ft). The primary developed area (fig. 24) is approximately 4,100 ft wide by 14,000 ft long, which is equivalent to about 1,310 acres. The less developed flank area is the total unit area (2,770 acres) minus the developed area (1,310 acres) for a net flank area of 1,460 acres.

The combined OGIP of the G-2 and G-4 intervals is estimated to be 63,007 MMcf, and the technically RGIP is estimated to be 23,109 MMcf. The technically RGIP of the developed area is 16,298 MMcf. The RGIP assumes a sufficient number of wells to contact all the mobile gas in the reservoir.

The projected recovery of each Wilcox G completion was determined from the decline of producing rate with time and cumulative production. Initial reservoir pressures and flowing well-head pressures were used to forecast production and match the production-decline trends. The summation of the projected recoveries (table 9) for the G-2 and G-4 completions is 14,430 MMcf. The extrapolated ultimate recoveries of the individual wells can be found in appendix 3.

Effective Recovery

The apparent RGIP for the Wilcox G reservoir, based on volumetric methods, is greater than the projected ultimate recovery of the existing Wilcox G reservoir completions. The projected recovery of 14,430 MMcf from the existing completions compares favorably with the RGIP of 16,298 MMcf estimated for the developed area (table 10). However, the combined RGIP of the developed and flank areas suggests that an additional 8,679 MMcf may be technically possible if additional wells are completed in the G reservoir, primarily in the flank area of the field. The economic feasibility of drilling and producing this remaining potential resource was not addressed in this study. The potential additional resource of 8,679 MMcf, compared with the projected recovery from the existing completions of 14,430 MMcf, represents a potential reserve growth of 60 percent.

CONCLUSIONS

The Paleocene to lower Eocene G sandstone is part of the Rockdale delta system of the Wilcox Deltaic Sandstone in the Houston Embayment (WX-1) play. The G sandstone varies from 150 to 300 ft in gross interval thickness. The G sandstone reservoir in the Lake Creek field is divided into four parasequences that are typical of the stratigraphic variability of deltaic depositional sequences in many major gas-bearing reservoirs. These parasequences are bounded by nonreservoir units composed of thin lignitic-rich zones and shales

Table 9. Projected recovery of existing completions.

Interval	Completions	Cumulative	Ultimate
G-2	9	5,576 MMcf	7,763 MMcf
G-4	4	2,985 MMcf	6,667 MMcf
Total	13	8,561 MMcf	14,430 MMcf

Table 10. Original and recoverable gas in place (OGIP and RGIP).

	Distributary channel	Channel-mouth bar	Delta front	Delta plain	Total
Developed area—crest					
Wilcox G-2					
Area (acres)	445	367	92	406	1,310
OGIP (MMcf)	4,992	4,597	462	0	10,051
RGIP (MMcf)	3,295	1,434	81	0	4,810
Wilcox G-4					
Area (acres)	354	786	131	39	1,310
OGIP (MMcf)	6,167	15,324	1,026	0	22,517
RGIP (MMcf)	4,508	6,666	314	0	11,488
Total G-2 and G-4					
OGIP (MMcf)	11,159	19,921	1,488	0	32,568
RGIP (MMcf)	7,803	8,100	395	0	16,298
Undeveloped area—flank					
Wilcox G-2					
Area (acres)	73	628	263	496	1,460
OGIP (MMcf)	4,735	4,290	393	0	9,418
RGIP (MMcf)	1,463	448	9	0	1,920
Wilcox G-4					
Area (acres)	409	292	584	175	1,460
OGIP (MMcf)	5,849	14,299	873	0	21,021
RGIP (MMcf)	2,039	2,774	78	0	4,891
Total G-2 and G-4					
OGIP (MMcf)	10,584	18,589	1,266	0	30,439
RGIP (MMcf)	3,502	3,222	87	0	6,811
Combined crest and flank					
Total G-2 and G-4					
OGIP (MMcf)	21,743	38,510	2,754	0	63,007
RGIP (MMcf)	11,305	11,322	482	0	23,109

interpreted as flooding surfaces that subdivide the G sandstone reservoir into four fieldwide mappable units, termed the G-4, G-3, G-2, and G-1 in ascending stratigraphic order. Detailed stratigraphic, petrographic, and petrophysical analyses using whole cores calibrated to well logs form the basis of an integrated study that included engineering analysis of field-production and pressure history and incorporated the results from recent infield development completions by the current operator of the Lake Creek Unit.

A log-interpretation model that predicts effective permeability to gas has been developed and takes into account the effects of fibrous illite on permeability measurements. The model was calibrated to permeability measurements obtained from special core analysis, namely, specific permeability to brine and relative permeabilities obtained from preserved core samples of the Wilcox G reservoir. Using the results from other special core analyses of electrical factors, water saturations, and permeabilities, an excellent fit was obtained between log-derived and core-derived petrophysical parameters of porosity, shale volume, and water saturation. Calibration methods such as these can improve confidence in accurately predicting producibility in zones of interest and can evaluate potential bypassed gas in low-permeability reservoirs found in the lower Wilcox. This model has been applied locally at Lake Creek, but a more general model can be applied worldwide. If the technique is transfered to other basins, it will be improved through the acquisition of capillary-pressure measurements in the field being evaluated.

The statistics of productivity and recovery from the Wilcox G reservoir demonstrate the importance of identification of facies and facies trends to maximize recovery from this depositional environment in the most efficient manner. Analysis of the productivity by facies in the G sandstone indicates that the distributary-channel completions have about three times the effective kh as do nonchannel-facies completions. The average projected ultimate recoveries from distributary-channel completions is about four times that of the nonchannel-facies completions.

A volumetric assessment of the Wilcox G reservoir indicates that the apparent original recoverable gas in place is greater than the projected ultimate recovery of past and existing completions. The incremental recovery potential lies primarily in the flank areas of the field. The capillary-pressure model predicts that productive rock facies should be found downdip, beyond the unit boundary. This prediction is supported by log evaluation and production. It is estimated that there may be a potential incremental resource of 60 percent more than the current estimate of ultimate recovery. This could be converted to producible reserves by additional completions or additional wells in the reservoir. The location, number, and economic feasibility of these wells were not evaluated.

ACKNOWLEDGMENTS

This study was part of a research program funded by the Gas Research Institute under contract no. 5088-212-1718, the U.S. Department of Energy under contract no. DE-FG-88MC25031, and the State of Texas. The cooperation of Nanette Kuich of Mobil Exploration and Producing U.S., Inc., is gratefully acknowledged. SEM photomicrographs were by J. M. Mendenhall. Core handling and thin-section preparation were done by the Core Research Center under the direction of Allan Standen. Figures were prepared by ResTech, Inc., and by the cartographic staff of the Bureau of Economic Geology. Others contributing to the publication were Susan Lloyd, word processing, Jamie H. Coggin, design; Bobby Duncan, editing; and Jeannette Miether and Kitty Challstrom, proofreading.

REFERENCES

Bebout, D. G., Weise, B. R., Gregory, A. R., and Edwards, M. B., 1982, Wilcox reservoirs in the deep subsurface along the Texas Gulf Coast: their potential for production of geopressured geothermal energy: The University of Texas at Austin, Bureau of Economic Geology Report of Investigations No. 117, 125 p.

Brooks, R. H., and Corey, A. T., 1964, Hydraulic properties of porous media: Fort Collins, Colorado, Colorado State University, hydrology paper, 27 p.

Clarke, T. G., 1962, Lake Creek field, Montgomery County, Texas, *in* Denham, R. L., ed., Typical oil and gas fields of southeast Texas: Houston Geological Society, p. 95–99.

Clavier, C., Coates, G., and Dumanoir, J., 1977, The theoretical and experimental basis for the dual water model for the interpretation of shaly sands: Society of Petroleum Engineers, SPE paper no. 6859, p. 3–18.

Craft, B. C., and Hawkins, M. F., 1959, Applied reservoir engineering: Englewood Cliffs, Prentice-Hall, p. 333.

Finley, R. J., Fisher, W. L., Seni, S. J., Ruppel, S. C., and others, 1988, An assessment of the natural gas resource base of the United States: The University of Texas at Austin, Bureau of Economic Geology Report of Investigations No. 179, 69 p.

Fisher, R. S., Tyler, Noel, and Barton, Mark, 1992, Quantification of flow unit and bounding element properties and geometries, Ferron Sandstone, Utah: implications for heterogeneity in Gulf Coast Tertiary deltaic reservoirs, *in* Memorandum of understanding between the United States Department of Energy and the State of Texas, annex I, characterization of oil and gas reservoir heterogeneity, final report, p. 130–164.

Fisher, W. L., and McGowen, J. H., 1967, Depositional systems in the Wilcox Group of Texas and their relationship to occurrence of oil and gas: Gulf Coast Association of Geological Societies, Transactions, v. 17, p. 105–125.

Guevara, E. H., and Grigsby, J. D., 1992, Deltaic deposits of the Wilcox Group in the Houston Embayment: example from Lake Creek field, *in* Levey, R. A., ed., Core and log analysis of depositional systems and reservoir properties of Gulf Coast natural gas reservoirs: an integrated approach to infield reserve growth in Frio, Vicksburg, and Wilcox sandstones: The University of Texas at Austin, Bureau of Economic Geology Geological Circular 92-7, p. 45–52.

Guevara, E. H., Tyler, Noel, Grigsby, J. D., and Kuich, Nanette, in press, Outcrop-constrained characterization of stratigraphic architecture in deltaic gas reservoirs, Lake Creek Unit, Texas: Gulf Coast Association of Geological Societies Transactions, v. 42.

Guven, N., Hower, W. F., and Davies, D. K., 1980, Nature of authigenic illites in sandstone reservoirs: Journal of Sedimentary Petrology, v. 50, p. 761–766.

Kosters, E. C., Bebout, D. G., Seni, S. J., Garrett, C. M., Jr., Brown, L. F., Hamlin, H. S., Dutton, S. P., Ruppel, S. C., Finley, R. J., and Tyler, Noel, 1989, Atlas of major Texas gas reservoirs: The University of Texas at Austin, Bureau of Economic Geology Publication, 161 p.

Langford, R. P., Grigsby, J. D., and Howard, W. E., 1992, Use of the enhanced density and microresistivity logs in interpreting diagenetic facies in Tertiary Gulf Coast sandstones,

Proceedings, 1992 Society of Petroleum Well Log Analysts Annual Logging Symposium (June 14–17), paper BB, p. 1–16.

Luffel, D. L., Herrington, K. L., and Harrison, C. W., 1991a, Fibrous illite controls productivity in Frontier gas sands, Moxa Arch, Wyoming: Society of Petroleum Engineers, SPE paper no. 21876, p. 695–704.

Luffel, D. L., Howard, W. E., and Hunt, E. R., 1991b, Travis Peak core permeability and porosity relationships at reservoir stress: Society of Petroleum Engineers, SPE paper no. 19008, p. 310–318.

Luffel, D. L., Herrington, K. L., and Walls, J. D., 1990, Effect of extraction and drying on flow, capillary, and electrical properties of Travis Peak cores containing fibrous illite: Society of Petroleum Engineers, SPE paper no. 20725, p. 131–138.

National Petroleum Council, 1992, NPC natural gas study, v. 2, Supply availability: Washington, D.C., variously paginated.

May, J. A., and Stonecipher, S. A., 1990, Depositional environments of the Wilcox Group, Texas Gulf Coast: Stratigraphic and early diagenetic signatures: Gulf Coast Association of Geological Societies Transactions, v. 40, p. 551–583.

Pittman, E. D., 1992, Relationship of porosity and permeability to various parameters derived from mercury injection capillary pressure curves for sandstone: American Association of Petroleum Geologists Bulletin, v. 76, no. 2 (February), p. 191–198.

Swanson, B. F., 1981, A simple correlation between permeabilities and mercury capillary pressures: Journal of Petroleum Technology, p. 2498–2504.

Thomeer, J. H. M., 1960, Introduction of a pore geometrical factor defined by the capillary pressure curve: Journal of Petroleum Technology (March), p. 73–77.

Tyler, Noel, Barton, Mark, Fisher, R. S., and Gardner, M. H., 1991, Architecture and permeability structure of fluvial-deltaic sandstones: a field guide to selected outcrops of the Ferron Sandstone, east-central Utah: The University of Texas at Austin, Bureau of Economic Geology, 80 p.

APPENDIX 1: DERIVATION OF THE ADVANCED CAPILLARY-PRESSURE MODEL (ADCAP)

Three empirical equations resulting from studies of large core data bases at Shell and Amoco are the foundation of the ADCAP model. The two Shell equations, by Thomeer (1960) and Swanson (1981), are now widely accepted in industry. Pittman's equation (1992), derived from Amoco's data base, is more recent. Working with multiple sets of capillary-pressure data covering a wide range of sand conditions, we independently verified Pittman's work.

Thomeer's Equation

In 1960, Thomeer proposed that mercury capillary-pressure data could be fit with hyperbolic curves employing three parameters

$$\frac{S_b}{S_{b\infty}} = e^{-F_g/\log(P_c/P_d)} \tag{1}$$

where

S_b = bulk volume occupied by mercury (percent of total rock volume),

$S_{b\infty}$ = bulk volume occupied by mercury at infinite pressure, or total interconnected pore volume (percent of total rock volume),

P_c = mercury capillary pressure (psi),

P_d = mercury extrapolated displacement pressure (psi), and

F_g = pore geometrical factor (dimensionless).

This equation can be simplified and restated in more common oil-field terms, if we assume $S_{b\infty}$ is porosity and S_b is porosity times hydrocarbon saturation,

$$\log P_c = -F_g / \ln (1-S_w) + \log P_d \tag{2}$$

where S_w = water saturation (fraction). We have found that this simplified Thomeer equation adequately represents capillary-pressure data.

Swanson's Equation

In 1981, Swanson demonstrated that the coordinates from a certain point A on the capillary-pressure curve could be used to calculate air permeability. His equation, again restated in oil-field terms, is:

$$k_{air} = 399\left[\frac{\varnothing(1-S_w)}{P_c}\right]^{1.691} \tag{3}$$

where

$\varnothing$ = porosity (percent),

k_{air} = air permeability (millidarcys), and

S_w and P_c = values at point A.

It can be shown that the fundamental point A is related to the parameters in equation 2 by the following simple equations:

$$F_g = \left[\ln(1-S_w)\right]^2 / 2.303 \tag{4}$$

and

$$P_d = P_c\,(1-S_w) \tag{5}$$

where S_w and P_c are values at point A. These relations imply that a knowledge of porosity and point A is enough to determine the entire capillary-pressure curve.

Pittman's Equation

Recently, Pittman (1992) demonstrated a correlation between the pore-throat radius at point A and air permeability in sandstones. His empirical equation is

$$\log r_{apex} = .226 + .466 \log k_a \tag{6}$$

where

r_{apex} = the pore-throat radius in microns at point A.

This relation was established using multiple regression on a data base of 202 samples of sandstone from 14 formations ranging in age from Ordovician to Tertiary. These sandstones are variable in

composition and texture. The porosities and permeabilities of the data set ranged from 3.3 to 28 percent and .05 to 998 millidarcys, respectively. The correlation coefficient for equation 6 is .919. We can solve for P_c at point A with the standard equation converting pore-throat radius to capillary pressure:

$$P_c = 107 / r_{apex} \tag{7}$$

which yields

$$P_c = 180 / k_a{}^{.466} \tag{8}$$

If we substitute equation 8 in equation 3, we can solve for S_w at point A in terms of porosity and permeability. Further algebraic manipulation with equations 4 and 5 allows us to obtain

$$F_g = \left[\ln\left(5.21\frac{k_{air}\cdot.1254}{\varnothing}\right)\right]^2 / 2.303 \tag{9}$$

and

$$P_d = 938 / k_{air}{}^{.34}\,\varnothing \tag{10}$$

This completes the derivation of the "generalized" model, which is embodied in equations 2, 9, and 10. Considering the large core data bases supporting the original three equations, 1, 3, and 6, this model can be viewed as a worldwide correlation for capillary-pressure curves. In the absence of measured laboratory data, ADCAP could be used to generate capillary-pressure curves characterizing a reservoir. As with any general correlation, it is to be expected that although in many cases these ADCAP curves should be reasonable approximations of the actual curves, in some cases there could be a significant difference.

We have worked with the model on six widely different reservoirs where measured capillary pressure was available and have found it useful to adjust the constants in equations 9 and 10 in order to closely approximate the measured data.

P_c to Height Conversion

To apply ADCAP to well data, mercury capillary pressures must be converted to height above the free-water level (FWL). This conversion is given by

$$h = \frac{P_c}{\rho_w - \rho_h}\left(\frac{\sigma_r \cos\theta_r}{\sigma_l \cos\theta_l}\right) \quad (11)$$

where

h = height above FWL (in feet),

P_c = mercury capillary pressure (psi),

ρ_w = formation water density (psi/ft),

ρ_h = formation hydrocarbon density (psi/ft),

σ_r = interfacial tension between the fluids in the reservoir (dynes/cm),

σ_l = interfacial tension between the fluids used in the laboratory (dynes/cm [480 for mercury]),

θ_r = contact angle between the fluid interface and the rock in the reservoir (typically 0°), and

θ_l = contact angle between the fluid interface and the rock in the laboratory (140° for mercury).

Regression Analysis

With centrifuge capillary-pressure data on selected plugs from the G-2 sandstone in the LCU No. 48 well, we adjusted the standard ADCAP to derive an initial local model. Equations for this model are the following:

$$\log P_c = -F_g/\ln(1-S_w) + \log P_d \quad (12)$$

$$F_g = \left[\ln\left(4.78\frac{k_{air}.009}{\varnothing}\right)\right]^2 / 2.303 \quad (13)$$

and

$$P_d = 439 / k_{air}^{.72}\ \varnothing \quad (14)$$

Appendix figure A1-1 shows the good correlation obtained between the water saturations calculated from the local ADCAP and those measured on the selected plugs. Air permeability of the plugs ranges from .21 to 7.92 md.

Data required for the regression analysis to predict free-water level are porosity, water saturation, and air permeability values at multiple depth levels. Data from 43 coring points in the G-2 sandstone was selected, all having air permeabilities greater than .05 millidarcys.

The initial model used in the regression consisted of equations 12, 13, and 14, together with the conversion of capillary pressure to height given by

$$h = .217\, P_c \tag{15}$$

This model produced unsatisfactory regression results from a least squares adjustment point of view because the residuals showed trends versus depth. In a satisfactory adjustment, residuals, when plotted versus depth, show a random scatter. In this case, the residuals are the adjustments that the regression makes to the porosity, water saturation, and permeability values to arrive at the "correct" values that fit the model.

Appendix figure A1-2 illustrates a trend in error terms versus depth. For convenience, instead of the residuals mentioned above, these error terms have been calculated by subtracting the right side of equation 12 from the left side. If the equation were perfectly satisfied, then all of the error terms would be zero. As it is, the figure shows a pattern of increasing error term values with decreasing depth. This violates a basic principle of regression analysis, namely that errors are randomly distributed.

Trends in residuals can be caused by employing an "incorrect" model. This is thought to be the case here because the initial model was adjusted to capillary-pressure measurements made at ambient conditions rather than in situ conditions. A regression was run in which two of the constants in equations 13 and 14 were adjusted along with the value for the free-water level. The conventional core data were essentially used to adjust the local model to in situ conditions. The final version of the local model is given by equations 16 and 17.

$$F_g = \left[\ln\left(2.54\frac{k_{air}\cdot.009}{\emptyset}\right)\right]^2 / 2.303 \tag{16}$$

and

$$P_d = 120 / k_{air}{}^{.72}\,\emptyset \tag{17}$$

Figure A1-3 shows that after the final regression run the new error terms no longer exhibit a trend versus depth. Note also that the scatter of error terms is much reduced from that shown in figure A1-2.

The final model implies that in situ capillary-pressure curves are different from those measured at ambient conditions. Figure A1-4 shows comparative capillary curves for SCAL sample 129. Two curves are shown for sample 129C, one representing measurements made at ambient conditions and one approximating the measured curve derived from the initial ADCAP model. The third curve, based on the stressed porosity and permeability measured on sample 129A, was derived from the final ACAP model and represents our best estimate of a curve measured under in situ conditions. In general, the "stressed" curve shows higher water saturations than do the unstressed curves, which is the qualitative relationship to be expected.

Indirect support for the saturation differences shown in figure A1-6 comes from comparative gas-water relative permeability plots shown in figures A1-5 and A1-6. The stressed curves measured on sample 129A in figure A1-6 are shifted to the left, in comparison with the unstressed curves measured on sample 129B in figure A1-5. This pattern holds for all such comparisons between stressed and unstressed companion samples.

The crossover point in figure A1-6 has a water saturation that is approximately 19 percent higher than the crossover point in figure A1-5. Because Purcell and Burdine have demonstrated in classic papers that a strong relation exists between capillary-pressure curves and relative permeability curves, this implies that comparative capillary-pressure curves for the two samples would agree with figure A1-4.

In spite of the saturation differences between the stressed and unstressed ADCAP models illustrated in figure A1-4, the predicted water levels for the two models are only 29 ft apart. The unstressed (initial) ADCAP model predicted a free-water level at –11,444 subsea, whereas the value for the stressed (final) ADCAP model was –11,473 subsea. Either value supports an important conclusion in the section "Example of a Free-Water Level," namely that productive limits for the field are partially controlled by stratigraphy.

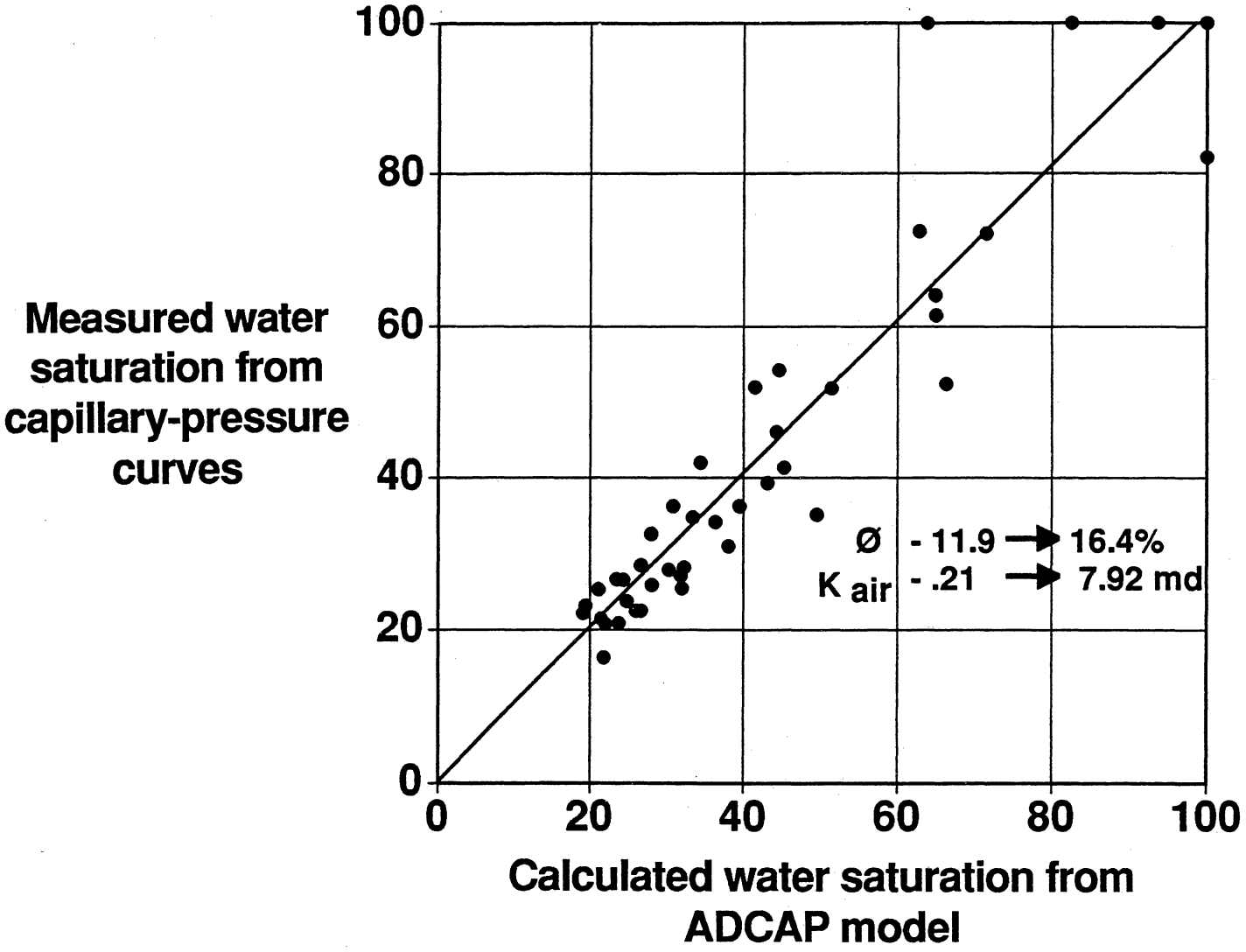

Figure A1–1. Comparison of water saturation calculated from the capillary-pressure model with that measured from capillary-pressure curves for the LCU No. 48 well.

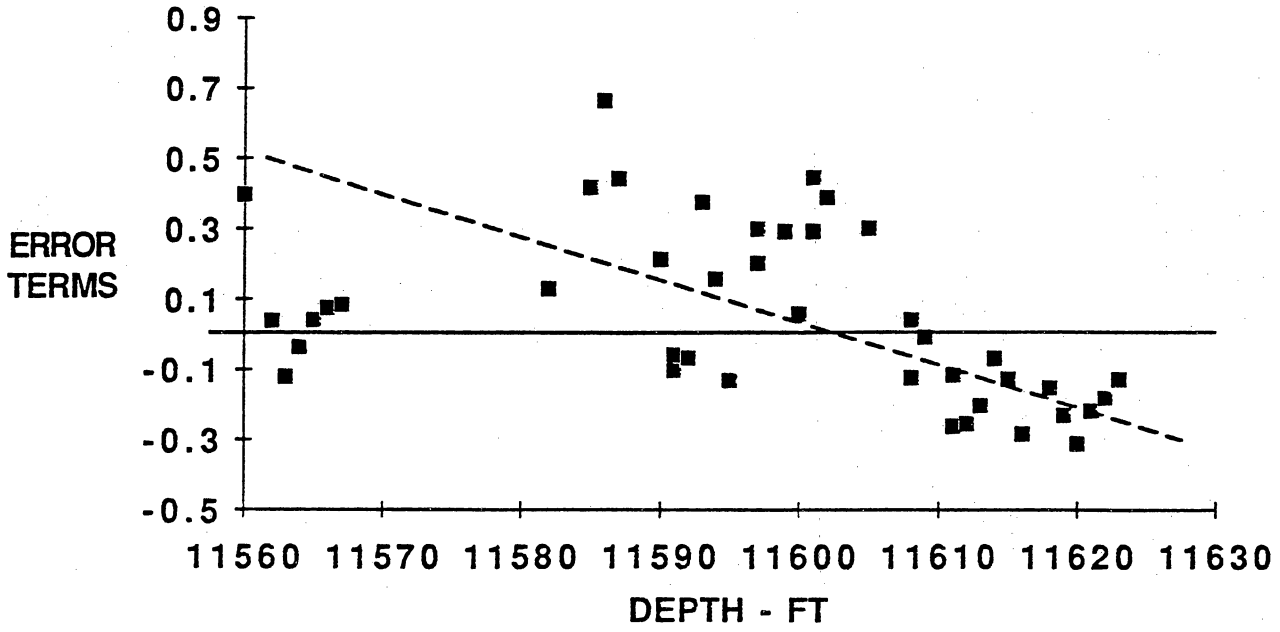

Figure A1-2. Error terms showing trend versus depth (original model—unstressed).

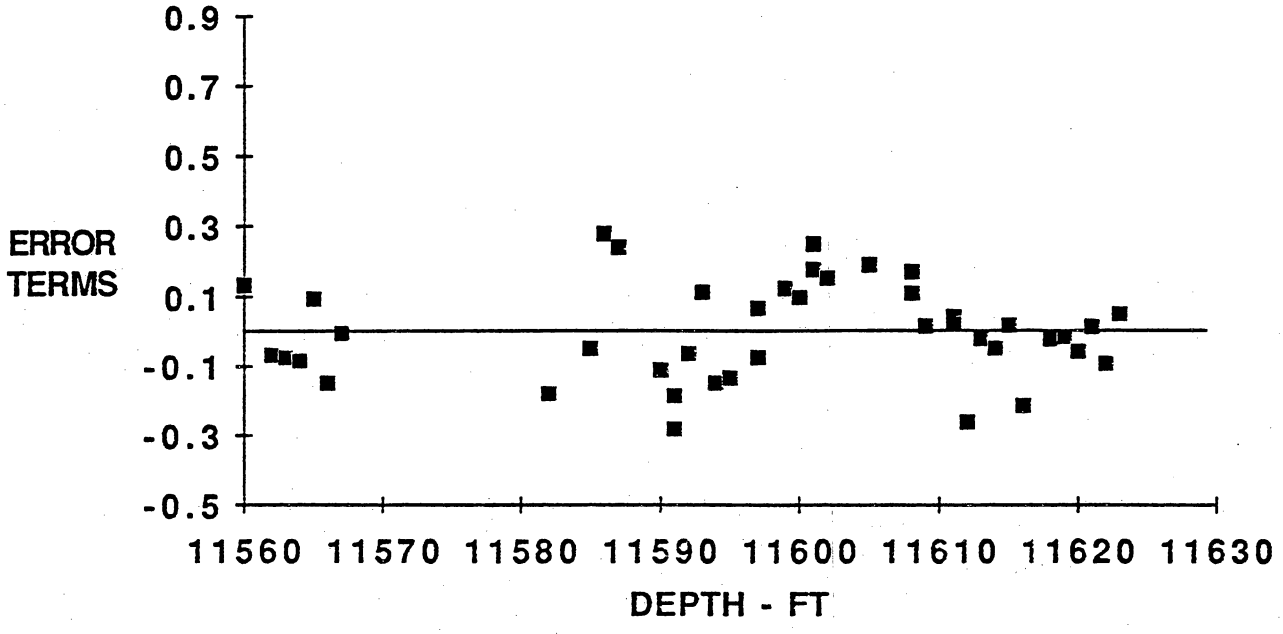

Figure A1-3. Error terms showing no trend versus depth (final model—stressed).

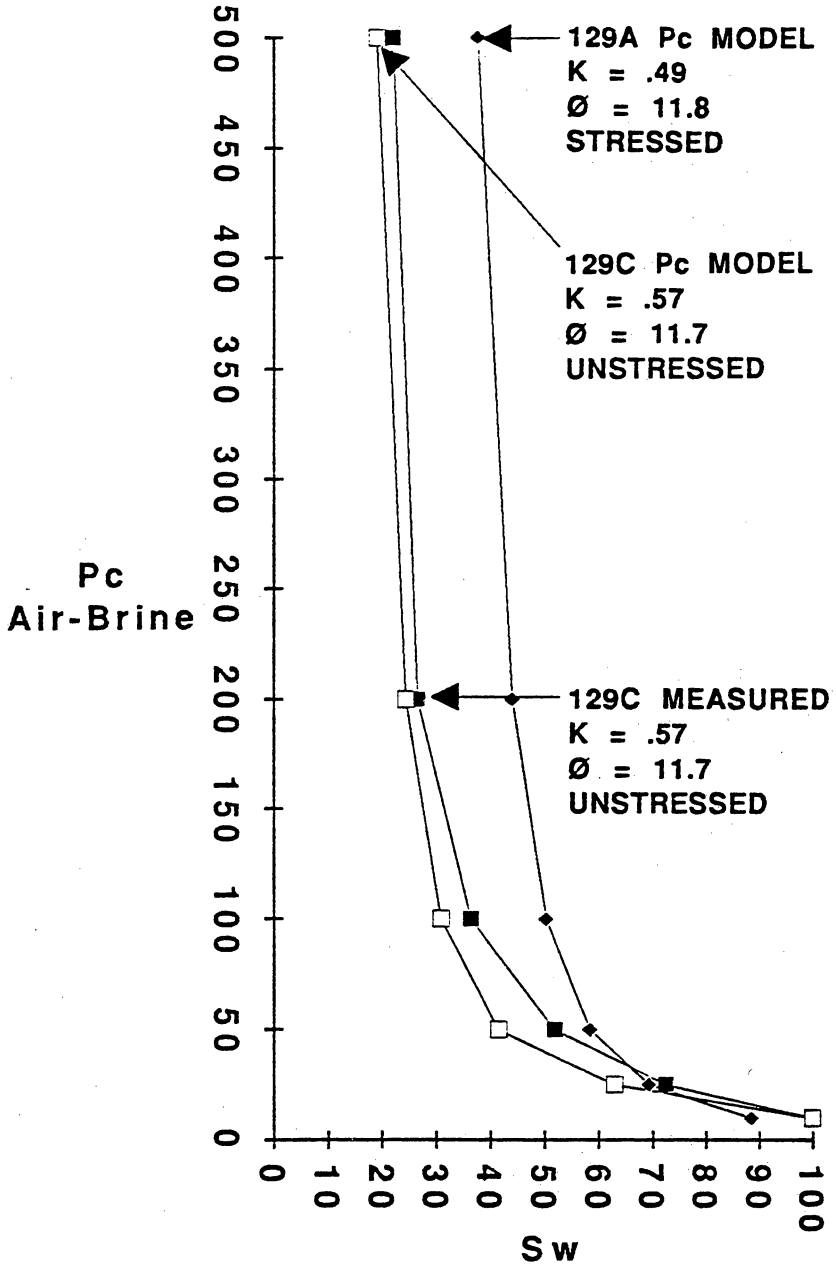

Figure A1-4. Stressed versus unstressed P_c curves.

RESTECH HOUSTON
MOBIL LAKE CREEK UNIT NO. 48 WELL
WILCOX FORMATION
LAKE CREEK FIELD
MONTGOMERY COUNTY, TEXAS

SAMPLE I.D.	: 129B
DEPTH, ft	: 11605.4
Ka, md	: 0.556
POROSITY, %	: 11.7
Kw, md	: 0.10

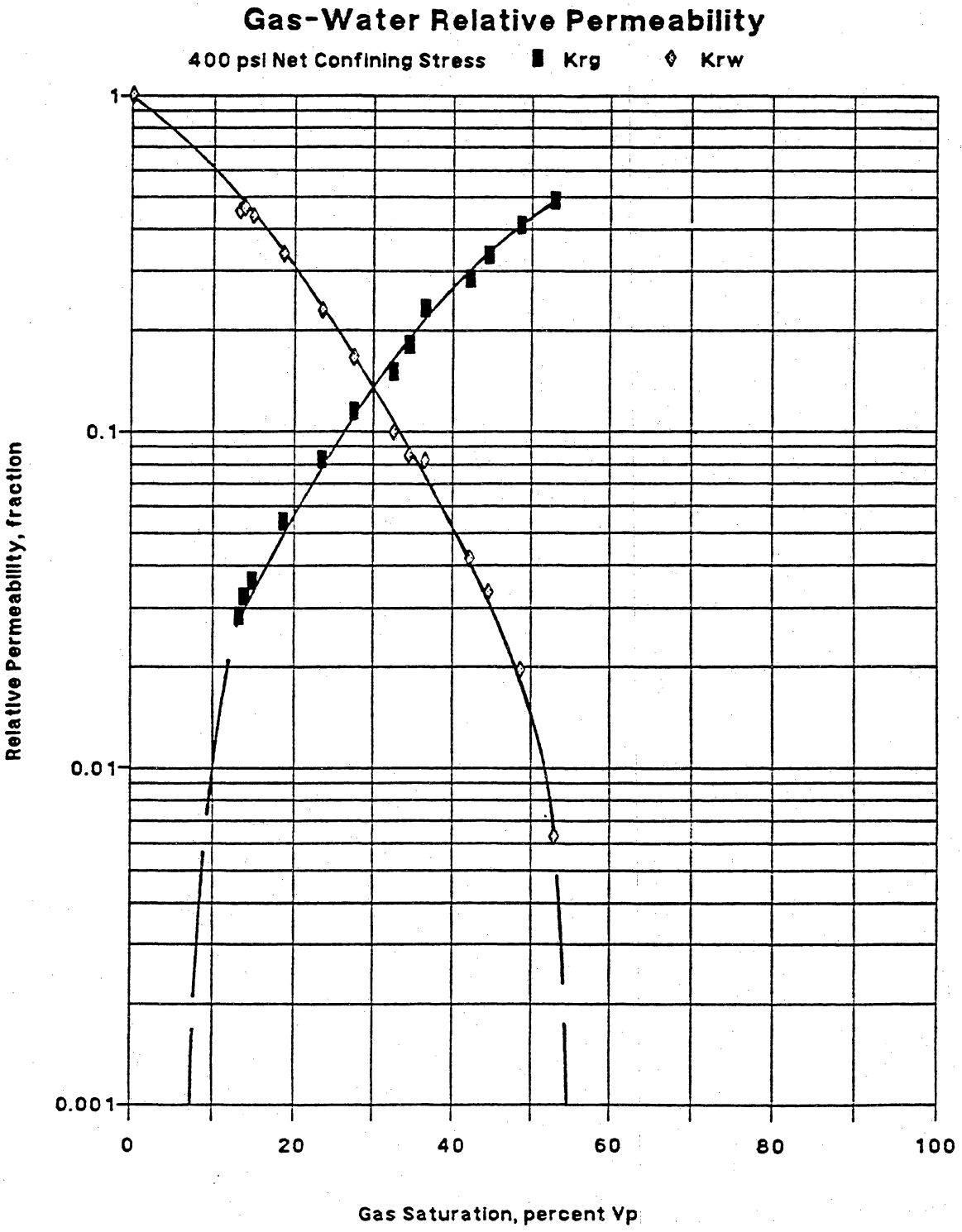

Figure A1-5. Gas-water relative permeability at 400 psi.

RESTECH HOUSTON		SAMPLE I.D.	: 129A
MOBIL LAKE CREEK UNIT NO. 48 WELL		DEPTH, ft	: 11605.4
WILCOX FORMATION		Ka, md	: 0.485
LAKE CREEK FIELD		POROSITY, %	: 11.8
MONTGOMERY COUNTY, TEXAS		Kw, md	: 0.072

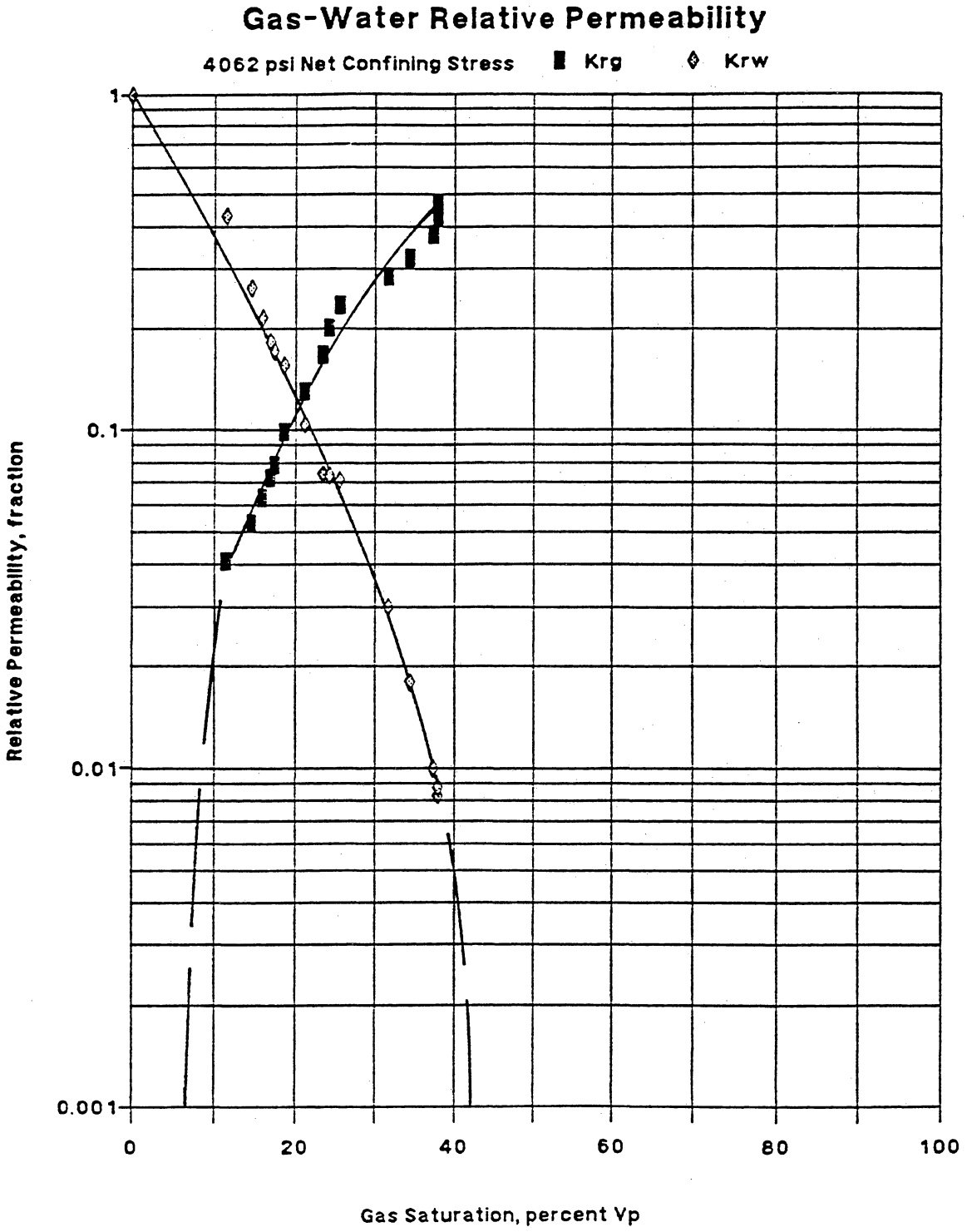

Figure A1-6. Gas-water relative permeability at 4,062 psi.

APPENDIX 2: PRODUCTION SUMMARY OF WILCOX G COMPLETIONS, LAKE CREEK UNIT

Table A2–1. Production summary (as of April 1992).

Well no.	Gas cum. (Mcf)	Oil cum. (Bbl)	Sep. gas gravity	Liquid gravity	GLR cf/bbl	Well gravity
16	1,579,877	na				
22	684,383	na				
24	250,288	na				
32	390,328	22,308	0.694	47.9	13,667	0.886
36	943,553	62,783	0.696	52.0	30,378	0.784
37	2,215,707	67,698	0.701	50.0	29,657	0.791
43	727,632	37,170	0.710	55.7	11,000	0.930
44	525,820	18,299	0.726	53.5	19,559	0.856
45	348,890	12,674	0.723	50.8	11,937	0.934
46	661,173	44,531	0.675	54.4	10,780	0.905
48	521,106	13,496	0.724	54.4	29,889	0.810
Total	8,848,757	278,959				
Average			0.706	52.3	19,608	0.862

na = not available

Original Gas in Place

The original reservoir pressure was 5,700 psi at the depth of the Wilcox G reservoir. This pressure was determined from wireline pressure and depth data. The G reservoir completion reports indicate an average dry gas gravity of 0.706 (air = 1), condensate gravity of 52.3°API, a gas/oil ratio of 31,721 scf/bbl, and a well-stream gravity of 0.862. An initial gas in place equivalent of 575 Mcf/acre-ft is determined from these fluid parameters and petrophysical parameters of 11 percent porosity and 53 percent water saturation. The cumulative condensate and gas production figures have been used to estimate a reservoir gas mole fraction of 97.6 percent and a condensate mole fraction of 2.4 percent. The reported condensate production, accounting for only 2.4 percent of the reservoir gas, is considered negligible in calculations of resource recovery.

APPENDIX 3: CUMULATIVE AND PROJECTED PRODUCTION, WILCOX G RESERVOIR, LAKE CREEK FIELD

Table A3–1. Cumulative and projected production, Wilcox G Reservoir, Lake Creek field (as of April 1992).

	Perforated		Allocated			
Well no.	Cum. (MMcf)	Ult. (MMcf)	G-2 cum. (MMcf)	G-2 ult. (MMcf)	G-4 cum. (MMcf)	G-4 ult. (MMcf)
16	1,580	1,580	1,580	1,580	0	0
22	684	684	342	342	342	342
24	250	250	250	250	0	0
32	390	509	160	209	195	255
36	944	1,791	944	1,791	0	0
37	2,216	3,567	0	0	2,216	3,567
43	728	1,608	728	1,608	0	0
44	526	664	526	664	0	0
45	349	523	321	481	0	0
46	661	855	383	496	53	68
48	521	2,777	0	0	521	2,777
Total	8,849	14,808	5,576	7,763	2,985	6,667

Allocation of cumulative and ultimate production was based on the relative thickness of each interval.

APPENDIX 4: DETERMINATION OF ORIGINAL GAS IN PLACE AND RECOVERY FACTOR

Step 1: Determination of a kh cutoff for reservoir productivity was established as 0.2 md air permeability. This permeability cutoff, based on the marginal producibility performance and the buildup test for kh of LCU Well No. 34, was applied to the probability distribution for air permeability for each of the three reservoir facies (distributary channel, channel-mouth bar, and delta front).

Step 2: The percentage of aerial distribution of each reservoir facies type was determined for the G-2 and G-4 reservoir intervals within the developed area and also with the flank area by projecting each of the reservoir facies into that area.

Step 3: Median permeabilities of each of the three reservoir facies were determined by eliminating those permeabilities that were less than the 0.2-md cutoff.

Step 4: For each of the three reservoir facies (distributary channel, channel-mouth bar, and delta front), and for each reservoir unit at structural positions corresponding to the average height above the free-water level in the developed area and on the flanks (total of 12 rock units), average water saturations and corresponding effective gas permeabilities were derived from the petrophysical model using the median air permeabilities from step 3.

Step 5: Using Darcy's law (appendix 5) abandonment pressures and corresponding recovery factors were calculated for each of the 12 rock units (six rock units in the G-2 and six in the G-4 reservoir).

Step 6: Volumetric calculations of the OGIP and theoretically recoverable gas were made for each of the 12 rock units using parameters derived above and the previously derived average porosities and pay thicknesses.

Step 7: Recoverable gas computed for the flank area was reduced by 50 percent to account for possible pay deterioration and a lack of well control in the flank area of the Lake Creek Unit.

Table A4–1. Estimation of water saturation and effective gas permeability by facies for the G-2 sandstone using the capillary-pressure model.

	Distributary channel	Channel-mouth bar	Delta front
Top of structure (–11,327 ft [msl])			
Depth from crest (ft)	0	0	0
Water saturation (%)	50	55	57
Effective gas k (md)	0.123	0.030	0.019
Developed area (–11,347 ft [msl])			
Depth from crest (ft)	–20	–20	–20
Water saturation (%)	51	57	60
Effective gas k (md)	0.115	0.027	0.017
Undeveloped area—flank (–11,387 ft [msl])			
Depth from crest (ft)	–60	–60	–60
Water saturation (%)	57	64	68
Effective gas k (md)	0.092	0.019	0.011

Note: The air permeability for distributary-channel facies is 1.5 md, for channel-mouth-bar facies is .55 md, and for delta-front facies is .40 md. The free-water level is –11,473 (±29) ft.

Table A4–2. Area by facies in the Wilcox G-2 and G-4 intervals.

	Fraction	Area (acres)
Wilcox G-4		
Developed area (1,310 acres total)		
Delta plain	0.03	39
Distributary channel	0.27	354
Channel-mouth bar	0.60	786
Delta front	0.10	131
Flank area (1,460 acres total)		
Delta plain	0.12	175
Distributary channel	0.28	409
Channel-mouth bar	0.20	292
Delta front	0.40	584
Wilcox G-2		
Developed area		
Delta plain	0.31	453
Distributary channel	0.34	495
Channel-mouth bar	0.28	409
Delta front	0.07	103
Flank area		
Delta plain	0.34	496
Distributary channel	0.05	73
Channel-mouth bar	0.43	628
Delta front	0.18	263

Developed area	1,310 acres
Flank area	1,460 acres
Total area	2,770 acres

APPENDIX 5: ESTIMATION OF FINAL DEPLETION PRESSURE BY FACIES

A well completed in a distributary-channel facies on the crest of the Lake Creek field is used to demonstrate the method of estimating the final or abandonment pressure in the drainage area of a well. A final pressure (P_s) of 1,300 psi is determined from the following equation (Craft and Hawkins, 1959) for the pseudo-steady-state flow of gas:

$$q = kh\left(P_s^2 - P_f^2\right) / (1422\mu Tz)\ (\ln(r_e / r_w) - .75 + S)\ \text{Mcf/d}$$

where

q = 100 Mcf/d (flow rate at abandonment),

k = 0.115 md (mean gas permeability of distributary-channel facies),

kh = 42 ft (average G-4 net-pay thickness),

P_s = psia (static reservoir pressure),

P_f = 1,000 psia (flowing wellbore pressure),

μ = 0.015 cp (gas viscosity),

T = 280°F, 740°R (reservoir temperature),

z = 0.9 (gas deviation factor),

r_e = 1,800 ft (drainage radius based on well spacing),

r_w = 0.25 ft (wellbore radius), and

S = –3 (typical skin coefficient for a fracture-stimulated well).

The final depletion pressure for each of the reservoir facies was determined for depths of 20 ft below and 60 ft below the crest. These depths represent the average structural position of the wells currently completed and of potential wells to be completed in the flank area. The final pressure-depletion pressure is that pressure that would support a production rate of 100 Mcf/d (an assumed economic limit) when wells are spaced at 80 acres per well. A skin factor of –3 was used because the Wilcox completions are typically hydraulically fractured. A flowing pressure of 1,000 psi was assumed to be reasonable for wells completed at these depths. The following table summarizes the final depletion pressure of each rock unit by facies and structural position. Different pressures were calculated for the G-2 and G-4 intervals because the G-4 thickness is 42 ft and the G-2 thickness is 27 ft.

Table A5–1. Depletion pressure of each rock unit by facies and structural position.

	Distributary channel	Channel-mouth bar	Delta front
Developed area—crest			
Depth from crest (ft)	–20	–20	–20
Mean air permeability (md)	1.500	0.550	0.400
Water saturation (fraction)	0.510	0.570	0.600
Effective gas permeability (md)	0.115	0.027	0.017
G-2 final pressure (psi)	1,630	3,363	4,238
G-4 final pressure (psi)	1,307	2,696	3,398
Undeveloped area—flank			
Depth from crest (ft)	–60	–60	–60
Mean air permeability (md)	1.500	0.550	0.400
Water saturation (fraction)	0.570	0.640	0.680
Effective gas permeability (md)	0.092	0.019	0.011
G-2 final pressure (psi)	1,822	4,009	5,269
G-4 final pressure (psi)	1,461	3,214	4,224